

Land Subsidence: Environmental risk in housing markets in Mexico City*

Lucy Hackett[†] Carolina Rodríguez Zamora[‡]

October 14, 2025

[LINK TO LATEST VERSION](#)

Abstract

We study the costs of and the housing market response to subsidence, the sinking of land areas due to groundwater over-extraction, in Mexico City. We propose an equilibrium model of the housing market that features housing re-development in the face of an evolving environmental hazard that has both realized and expected future impacts to home quality. Guided by model-derived estimating equations for key parameters of the model, we exploit quasi-random variation in sinking intensity to estimate the impact of both realized and future subsidence on home values and redevelopment. We find that realized subsidence imposes substantial costs, lowering prices by 1.5% on average. However, prices are unresponsive to measures of expected future sinking, and novel survey evidence on residents' beliefs and information about sinking suggest that information frictions affect the ability of homebuyers to capitalize predictable future risk. Consistent with model predictions, units that have experienced more sinking are more likely to be redeveloped, as these have lower opportunity cost of being re-built. Evaluating welfare using our parameter estimates implies that subsidence costs Mexico City a total of \$33 billion USD, about \$18 billion of which are due to information frictions that inefficiently increase the housing stock in risky areas. Our findings show that groundwater depletion imposes a costly externality on the built environment, and that frictions affecting the capitalization of environmental hazards in the housing market exacerbate these costs by putting more value in harm's way.

*We are grateful to Marco Gonzalez-Navarro, Kirill Borusyak, Lucas Davis, and Joe Shapiro for their guidance and support. We also thank Lorenzo Aldeco, Nano Barahona, Benjamin Faber, Cecile Gaubert, Amir Kermani, Antoine Levy, and numerous seminar participants for feedback and suggestions. We thank Dr. Natalia Volkow and the staff members at the Microdata Lab at INEGI and the staff of the Econlab for facilitating access to restricted microdata and Rodolfo Oviedo Moguel for invaluable data support. We gratefully acknowledge funding from the Clausen Center, the Fisher Center, and CEGA at UC Berkeley.

[†]Department of Agricultural and Resource Economics, UC Berkeley

[‡]Banco de México

1 Introduction

As groundwater levels decline in places of high population density worldwide, policymakers are increasingly concerned about the environmental and economic consequences of falling water tables (Carleton et al., 2024; Rodella et al., 2023). One important yet under-studied externality resulting from groundwater decline is land subsidence, the sinking of the Earth’s surface due to groundwater depletion. Land subsidence occurs when aquifer levels fall within a groundwater basin, leading to the irreversible compaction of fine-grained sediments and the loss of elevation for the overlying land along with any infrastructure located in the area.¹ Subsidence is an externality because aquifers are hydraulically connected: a drop in water levels caused by pumping in one location eventually equalizes over space, causing land to sink in potentially distant areas within the same basin.

While the physical sinking process is slow—with rates in “severe” cases ranging from 10 to 30 centimeters per year of elevation loss—the cumulative impact creates significant hazards for the built environment. Over time, structures endure increasing stress that leads to tilting, cracking, and eventual loss of structural integrity as the foundation shifts below them. Large public infrastructure is also vulnerable to uneven sinking across broad areas, which causes fissures and sinkholes in roads and damages subterranean assets like water mains and subway tunnels by distorting their required slopes (Cigna and Tapete, 2021; Gambolati and Teatini, 2021).

These structural and infrastructural issues are particularly acute in large cities overlying severely over-drafted groundwater sources, with prominent examples including Jakarta, Tehran, and Mexico City.² These major world cities have experienced cumulative losses of several meters in recent decades (Bagheri-Gavkosh et al., 2021; Werner et al., 2013),

¹Subsidence can also be induced by intensive mining activities or volcanic eruptions; in this paper we focus on groundwater depletion as this is the predominant cause in cities.

²Subsidence “hot spots” can be found on every continent, and there are particularly fast-sinking areas in coastal East Asia, Iran, Mexico, and the United States with areas of intense sinking in 45 states in the United States and more than 95 cities in China (Bagheri-Gavkosh et al., 2021). As Figure B1 illustrates, this issue tends to be particularly acute in developing countries with water management challenges.

resulting in severe consequences for the physical capital overlying sinking areas.³

We study the costs of subsidence and the equilibrium housing market response to this evolving hazard in one of the largest and fastest-sinking urban areas in the world: Mexico City. Mexico City has experienced rapid sinking with the worst-hit parts of the city losing approximately a meter of elevation every 3-4 years since 1950 (Chaussard et al., 2021). Figure 1 depicts some examples of what the consequences of subsidence look like in the city: sinking buildings become damaged and potentially uninhabitable, or require extensive repairs to remain usable. Additionally, subsidence has caused damage to pavement and other infrastructure laid on or below the surface, especially in areas sinking unevenly.

We structure our approach to estimating the costs of subsidence by proposing an equilibrium model of the housing market from which we derive model-consistent estimating equations that identify and provide interpretation of the key parameters governing the market response to subsidence. On the demand side, our estimating equation identifies the willingness to pay to avoid sinking when (i) forward-looking housing demand must consider the future risk of sinking even for homes that have not yet sunk, and (ii) there may be information frictions affecting valuation of future risk, as this may be difficult for home buyers to internalize for yet-unaffected homes. On the supply side, we model a housing developer who considers whether and where to re-develop housing units by re-building existing units on a plot, taking into account that redevelopment re-vitalizes homes that have been impacted by subsidence.

The supply framework highlights the dual role that evolving hazards that affect housing play in the incentive to redevelop; while worsening expectations about future impacts dissuade development, the depreciation caused by subsidence lowers the opportunity cost of renewing existing units, leading to increases in development in affected areas. Conditional on

³In subsiding coastal areas, it is estimated that up to 30% of projected sea level rise is in fact due to these areas sinking into the sea (Nicholls et al., 2021), and currently 11 coastal cities are at risk of becoming totally inundated by the end of the century. In a striking example, Indonesia has developed a plan to move the capital away from Jakarta, which is rapidly subsiding below sea level due to groundwater extraction (Press, 2022).

development, information frictions about future damages lead to inefficiently high housing supply in hazardous areas, as developers receive too high a price for units that will sink in the future. These forces are general to settings where environmental hazards like floods or erosion lead to accelerated housing stock deterioration, and our model provides a way to think about what types of housing market responses are symptomatic of market failures that affect the capitalization of environmental hazards into home values.

The model also elucidates that three parameters are central to this relationship: the willingness to pay of residents to avoid subsidence, the extent of information frictions, and the housing supply elasticity. We derive estimating equations from the structure for these parameters and estimate them using a quasi-experimental design that combines original survey evidence on resident beliefs and information about subsidence, administrative data on bank appraisals, and data on housing developers in Mexico City with novel subsidence measures that we construct for Mexico City.

We measure subsidence by combining original processing of radio wave-based satellite products together with pre-existing measures created by geophysicists to create the longest panel ever constructed of annual subsidence rates in Mexico City at 100m resolution from 2007-2025. We do so using a process called Synthetic Aperture Radar interferometry, a tool used by geophysicists to measure distortions in the earth with applications related to subsidence, volcanic eruptions, and glacier movement, among others. We then use these data to infer the subsidence history of individual properties in our appraisal and survey data, measuring how much a specific property has sunk over its life and its sinking post-transaction.

With these measures in hand we take our model to the data, estimating the willingness to pay of home buyers to avoid subsidence and the capitalization of future subsidence into home values using the universe of mortgage appraisals in Mexico City. In order to causally identify this parameter, we exploit the geophysical determinants of sinking in Mexico City over time and space to isolate exogenous variation in sinking, and use a rigorous repeat

appraisal design that allows us to flexibly control for all static quality and neighborhood differences between different buildings. By using repeat bank appraisals conducted for the purpose of home sales, we employ gold standard approaches to measuring housing price changes, an opportunity that is rarely available in middle income or developing countries due to data limitations. We find that subsidence has important impacts on home values: a meter of sinking causes a loss of 6% in appraised value, and the average home in our sample lost 1.5% of its value to sinking over 10 years. Exploring mechanisms of how sinking impacts home values, we find evidence that losses are a product of both physical impacts to the home and increased maintenance costs. Including uneven neighborhood sinking explicitly in estimation shows that a neighborhood's relative sinking compared to its neighbors also matters: The average relative change in the altitude of a neighborhood causes a 2.4% loss in appraised value over 10 years, and is correlated with an almost doubling of the probability of residents reporting issues with flooding in their neighborhood.

We estimate the extent of information frictions using a combination of model-informed tests and survey evidence. Evidence from the model-derived specification shows that home prices have no detectable relationship with multiple ways of specifying expectations about the future intensity of sinking. We complement this approach using a novel survey of homeowners and long-term occupiers of their housing unit in Mexico City that documents residents' beliefs about subsidence, how they infer sinking risk, and the direct impacts of subsidence to their home and neighborhood. We find evidence that residents of high-sinking plots experience high rates of surprise about the severity of sinking they have experienced, and that these same residents are the least likely to report having considered sinking when they moved in, a finding robust to rich controls for respondent socioeconomic status and survey measures of risk and discounting preferences. Together, these facts point to the presence of important frictions in residents' ability to price future sinking into home prices, and guide us in calibrating the structural information friction parameter in our model.

On the supply side, we leverage the developer's decision to purchase and rebuild on a

plot to estimate the supply elasticity using a survey of housing developers. We infer that a property was re-developed by matching appraisals to the locations of new builds, and find that a meter of sinking increases the probability that a plot is redeveloped by 9.1 percentage points. This finding echos our model intuition that realized sinking lowers the opportunity cost of re-developing a plot, and interpreting our estimates structurally provides an estimate of the supply elasticity.

Using our parameter estimates to evaluate welfare, we find that subsidence costs Mexico City a total of \$33 billion US dollars, which annualized represents almost 1% of Mexico City's GDP. Converting this total to dollars-per-unit of groundwater pumped allows us to estimate the Pigouvian tax on groundwater pumping, which we estimate to be \$0.89 per cubic meter. This is a large tax, which if passed on to consumers would imply a 137% increase in the average water bill. We also estimate the potential gains from policies that address the information friction in the housing market. As is the case in many developing and middle income countries, there are no disclosure laws in Mexico requiring the reporting of relevant hazards as in the United States, despite the fact that developers have detailed information about subsidence risk at the plot level. We find that fully mitigating information frictions would offset 55% of the total costs of subsidence. While all market participants benefit from slowing subsidence, the developer loses market surplus when information frictions are addressed, as information frictions cause the price they receive for new units to be inefficiently high.

Finally, we use our estimates to conduct cost-benefit analysis of policies that would permit groundwater recharge, as the costs of subsidence represent the benefits of these investments. We focus on three policies that have already been implemented by the city government to some extent: building wastewater recycling facilities, investing in artificial aquifer recharge stations, and repairing the extensive leaks that cause technical losses in the domestic water supply system. We find that artificial recharge shows the most promise in terms of a cost-effective policy, but caution that our analysis is limited by the use of rough or dated cost

estimates.

These findings represent the first comprehensive economic analysis of subsidence. While a large body of work has focused on the costs of environmental externalities such as air pollution, floods, and wildfires, subsidence is a natural hazard that has been relatively understudied by economists despite the fact that it is an important groundwater externality affecting many major cities around the world.⁴ We contribute to the sparse economics literature that has studied subsidence (Willemsen et al., 2020; Yoo and Perrings, 2017) by combining improved causal inference with market valuation to estimate costs, and by providing empirical and theoretical analysis of the equilibrium housing market response to sinking. Our original satellite work and survey contribute novel evidence on the physical impacts of sinking on buildings and public infrastructure, which to our knowledge is the first representative measure of damages for a city.

More broadly, our framework provides a way to think about the equilibrium response of housing to evolving environmental hazards, with a particular focus on contexts with imperfect information. We build on recent empirical findings from work in environmental, urban, and real estate economics that study how information frictions about environmental risk impact housing markets (Bakkensen and Barrage, 2022; Bakkensen et al., 2019; Gallagher, 2014; Gourevitch et al., 2023; Hino and Burke, 2021; Ortega et al., 2025; Ortega and Taşpinar, 2018; Petkov and Ortega, 2025; Wagner, 2022), and go further by embedding these frictions in an equilibrium spatial model of the housing market to quantify the aggregate costs of these frictions.⁵ We also provide rich empirical evidence on the housing market response to an important externality from a middle income context, a rare

⁴Engineering-style estimates of the costs of subsidence suggest that these may be large, especially in urban areas; case studies from China (Lixin et al., 2010), Indonesia (Mahya et al., 2021), Mexico (Fernández-Torres et al., 2025; Novelo-Casanova et al., 2022), and California (Borchers and Carpenter, 2014; Fowler, 1981) find damages in the billions for specific cities or counties. However, the general approach in these studies is to estimate replacement costs for damaged infrastructure without considering market values or forces.

⁵Relatedly, our forward-looking demand framework draws on insights from recent dynamic hedonic approaches (Rosen, 1974; Benetton et al., 2023; Bishop and Murphy, 2019), and we propose a way of incorporating information frictions into these methods.

opportunity due to the infrequency of housing value data in these settings.⁶ In particular, we provide evidence on the value of disclosure laws from a middle income context, a first that we are aware of (Dranove and Jin, 2010; Frondel et al., 2020; Nanda and Ross, 2012; Sinha, 2022).

By modeling the market response to environmental risk in equilibrium, this paper is related to the literature on urban development and adaptation (Gechter and Tsivanidis, 2025; Hsiao, 2023; Ospital, 2024; Ostriker and Russo, 2023), and more generally to a body of work that studies the costs of slow-moving disasters such as climate change (Balboni, 2025; Desmet et al., 2021; Hsiang et al., 2017). Our model contributes to these papers by modeling redevelopment in the context of an evolving hazard, which allows us to carefully examine the different roles that *realizations* and *expectations* of environmental risks play in driving housing supply and re-development.

The rest of this paper is organized as follows. Section 2 introduces the context and our satellite data for measuring subsidence. Section 3 presents the economic data we use. We present our theoretical framework in Section 4. Section 5 presents the estimation strategy and results from our survey work and the demand and supply estimation. We present policy analysis in Section 6, and Section 7 concludes.

2 Subsidence in Mexico City

Mexico City has experienced severe rates of subsidence over the last 100 years, which geophysicists have established is caused by sustained groundwater pumping on the Mexico Valley aquifer (Cabral-Cano et al., 2008; Chaussard et al., 2021; Solano-Rojas et al., 2015).⁷ This pumping is primarily conducted by the city government and the federal water authority

⁶One important exception is Gonzalez-Navarro and Quintana-Domeque (2016), who also use professional appraiser data to study road paving in Mexico.

⁷Mexico City has a long history of water management and scarcity; the Aztec empire had built their capital city around and interwoven with the large lake system in the area, but the lake was subsequently drained by the Spanish colonial government. Because such a large part of the city is built on the soft, silty lake bed of the drained lake, this area is particularly prone to subsidence.

CONAGUA for the purpose of supplying the city with about two-thirds of its total water consumption, the other third of which is supplied by surface water sources.⁸ Because the aquifer is hydraulically connected, pumping anywhere affects the water table everywhere ([Cigna and Tapete, 2021](#)), which is why the city itself experiences high rates of subsidence despite the fact that there is no groundwater pumping conducted within city limits.⁹

Thus sinking rates are primarily a product of two factors: the height of the water table and the propensity of overlying geologies to compact and sink. Given that the water table is currently far below historic levels, sinking accelerates when the water table is relatively lower (and vice versa), and could only be fully stopped if the aquifer is recharged either naturally or via water injection ([Gambolati and Teatini, 2021](#); [Liu et al., 2019](#)). While it is conceivable that the weight of human development could increase sinking, empirical studies in Mexico City have found no correlation between localized sinking rates and population density, pumping rates, or land use type ([Chaussard et al., 2021](#)).¹⁰ Our own analysis in Appendix E.1 supports this conclusion, as we find that construction on a pixel does not predict subsequent sinking rates.

2.1 Measuring subsidence

Historically, subsidence was measured by inserting poles deep into the ground at discrete points and measuring the change in how exposed the pole became over time as the ground subsided away from it; this method was used as early as the 19th century by the Spanish

⁸Bringing surface water into Mexico City is very expensive due to how far large surface water sources are and the fact that most sources need to be pumped over the surrounding mountain ranges. The most important surface water source for the city is the Cutzamala system, which involves seven dams and over 330 kilometers of canals and pipes that use over 2 billion kWh of electricity per year to transport water to Mexico City.

⁹The government has limited all pumping on the aquifer to the periphery of the city- a policy decision made after an episode of intense sinking in the 1950s ([SACMEX, 2012](#)), which resulted from the fact that water table levels take time to equalize over space. Pumped water is first sent to treatment facilities then to distribution stations, making the relationship where water is pumped and supply of water to a specific area tenuous.

¹⁰Studies have found that the weight of New York City has caused sinking of a couple millimeters, but New York has much higher population density than Mexico City, and this effect is orders of magnitude smaller than the rates observed in Mexico ([Parsons et al., 2023](#)).

colonial government to measure sinking in Mexico City ([CONAGUA, 2009](#)). Today, measuring sinking over larger areas at fine geographic scale is possible thanks to Synthetic Aperture Radar (SAR) instruments on satellites.

SAR instruments emit energy at the Earth in the form of radio waves and record a transformation of the number of oscillations that the wave undergoes between the earth and the satellite. While these measurements are meaningless on their own, constructing the difference between two images through a process called interferometry creates high-accuracy measures of vertical displacement.¹¹ Interferometry is the go-to tool of geophysicists studying events involving land deformation, and because this is a popular and well-established tool the measurement error associated with SAR measurements of subsidence is well-studied, with inaccuracies on the scale of 1-10 millimeters for modern satellites ([Wu and Madson, 2024](#)), an order of magnitude smaller than the subsidence rates we measure in Mexico City.¹²

We apply gold standard tools for conducting interferometry and subsidence time series construction at the pixel level that correct for distortions caused by terrain, tropospheric factors, and orbital error to construct the longest panel of subsidence rates in existence for Mexico City ([Fattah et al., 2017](#); [Yunjun et al., 2019](#); [Yu et al., 2018b](#)). We do this by combining three series of data, summarized in Appendix Figure [B2](#), performing original interferometry using data produced by the ALOS-1 (2007-2011) and Sentinel-1 (2021-2024) satellites to complement measures created by [Chaussard et al. \(2021\)](#), a team of geophysicists who used Sentinel-1 readings to study sinking in Mexico City at a 90-meter resolution from 2014-2020. By using three separate series, we are able to address the computational challenge

¹¹These calculations are deterministic in nature, and are not the result of machine learning algorithms like those well known in applications such as remote sensing of pollution or applications that use image-based sensors.

¹²Interferometry achieves higher accuracy in urban areas because the hard reflective surfaces minimize noise generated by signals intercepting vegetation. We provide a detailed discussion of the sources and potential magnitudes of measurement error when conducting interferometry in Appendix [E.1.1](#), but by using state-of-the-art algorithms we address the main sources of error that could affect our estimates, including distortions potentially generated by construction. Intuitively, construction does not have a strong impact on our measurements for two reasons. One, because satellites take measurements at an angle, interferometry has trouble detecting building height in general. Second, because the construction of the time series involves linearly projecting through high-frequency measurements every 6 days by year on a pixel-by-pixel basis, this minimizes the noise from irregular measurements or changes induced by demolition/construction.

presented by calculating a single time series: The raw Single-Look Complex (SLC) SAR data and its processed output for just one orbit direction (ascending) for 5 years contains almost five terabytes of data and takes over three weeks of continuous computational time to process.

In order to characterize the gradient of sinking over larger spatial areas, the principal risk factor for damage to roads and water mains, we define a 500-meter resolution grid (the median census tract size) over Mexico City and construct two complementary measures of how uneven sinking is over space. The first measure is the standard deviation of sinking among pixels overlaying the grid cell, an intuitive measure of unevenness. The second measure takes inspiration from the horizontal gradient used in geophysics studies such as [Fernández-Torres et al. \(2020\)](#) and calculates the absolute value of the grid cell's *relative* displacement between periods t and t' as the absolute value of the difference in grid cell sinking and the average of its neighbors:

$$\text{Abs. relative elevation change}_{gtt'} = \sum_{\tau=t}^{t'} |s_{g\tau} - \bar{s}_{g\tau}^{nbrs}| \quad (1)$$

The absolute value allows us to capture the potentially damaging macro-infrastructure effects of areas that are sinking more or less than their neighbors. Because this measure accumulates over time, it captures the cumulative impact of relative altitude change in the environment, which may matter more for infrastructure like water mains and sewers than unevenness alone.

2.2 Sinking over time and space

Our subsidence data paint a detailed picture of how sinking has evolved in Mexico City in recent decades. Figure 2, Panel (a) plots the sinking rate in 2010. The highest rates of subsidence across the city reach between 20-25 centimeters per year, rates that are among the highest in the world ([Werner et al., 2013](#)). These fast rates are strongly localized in the eastern part of the city, which overlies particularly vulnerable geologies prone to subsidence.

Geophysicists estimate that this part of the city could sink up to 30 more meters given the thickness of the features of the subterranean geology prone to compaction ([Chaussard et al., 2021](#)).

Panel (b) depicts the change in the rate from 2010 to 2020, and shows that by 2020 the northeast corner of the city actually slows somewhat whereas other parts of the valley begin to sink. These areas have started sinking in recent years, as aquifer levels remain low and some destabilizing drought periods and seismic events have weakened these historically resistant areas. Despite these changes, subsidence on a broad scale is still very predictable over space due to the concentrated geological features that determine risk.¹³ Perhaps because of this broad systematic predictability, subsidence is uninsurable in Mexico City, and is explicitly listed in home insurance policies as a non-covered event.¹⁴

Finally, Panels (c) and (d) plot our measures of uneven sinking, showing that high relative altitude change and standard deviation of sinking are concentrated around the edges of the high-sinking area, as well as around relatively fixed geologic features that maintain their altitude as the neighborhoods around them sink.

2.3 Sinking is prominent, but poorly understood by residents

Subsidence is a familiar issue to Mexico City residents: In our survey, before we mention the word subsidence, 56% of respondents included “sinking” in their response when asked about the likely causes of the degraded state of a photograph of a tilted and cracked building. Additionally, only 18.5% of respondents could not provide a guess when asked where in the city has the most issues with subsidence.

Despite this familiarity with subsidence as a local issue, survey respondents show several “symptoms” of experiencing information frictions around how future subsidence will impact

¹³Appendix F provides detailed discussion of the data generating process of subsidence and its predictability, and we show that while sinking is very predictable over large spatial areas, sinking rates are more idiosyncratic within a city-block.

¹⁴Subsidence was recently included in “home quality insurance” policies that cover INFONAVIT mortgages from the federal government, but these policies only cover the first 10 years of the home’s life, within which the most severe impacts of sinking would not yet be observed.

their home. Figure 3 plots the relationship between a measure of expected 5-year sinking on a respondent’s plot, estimated as five times the average rate over the panel, and two survey measures of information frictions. In Panel (a), this sinking intensity is plotted against the probability that the respondent reports having considered sinking when they moved to their unit. We see that for most of the support, residents living in units sinking at higher intensity are less likely to have considered sinking when they moved in than residents of low-sinking intensity plots. Complementing this in Panel (b), we find that the more a resident’s plot has sunk, the more likely they are to report that sinking on their property has been worse than expected, providing evidence that residents do not buy sinking homes “eyes wide open” about the future impacts they will experience.

These patterns have a couple of competing explanations. First is that some residents experience information frictions or are inattentive to future sinking, and that these residents end up sorting into high-sinking areas. Alternatively, some residents may have high discount rates that lead them to systematically ignore future sinking. This mechanism is unlikely for housing which has an important asset value, and which should tie discounting of future values to other financial products. We show in Appendix Table A4 that measured values of discount rates and risk aversion are uncorrelated with sinking intensity, suggesting that this is not playing a strong role here.¹⁵

We will provide more quantitative and qualitative evidence for information frictions in Section 5, but motivated by these stylized findings we incorporate potential underestimation of the severity of future sinking into our theoretical framework.

¹⁵It is also possible that some residents simply do not value the impacts of subsidence on their home, causing them to be inattentive to future sinking. However, if this were the case we would not expect these residents to also report that subsidence has been worse than expected, as they should also be inattentive to realized subsidence.

3 Economic Data

3.1 Measuring home prices: Appraisals

We measure housing values using confidential data on the universe of mortgage appraisals for the purpose of home sales performed by the Federal Mortgage Society (SHF, *Sociedad Hipotecaria Federal*) in Mexico City from 2005-2020, which were made available through freedom of information request.¹⁶ We use property characteristics and exact locations to identify identical units from the same building, a matching process that results in 17.4% of our sample as being identified as a repeat appraisal.¹⁷ We assign sinking to transactions by matching appraisals spatially to pixels using the exact location to calculate the total amount of subsidence that the unit has experienced since the year of construction.

An advantage of our data is that mortgages represent relatively arms-length transactions, which are less likely to be affected by relational contracting or fraudulent reporting for the purpose of tax evasion, two common issues affecting price data from other sources in Mexico ([Gonzalez-Navarro and Quintana-Domeque, 2016](#)). However, in order for appraisals to capture the true valuation of subsidence by homebuyers as opposed to the appraiser's algorithm, they must contain a strong signal of the transaction price ultimately paid. Conceptually, this is likely as appraisals are used for the purpose of valuing a mortgage, and appraisers have a strong incentive to appraise the home at the price a buyer is willing to pay. We validate this using a confidential dataset of appraisal and transaction prices called the R04, whose access was provided by the *Banco de México*. The R04 data only contain

¹⁶An SHF appraisal is required as a condition of obtaining a mortgage from a private bank or the public mortgage financier, and all SHF appraisals must be done by an SHF-certified appraiser. Thus, these data contain the universe of SHF appraisals, but do not include unofficial appraisals that may have been done for cash purchases of homes. The 2020 National Housing Survey suggests this restriction is important: only 30% of home purchase in Mexico City in 2020 were financed with some form of formal credit, with the majority of homes obtained via self-financing of own construction.

¹⁷We exactly match appraisals on the built square footage, the square footage of the property, the number of rooms and bathrooms, number of floors, number of parking spaces, and whether the building has an elevator, and require the coordinates of the appraisal to imply a less than 100-meter distance between them. Table A2 in the Appendix describes how repeat sales properties differ from single sales in the data; properties with repeat sales are much more likely to be apartment as opposed to single family homes, and are generally newer, smaller, and less valuable than the full sample.

approximate locations, but allow us to directly compare appraisals and transaction prices.

Using these data, we find that 73% of observations have identical appraisal and transaction values, and that appraisal values closely track transaction prices. Figure 5 plots transaction prices against appraisals, showing that points are closely centered around the 45° line.¹⁸ Appendix Table A1 reports coefficients and goodness-of-fit statistics for regressions of transaction prices on appraised values with and without an intercept. We estimate a coefficient of determination of 0.97 (Column (1)), highlighting the close relationship between appraisals and transaction prices. Importantly, Column (3) shows that deviations of appraisal values from sales prices are not correlated with subsidence; total sinking on the locality from 2007-2020 is not a statistically or economically significant predictor of the absolute deviation of appraised values from transaction prices.

3.2 New survey on subsidence impacts and beliefs

In March 2025 we conducted a representative in-home survey of long-term Mexico City residents about subsidence impacts and their beliefs and information about subsidence. Respondents were restricted to owner-occupiers (73%) or those who had lived in their home for at least five years (27%). The survey was stratified based on subsidence risk, with two-thirds of the sample drawn from the seven high-risk boroughs and one-third from the remaining nine boroughs.¹⁹

This first-of-its-kind survey asked homeowners about the damages from subsidence to their housing unit and the urban environment, as well as residents' beliefs and attention to the issue when making housing decisions. First, we surveyed residents on the physical quality of their home and neighborhood as well as maintenance expenditures and activities before mentioning subsidence. In the second module, we then mentioned subsidence by name, surveying residents on their knowledge about subsidence, how they thought about subsidence

¹⁸Figure B3 in the appendix reports the distribution of deviations between appraised and transaction values, showing the full distribution of differences.

¹⁹More details about survey sample definition and implementation can be found in the Data Appendix E.2.

before living in their current home, and their experience with sinking since arriving at their current unit. We use the location of respondents' homes to map their property to our satellite measures of sinking and infer the total amount of sinking their home has experienced since construction (or 2007, whichever is later), the amount of sinking on their property over the last 5 years, and the unevenness measures associated with their grid cell.

3.3 Housing development

We examine the supply side of the market using the DIME (*Dinámica del Mercado Inmobiliario*) dataset, which is a quarterly survey of new housing developers. These data are compiled by a private real estate consulting firm and access was granted through *Banco de México*. From this survey we construct a dataset of new housing developments from 2007-2020, which are new construction projects that comprise one or more housing units.²⁰

We use these data in two ways. First, we use a combination of address matching and spatial methods to match new developments to appraisals previous to when construction started to identify appraisals that were sold to developers. Because addresses are not always consistently recorded in the data and may change when a plot is redeveloped, we likely miss some appraisals that subsequently became redeveloped in our data. We address this in an alternative analysis that characterizes the geography of new development by creating a panel at the pixel level that measures the number of units built and the probability of new development.

²⁰Given that new homes comprise 70-80% of the housing market in Mexico and that real estate developers built 60% of new homes, the DIME data observes 42-48% of the housing market in a given quarter (Rodríguez Zamora, 2010). This is likely a lower bound for Mexico City, which has a more formal construction sector than other areas of the country. Appendix E.4 discusses coverage in more detail. There were 20,380 new developments over the study period, which contain 977,221 new housing units. The median housing development included 20 new units, but some developments have hundreds of new units.

4 Theoretical framework

In order to structure estimation of a hazard that has both *realized* and *anticipated* impacts, we propose a model of the housing market that incorporates forward-looking housing demand that values subsidence as a negative home attribute. Our model yields welfare expressions that allow us to quantify the costs of subsidence, and estimating equations for the key parameters needed to conduct welfare analysis.

Time is discrete, and in each period households rent housing from property managers who serve as intermediaries between renters and a housing developer who builds the housing stock. The developer purchases existing housing from property managers and builds new housing that is subsequently sold back to property management firms. Each period begins with an existing continuous measure of housing on each plot j , H_{jt-1} , which is owned by property management firms. There is an initial period $t = 0$ with a measure H_{j0} of housing on each plot. In each period t , the following sequence occurs:

1. The developer draws cost shocks for each plot and all housing units go up for sale on the market to own housing.²¹ Units may be purchased by another property management firm or the developer. If they are purchased by the developer, then new units are built, which have zero realized sinking and re-enter the market for purchase by property managers.²²
2. The ownership market clears on the price of owning a home p_{jt} . Given the development that may have occurred, this implies a housing stock on each plot H_{jt} that is fixed until the next period.
3. Renters draw iid preference shocks over plots and make a discrete choice over which plot to live on. Property management firms supply rentals from the housing they purchased

²¹By putting the full stock on the market in each period, we abstract from housing inventory and matching buyers to available housing.

²²We assume the market lasts long enough for these units to compete with a meaningful share of the stock when put back on the market.

in the previous step. Equilibrium rents R_{jt} adjust to clear the rental market.

We describe these steps in reverse order, as the decision of property management firms to purchase is a function of their expectations over the rental market.

4.1 Renters

A continuum of renters in Mexico indexed by i with mass \bar{L} decide which discrete plot j to rent a unit of housing on. They draw preference shocks over plots in each period, and can choose from plots in Mexico City or choose the outside option of living outside the city ($j = 0$), where rental units are supplied perfectly elastically at zero price. All rental units on a given plot are identical, and they derive utility/disutility from paying rent R_{jt} , how much the unit has sunk to date, S_{jt} , other observable attributes Z_{jt} and unobserved attributes e_{jt} , each of which are unaffected by subsidence. Total subsidence S_{jt} is the accumulation of sinking rates on the plot $s_{j\tau}$ from the time of construction to t :

$$S_{jt} = \sum_{\tau=\text{Year built}_j}^t s_{j\tau} \quad (2)$$

Their utility is given by:

$$V_{jt}^i = \gamma S_{jt} + Z_{jt}\delta + e_{jt} - \log(R_{jt}) + \epsilon_{jt}^i \quad (3)$$

We assume $\epsilon_{jt}^i \sim \text{iid EV}(1)$ with variance 1, and normalize mean utility from the outside option to zero: $V_{0t}^i = \epsilon_{jt}^i$.

The probability that a renter chooses plot j is:

$$\lambda_{jt} = \frac{\exp(\gamma S_{jt} + Z_{jt}\delta + e_{jt} - \log(R_{jt}))}{1 + \sum_l \exp(\gamma S_{lt} + Z_{lt}\delta + e_{lt} - \log(R_{lt}))} \quad (4)$$

and total rental demand is given by:

$$H_{jt}^D = \bar{L}\lambda_{jt}(R_{jt}) \quad \forall j \quad (5)$$

4.2 Property management firms

In each period a mass of competitive property management firms, indexed by $k \in \Omega$, purchase housing (either used or newly developed) and rent units to renters. Their expected profits on a plot j from holding a measure of housing $H_{jt}(k)$ are given by:

$$\tilde{\mathbb{E}}_t(\pi_{jt}(k)) = H_{jt}(k)\tilde{\mathbb{E}}_t\left(\sum_{\tau=t}^{\infty} \rho^{\tau-t} R_{j\tau}\right) - p_{jt}H_{jt}(k) \quad (6)$$

Expected revenue is the present value of expected rents accruing from renting $H_{jt}(k)$ of the housing measure. These firms form subjective expectations $\tilde{\mathbb{E}}_t()$, which may differ from rational expectations $\mathbb{E}_t()$. Each unit of $H_{jt}(k)$ costs p_{jt} in a lump-sum payment to purchase from another property manager or the developer.²³ Their total expected profits sum over their holdings on all plots:

$$\tilde{\mathbb{E}}_t(\pi_t(k)) = \sum_j \tilde{\mathbb{E}}_t(\pi_{jt}(k))$$

The separation of the owners of housing from those who occupy it creates a helpful accounting separation between those who hold the asset value of the home and the use value. It is worth noting that in our context 65% of residents are owner-occupiers; this would correspond in the model to property management firms that rent to themselves.

4.2.1 Information frictions

Expectations over future sinking play an important role in (6); however, information frictions may complicate the valuation of yet-unrealized damages (Bakkensen and Barrage, 2022;

²³We abstract from leverage or other financial markets by assuming that they self-finance their capital investment into the property at zero opportunity cost.

(Gourevitch et al., 2023; Gallagher, 2014). We incorporate information frictions into the model by modeling expectations of future sinking rates as a function of rational expectations such that:

$$\tilde{\mathbb{E}}_t(s_{ju}) = \theta \mathbb{E}_t(s_{ju}), \quad \theta \in [0, 1], \quad u > t \quad (7)$$

In this expression, θ parameterizes the extent of information frictions or myopic behavior on forming expectations about future sinking; when $\theta = 1$, property managers have rational expectations about future sinking. As $\theta \rightarrow 0$, buyers shade their expectations about future sinking and prices become less responsive to expected future sinking, remaining inefficiently high as property managers overpay for homes that will sink in the future.²⁴. This behaves similarly to the β in the beta-delta behavioral model (Laibson, 1997; DellaVigna, 2018), except that the discounting is only over future sinking and not all future rents.

4.3 The housing developer

In each period, the developer receives plot-specific cost shocks ξ_{jt} , and decides which plots to purchase and redevelop. The developer operates only within Mexico City. Purchasing a plot means purchasing the measure of housing contained on it, H_{jt-1} . Developing involves building new units which have zero realized sinking; the key feature of development is that it allows the developer to adjust the housing stock on the plot and it “resets” realized sinking to zero. Their plot-specific profits conditional on developing are:

$$\pi_{jt} = \max_{H_{jt}} \underbrace{p_{jt}(0)H_{jt} - \xi_{jt} H_{jt}^{\frac{1+\eta}{\eta}}}_{\text{Variable profits from developing}} - \underbrace{p_{jt} H_{jt-1} D}_{\text{Cost of acquiring, renewing plot}}, \quad \eta > 0 \quad (8)$$

where η is the supply elasticity, and $p_{jt}(0)$ is shorthand for the price that a developer receives for new units that have experienced no sinking. D is renovation cost of the plot,

²⁴In this model, θ does not update with realized sinking, but the total welfare impacts of these frictions are the same in an alternative model in which $\theta < 1$ only for the period that the home is first sold as a new unit, which changes only which property developers experience negative profits. We model that θ is uniform among property managers, but note insights from papers such as Bakkensen et al. (2019) that show that only some mis-informed participants are needed to inflate prices.

which is proportional to the total value of the plot.²⁵ Because the developer competes with property managers (the used housing stock) both when selling their units and when purchasing plots, they take market prices as given but may make positive profits arising from favorable productivity shocks.

Conditional on developing, the developer chooses how many units to build optimally. Solving this problem gives:

$$H_{jt}^{opt} = \left(\frac{\eta}{(1+\eta)\xi_{jt}} p_{jt}(0) \right)^\eta$$

$$\pi_{jt}^* = \max\{0, \tilde{\eta}\xi_{jt}^{-\eta} p_{jt}(0)^{\eta+1} - p_{jt} H_{jt-1} D\}, \quad \tilde{\eta} = \left(\frac{\eta}{1+\eta} \right)^\eta \left(\frac{1}{1+\eta} \right)$$

The developer will re-develop a plot if variable profits are larger than the cost of acquiring the plot:

$$d_{jt} = 1(\tilde{\eta}\xi_{jt}^{-\eta} p_{jt}(0)^{\eta+1} \geq p_{jt} H_{jt-1} D) = 1(\tilde{V}_{jt}^S \geq 0)$$

$$\tilde{V}_{jt}^S = \log(\tilde{\eta}) + (\eta+1)\log(p_{jt}(0)) - \log(p_{jt}) - \log(H_{jt-1}) - \log(D) + \tilde{\xi}_{jt}$$

where $\tilde{\xi}_{jt} = -\eta \log(\xi_{jt}^S)$, and we assume $\tilde{\xi}_{jt} \sim \mathcal{N}(\mu, \sigma^2)$ for calculation of expected surplus and estimation. Intuitively, higher prices for new units increase \tilde{V}_{jt}^S by $\eta+1$ because this latent value is a function of log revenues (as opposed to quantities). We transform this expression into a function of observable data using the price decomposition given by the demand structure to separate realized subsidence from the rest of the price: $\log(p_{jt}(0)) = \log(p_{jt}) + \gamma S_{jt}$:

$$d_{jt} = 1(\tilde{V}_{jt}^S \geq 0) \tag{9}$$

$$\tilde{V}_{jt}^S = \log(\tilde{\eta}) + \eta \log(p_{jt}) - \gamma(1+\eta)S_{jt} - \log(H_{jt-1}) - \log(D) + \tilde{\xi}_{jt} \tag{10}$$

²⁵This allows demolition costs to increase with buildings that are built with better materials or that are larger, qualities that would be correlated with higher value.

and write housing supply as:

$$H_{jt}^S = d_{jt} H_{jt}^{opt} + (1 - d_{jt}) H_{jt-1} \quad \forall j \quad (11)$$

4.4 Equilibrium

Given exogenous parameters $\{\gamma, \theta, \eta, \bar{L}, \{H_{j0}\}_j, \delta, \rho, D\}$ and realizations of cost shocks $\{\xi_{jt}\}_{j>0}$, in each period the equilibrium consists of a set of prices $\{p_{jt}^*\}_j$, rents $\{R_{jt}^*\}_j$, and housing $\{H_{jt}^*\}_j$ that satisfy the following conditions:

- Renters choose the plot to rent on optimally. Property managers and the developer maximize profits.
- Property management firms make zero subjectively-expected profits:²⁶

$$p_{jt}^* = \tilde{\mathbb{E}}_t \left(\sum_{\tau=t}^{\infty} \rho^{\tau-t} R_{j\tau}^* \right) \quad \forall j \quad (12)$$

- The rental market clears on rents R_{jt}^* in each period such that rental demand given by (5) equals (11).²⁷
- The market for new homes clears on home prices p_{jt}^* according to (12) and (11) given the price function $\log(p_{jt}^*(0)) = \log(p_{jt}^*) + \gamma S_{jt}$.²⁸

Figure 4 visualizes these two markets. Demand for owning housing inherits its shape from the rental market, and may be too high if information frictions inflate the value of future rents. If re-development happens, then supply is upward-sloping from the developer's

²⁶This follows because these firms are competitive and we assume that there is no private information or other advantage that firms can leverage.

²⁷Given that (i) development decisions and the housing stock on each plot are determined before the rental market occurs, and (ii) conditional on ownership, property managers supply rentals at zero marginal cost, rental supply is inelastically supplied according to (11).

²⁸Because there is only one developer competing with many property managers to purchase units, the transaction price will be set by property manager demand. This also implies that the expectation that property managers form of the future stream of rents will be set by the value of those rents conditional on *not* redeveloping, as that is the price a developer will pay them for the asset even if the plot is subsequently redeveloped.

problem; otherwise it is inelastically set at the previous housing quantity. Once the housing stock has been set by this equilibrium, the rental market takes this as given, and the rental market clears on rents so that demand for a plot equals the supply of housing on that plot. As sinking occurs, rental prices fall on plots that have not been redeveloped to maintain all housing on the plot occupied. Deadweight loss in the housing market comes from the over-supply of units in sinking areas that result in losses for property managers as the flow of rents is lower than expected on those units.

4.5 Welfare and Model predictions

The total change in welfare in the housing and rental markets in Mexico City between counterfactuals corresponds to the total change in developer, property manager, and renter surplus between alternative equilibria.²⁹ Per-period developer's surplus is their total expected profits across all plots, taking expectations over the distribution of cost shocks:

$$PS_t = \sum_{j>0} \mathbb{E}_\xi(\pi_{jt}^*) \quad (13)$$

Objectively-expected property managers' profits are derived by substituting (6) into (12).

$$\Pi_t = \sum_j H_{jt}^* \left(\sum_{\tau=t}^{\infty} \rho^{\tau-t} \left(\mathbb{E}_t(R_{j\tau}^*) - \tilde{\mathbb{E}}_t(R_{j\tau}^*) \right) \right) \quad (14)$$

Under rational expectations, these are zero; in the presence of information frictions (rationally) expected profits will be negative.

To account for using log rents in utility, we calculate the equivalent variation Δ_t^D that equalizes average consumer surplus between counterfactuals to characterize the change in renter welfare. The present value of the difference in total welfare between counterfactuals

²⁹Derivations of the welfare terms and comparative statics in the next section can be found in Appendix G.4.

is:

$$\Delta W = \Delta \Pi_t + \frac{\Delta_t^D}{1 - \rho} + \frac{\Delta PS_t}{1 - \rho}$$

4.5.1 Model predictions

Examining how model outcomes and welfare behave in equilibrium sheds light on how the housing market responds to subsidence and market frictions; we list the main propositions here, and provide proofs in Appendix G.4. For each experiment, we consider the difference between equilibria under different parameter values, allowing prices and the housing stock to fully adjust.

Proposition 1: Information frictions ($\theta \rightarrow 0$) increase expected housing supply and producer surplus on sinking plots, but have no effect on the probability of re-development.

Proposition 2: Realized sinking increases expected producer surplus and the probability of re-development, but expected future sinking decreases expected producer surplus and has no impact on the probability of redevelopment.

Proposition 3: Information frictions make the profits of property managers more negative.

Intuitively, information frictions lead to an inefficiently high price being offered for new units in sinking areas, which leads to oversupply of housing conditional on developing and increased profits. However, because information frictions inflate housing density in sinking areas, both the developer's fixed cost of buying the plot (which is proportional to housing density) and revenue (a function of expected future sinking) are too high under information frictions, so re-development happens with the same probability as in the frictionless equilibrium.

Expected future sinking has an analogous though opposite effect: future sinking decreases both cost and revenues equally and has no net effect on redevelopment, but it decreases prices and therefore the number of units built. Realized sinking works through a different

mechanism; by directly lowering the costs of buying up a plot, realized sinking increases the probability of redevelopment by increasing the probability of positive profits.³⁰ Property managers make negative profits under information frictions, as they over-pay for units that will sink more than they expect.

The model makes clear that three parameters are crucial for quantifying the total costs of subsidence: γ , the per-period direct costs of subsidence, θ , the extent of information frictions, and η , which governs the shape of the supply curve and thus the responsiveness of supply to the market distortion. In the next sections, we derive estimating equations from the model for these parameters and estimate them using our data on mortgage appraisals and development.

5 Estimation

5.1 Costs of subsidence

Our granular data permits a direct approach to estimating the costs of subsidence and capitalization of future risk that leverages within-building variation to isolate plausibly exogenous variation in sinking.³¹ We solve Equation (4) for rents:

$$R_{jt} = \exp\{\gamma S_{jt} + \delta Z_{jt} + e_{jt} - \tilde{\lambda}_{jt}\}$$

where $\tilde{\lambda}_{jt} = \log(\lambda_{jt}) - \log(\lambda_{0t})$, and substitute this expression into (12) to derive a relationship between log prices and sinking:

$$\log(p_{jt}) = \gamma S_{jt} + \log \left(\exp(-\tilde{\lambda}_{jt} + Z_{jt}\delta + e_{jt}) + \tilde{\mathbb{E}}_t \left(\sum_{\tau=t+1}^{\infty} \rho^{\tau-t} \exp\{\gamma S_{j\tau}^{t+1} + Z_{j\tau}\delta + e_{j\tau} - \tilde{\lambda}_{j\tau}\} \right) \right)$$

³⁰The impact of these policies on renters is not a direct function of sinking, as they are perfectly compensated for sinking through decreased rents. However, they may experience benefits in alternative equilibria where rents are lower on average due to a higher housing stock, and vice versa.

³¹Our approach also allows us to recognize that sinking is an individual property attribute in our appraisals data. We also note the equivalence of hedonic and discrete choice estimators when the characteristic is continuously “supplied” in the market, as is the case of subsidence in our setting (Bayer et al., 2007).

where $S_{j\tau}^{t+1} = \sum_{u=t+1}^{\tau} s_{ju}$ is the cumulative sinking from $t+1$ to τ . We are able to factor out realized sinking from the expression because (i) its impact on homes is persistent, and (ii) because the transaction price is set by property manager's demand, expected future rents are those of the non-redeveloped property.

Stronger assumptions are required to make progress towards an estimating equation that teases expected sinking from the residual. We first assume that $Z_{j\tau}$ are time-invariant and can be written as Z_j . Next, we take two first-order approximations: first of $\mathbb{E}_t(\exp(\gamma S_{j\tau}^{t+1} + e_{j\tau} - \log(\lambda_{j\tau}) + \log(\lambda_{0\tau})))$ around the expectations of these variables, and then of the log function around $\mathbb{E}_t(e_{j\tau}) = e_{jt}$, $\mathbb{E}_t(\tilde{\lambda}_{j\tau}) = \tilde{\lambda}_{jt}$, and $\mathbb{E}_t(S_{j\tau}^{t+1}) = 0$ to arrive at.³²

$$\begin{aligned}\log(p_{jt}) &\approx \gamma S_{jt} + \gamma \theta \sum_{\tau=t+1}^{\infty} \rho^{\tau-t} \mathbb{E}_t(s_{j\tau}) + \delta Z_j - \log(H_{jt}^S) + \log(H_{0t}^S) + u_{jt}, \\ u_{jt} &= e_{jt} + (1-\rho) \sum_{\tau=t+1}^{\infty} \rho^{\tau-t} (\mathbb{E}_t(e_{j\tau}) - e_{jt} + \tilde{\lambda}_{jt} - \mathbb{E}_t(\tilde{\lambda}_{j\tau})) - \log(1-\rho)\end{aligned}\quad (15)$$

and formulate the estimating equation we take to the data as:

$$\log(p_{jt}) = \gamma S_{jt} + \gamma \theta \sum_{\tau=t+1}^{\infty} \rho^{\tau-t} \mathbb{E}_t(s_{j\tau}) + \alpha_j + \alpha_{z(j)t} + Z_j \cdot t\beta + \tilde{u}_{jt} \quad (16)$$

By including fixed effects for identical units in the same building α_j , we flexibly control for both observed and unobserved static quality differences between appraised units (Z_j, e_j), a concern that is first-order in many hedonic estimation strategies. The α_j also absorb $\log(H_{jt}^S)$, as housing supply on the plot is fixed between appraisals. Geography by year fixed effects $\alpha_{z(j)t}$ absorb housing supply outside Mexico City ($\log(H_{0t}^S)$), and allow demand shocks to vary flexibly across housing markets.³³ The inclusion of linear trends by a vector

³²Appendix G.1 provides more details and derivations. Note that the second-order approximation of the expectation would add the term $\frac{\gamma^2}{2} \exp(\gamma \mathbb{E}_t(S_{j\tau}^{t+1})) \text{Var}_t(S_{j\tau}^{t+1})$; given that the variance of sinking conditional on the property's location is relatively small as is the value of γ , the first-order approximation likely represents a good approximation of the expectation. The second approximation is as if homebuyers expect demand shocks and relative rental demand to follow a random walk.

³³We show robustness to specifications that define $z(j)$ as the borough and seismic zone. There are 16 boroughs and three seismic zones in Mexico City which delineate seismic risk and construction code requirements.

of building characteristics $Z_j \cdot t$ approximates the $\mathbb{E}_t(e_{j\tau}) - e_{jt}$ terms by allowing housing of different types to experience different market trends.³⁴

Identification in estimating (16) requires that the expected amenities and rental demand in the residual be independent of sinking and expected sinking conditional on the controls. Property-level fixed effects break up the strong cross-sectional correlation in both sinking and prices, as can be seen in a map of residualized sinking and prices in Figure 6. We argue that sinking is quasi-randomly assigned conditional on these controls because local forces cannot directly influence localized sinking. Groundwater is almost exclusively pumped outside the city for consumption by all residents, so a neighborhood's sinking rate is a function of lagged groundwater pumping and the local geology's resistance to subsidence at a given groundwater level. Additionally, there is little scope for local conditions to cause sinking, as discussed in the background. While these considerations motivate that shocks to sinking above the building's average rate may be quasi-randomly assigned, we conduct several tests for parallel trends to give more credibility to this approach.

First, we use the microdata from the Income and Expenditure Survey (ENIGH) test for whether future sinking predicts current rents. Rents need not be forward looking, so if they predict future sinking conditional on current sinking that would be evidence that local housing market shocks are correlated with subsidence. Table 1 reports coefficients of the impact of sinking and the present value of future sinking on rents, where the present value of future sinking aggregates observed sinking from the survey wave to 2020 at the location of the respondent and an estimate for sinking beyond 2020. Future sinking has no predictive power for log rents, providing reassurance that property values are not evolving systematically before sinking occurs.

We also test for parallel trends by examining the relationship of the composition of the housing market with subsidence. While our approach directly controls for quality, a correlation of the characteristics of units on the market with subsidence could be an indication

³⁴Our most stringent specification includes linear trends that vary by the borough and type (single family, apartment, etc.), but we show that our results are robust to using subsets of these controls.

that the market is evolving in other unobserved ways that confound our estimates. Figure 7 reports the coefficients and 95% confidence intervals from regressions of the Z-scores of unit amenities on sinking on the property. Sinking is uncorrelated with these amenities, and all point estimates imply a treatment effect less than 0.025 standard deviations in size. For the hedonic index that aggregates all of these, the (insignificant) treatment effect of a meter of subsidence is less than 0.01 standard deviations. These results are reassuring that the housing markets that sinking plots are located in are not becoming systematically lower quality.

Thus far we have found no evidence that housing markets in sinking areas have confounding trends that are correlated with sinking. In Section 5.3.1 we discuss other pre-trends tests and conduct placebo and other robustness exercises, but now proceed with the presentation of our results estimating the costs of subsidence.

5.1.1 Results

Table 2 reports the results of estimating Equation (16). Standard errors are clustered at the census tract. We formulate expectations as both an AR(1) process estimated at the plot level in Columns (1) and (2), and as a “perfect foresight” measure that uses observed sinking on the plot post-transaction in expectations in Columns (3) and (4). Regardless of the manner of specifying expectations or the discount rate chosen, realized sinking has a consistent and negative impact of appraised values, with a meter of sinking causing a 6.1% fall in appraised value. Given that the average property in our sample sank 15.1 centimeters, this implies a 0.9% decrease in values on average.

We cannot detect a role for future sinking in impacting prices in any specification, and in all cases estimate a value of θ that is statistically indistinguishable from zero. However, these estimates will be biased towards zero if we mis-specify the formulation of expectations or if the specification directly absorbs expectations (Dickstein and Morales, 2018). For example, we would expect to estimate estimate $\gamma\theta = 0$ for a home buyer that expects that the sinking

rate is a constant on the plot, since this would be absorbed by our fixed effects. We relax this slightly in Table 3, which shows the results of estimating (16) only for new builds, replacing our property fixed effects with 500-meter grid cell fixed effects. We again find that expected future sinking has no statistically detectable or economically meaningful impact on appraised values in both ways of specifying expectations. However, given that we are limited in our ability to mitigate the attenuation bias that may affect these estimates, we complement these findings with qualitative survey evidence that households struggle to draw accurate inference about future subsidence risk.

5.1.2 Survey evidence on information frictions

Measuring information frictions about environmental hazards is complicated by the fact that residents may have information that they cannot accurately communicate in easily comparable units- for example, a homeowner may know their home has sunk “a lot” and have a strong idea about future sinking, but is not sure about how many centimeters this represents. We address this issue by focusing on the symptoms of information frictions, such as difficulty inferring risk, attention, and surprise, as in the first set of survey results visualized in Figure 3.

Figure 8a plots the share of different responses to the question, “How can you know if a home will have issues with sinking in the future?”, separated by respondents in high and low risk boroughs.³⁵ 21% of respondents say it is impossible to know in advance whether a home will have issues with sinking, and despite the strong spatial correlation in sinking, only 21% report that you can infer risk by knowing the home is in a risky area. Grouping these responses into ex-ante ways of knowing, which do not require that a home be affected yet, such as asking an expert or the risk zone, and ex-post ways of knowing (seeing the effects in the home or plot) in Figure 8b, we find that residents of low sinking boroughs are 47% more likely to report using ex-ante available factors to infer risk. This suggests that residents

³⁵This question was free response, and we prompted respondents for more answers until they indicated they could not come up with any more.

with less information are less likely to locate in high-sinking homes, which would imply an inflated demand for units in high-sinking areas.

We show that this finding together with the results in Figure 3 are robust to controlling for respondent and housing unit characteristics, including the education of the respondent, in Table 4. Furthermore, Table A3 in the Appendix confirms that these effects are even stronger overall when limiting to residents who moved within the last 10 years, assuaging concerns that results are driven by selective recall or habituation.

We implement Falk et al. (2016) instruments for measuring risk preferences and discount rates to test whether these sorting patterns are driven by residents with higher tolerance for risk or higher discount rates locating in high-risk units, a first that we are aware of for the literature on environmental risk and housing markets. We test for whether plot-level sinking intensity is correlated with differences in measured risk aversion and discounting in Appendix Table A4. Discount rates are not correlated with either the sinking on the resident's plot over the last 5 years or the relative altitude change over the last 5 years. We pick up no correlation with plot-level sinking on measured risk aversion, and if anything residents of neighborhoods with highly uneven sinking show higher measured risk aversion, suggesting that our results cannot be explained by residents with high risk tolerance or discount rates buying sinking homes.

Finally, we conduct quantitative tests for information frictions that, while more model-consistent, require that respondents be able to quantify sinking in ways that may be unreasonable. Appendix Figure B4 plots respondents' belief about how much their property has sunk over the last five years to our satellite measure, and find that the slope of this relationship is only 0.05, showing that even in retrospect respondents have little idea about how much their property has sunk in quantitative measures. Appendix Figure B5 grades respondents on a question where we ask them to name boroughs that have had issues with sinking,³⁶ and shows that the median respondent commits substantial Type 1 and Type 2

³⁶We grade respondents on two measures: how many boroughs we consider to be high risk that they name, and how many boroughs they name that we would consider to be high risk. For the former, respondents

errors when trying to name high-risk areas.

Together, these findings suggest that respondents face substantial information frictions about subsidence, and that these frictions are particularly related to the ability to infer the probability of future subsidence absent realized sinking. We also find evidence that residents sort on information about subsidence, with less informed residents being more likely to live in high-sinking properties. These findings echo insights from papers in the United States that find that *realizations* of floods or hurricanes drive discounts of environmental risks in housing prices (Gibson and Mullins, 2020; Bakkensen et al., 2019; Ortega and Taşpinar, 2018), and that less informed residents sort into riskier settings (Bakkensen and Barrage, 2022; Wagner, 2022).³⁷

5.1.3 Mechanisms: How does realized sinking affect homes?

Our findings in Table 2 show that plot-level sinking imposes important losses to home values, but what is driving the losses from realized sinking? Sinking damages structures, but it is possible that homeowners are able to invest in maintenance and other remedies that offset these damages. We explore these mechanisms in Table 5, where we simplify estimation by only including realized subsidence. Column (1) reports the result of estimating our repeat appraisal specification, but replacing the outcome with the appraised years of life remaining for the home.³⁸ This measure captures the appraiser's estimate of the years of inhabitable life left for the structure, and provides an estimate of how degraded or depreciated the physical building is. We find that sinking has a pronounced negative impact on the appraised life remaining of the home: a meter of sinking causes a reduction of 4.1 years of remaining life, and the average home lost 1.1 years of life at the average sinking of 25 centimeters over 10 years compared to a home that experienced no sinking.

may interpret the question with different degrees of severity and name a subset of all high-risk boroughs. For the latter, respondents may be aware of outlier high-sinking cases in otherwise low-risk boroughs.

³⁷Consistent with this idea, we find suggestive evidence that capitalization of future sinking into the price of new builds is higher in boroughs with slower sinking rates on average in Appendix Figure B6.

³⁸Appendix Table A5 reports the result of all specifications for this outcome.

Our survey evidence on the relationship between the physical state of homes and sinking also provides correlational evidence that sinking depreciates structures. Columns (2) through (5) regress indicators for whether a respondent reports different structural issues in their home that could be caused by subsidence on our satellite measure of the total sinking on the survey respondent's home. Column (2) shows that a meter of sinking on the respondent's home increases the probability of reporting severe structural issues by 17% relative to the mean in the low-sinking strata and increases the probability of reporting issues with levelling and cracks in walls by 20% and 28%, respectively.

Do residents invest in maintenance in response to these damages? Table 6 reports the correlation of survey measures of maintenance investments with sinking on the respondent's plot. While we do not find that sinking is associated with intensive margin increases on the probability of incurring maintenance expenses, we do find that a meter of sinking is correlated with a large increase in spending on maintenance by 44% conditional on incurring any spending. Sinking is also associated with an 18.8% fall in the respondent's assessment of when they will have to make their next "large investment" in the home, suggesting that residents are pulling forward investments in the home.³⁹

Finally, we look for evidence that subsidence induces complementary investments in maintenance or home improvement activities that are not related to subsidence, as these could bias our estimates towards zero if they increase the market value of the home. We test for this in the last column of Table 6 by regressing an indicator for the respondent incurring any spending on non-sinking related issues (additions, remodeling, electric work, painting, or waterproofing) on sinking on the home. We find no statistically significant or economically meaningful relationship between sinking and complementary investments, assuaging concerns that these cause us to underestimate the costs of subsidence.

³⁹We find a similar result using spending on maintenance from the income and expenditure survey in Appendix Table A6, though in these data we are only able to detect extensive margin increases in the probability of incurring maintenance costs.

5.1.4 Mechanisms: Uneven sinking across neighborhoods

So far we have focused on the impact of plot-level sinking on home values, but uneven sinking at across neighborhoods also has the potential to reduce the desirability of a property through its impact on public infrastructure. We study this by introducing our measures of the unevenness of sinking over space: the cumulative relative sinking of the grid cell relative to its neighbors, and the standard deviation of sinking, into our main specifications.

Table 7 reports results. Columns (1) and (2) report the result of estimating the repeat appraisal design on plot-level sinking and our measures of uneven sinking: In Column (1) we include the cumulative relative altitude change across 500m grid cells , and Column (2) includes the standard deviation of sinking within the 500m grid cell. Both measures have a negative impact on price, but changes in the relative altitude have a larger effect on values: The average change in relative altitude across grid cells causes a 1% fall in appraised values. The impact of locally uneven sinking, as measured by the standard deviation *within* the grid cell, is much smaller, with the average change in the standard deviation of sinking causing a 0.07% fall in appraised values.

In Columns (3) through (6) we use survey reports of infrastructure issues in the neighborhood to estimate the physical impacts of uneven sinking on the probability that a neighborhood experiences flooding or fissures in pavement or roads. First, notice that plot-level sinking has no significant relationship with the probability of these infrastructure issues, underscoring the intuition from civil engineering studies ([Hu et al., 2013](#)) and the Mexico City government's own qualitative reports ([Secretaría de Gestión Integral de Riesgos y Protección Civil, 2018](#)) that the damages caused by subsidence on macro-infrastructure are driven by uneven sinking across neighborhoods, not just localized sinking.

Column (3) suggests that at the average relative altitude change of 2.8 centimeters of the 500m grid cell a respondent's home is located in is 2.85% more likely to report that their neighborhood has issues with flooding, and the standard deviation of sinking is not predictive of this outcome (Column (4)). Fissures in roads or sidewalks show the opposite

pattern: relative altitude change does not predict fissures, but a one standard deviation increase in the sinking of their grid cell is correlated with a 220% increase in the probability that a respondent reports issues with fissures. These findings suggest that what “type” of sinking matters depends on the infrastructure type one is interested in; while relative altitude change, which measures the change in relative slopes, affects the probability of flooding, it seems that local unevenness, as measured by the standard deviation, is more predictive of fissures in roads.

Summing up We have found that subsidence has large direct costs and that home values do not show evidence of strong capitalization of future risk. For welfare analysis, we set conservative values for our demand parameters, setting the costs of subsidence to $\gamma = -0.06$ and the extent of information frictions $\theta = 0.08$, the highest value estimated from Column (4) of Table 3. In the next section, we leverage the fact that uneven sinking across grid cells decreases demand, using this as an instrument for prices in supply estimation.

5.2 Supply response to subsidence

The supply model highlights the dual role that subsidence plays in the decision to re-develop. While higher expected subsidence should deter develop by lowering the price that developers can get for new builds, realized subsidence lowers the opportunity cost of redeveloping by lowering the value of existing, degraded units, and thus the opportunity cost of demolition. In this section, we estimate the supply elasticity using the responsiveness of re-development to realized sinking and prices.

5.2.1 Reduced-form evidence for model predictions

We begin by testing our model prediction that realized sinking draws in development in two ways. First, we use our matched development-appraisal data to test whether homes that have sunk more are more likely to be sold for redevelopment. Table 8 reports the

results of regressions of an indicator for the appraisal being redeveloped on sinking and a battery of property characteristics, including the age of the building. Strikingly, Columns (2) and (3) show that sinking strongly predicts whether an appraisal is for the purpose of re-development, with a meter of sinking increasing this probability by 0.5 percentage points over a mean probability of 0.89%. Consistent with irregular neighborhood sinking making neighborhoods less attractive, changes in relative altitude decrease the probability of redevelopment conditional on plot-level sinking, though noisily so. Including the appraised price as a control in Column (3) does not change these conclusions.

As an alternative test, we use our panel of pixels to estimate the impact of sinking on the probability of that construction begins on a new development in pixel j in year t . This approach allows for less detailed analysis of the exact characteristics of the unit, but does not require us to rely on accurate identification of transactions that were later redeveloped. Table 9 reports results for varying ways of controlling for time trends, and our most flexible specification in Column (3) implies that a meter of sinking on a pixel from 2007- t increases the probability that construction will begin on a new development in that pixel by 8.2%.

5.2.2 Estimating the supply elasticity

Our supply model given by (9) and (10) provides a way to estimate the supply elasticity using the response of development to subsidence, but we must address the potential endogeneity of cost shocks $\tilde{\xi}_{jt}$ with prices; supply shocks cause movement along the demand curve in equilibrium, biasing estimates that do not take this into account towards zero. We address this using a control function approach; by putting additional structure on the distribution of cost shocks and identifying a demand shifter as an instrument for prices, we derive a control function that absorbs the endogenous part of the error term (Petrin and Train, 2010).⁴⁰ We

⁴⁰Control functions are numerically equivalent to IV estimation in the linear case, and can be extended to non-linear estimation under certain conditions. Appendix G.5 provides a proof of the validity of using a control function in this context (Blundell and Matzkin, 2014).

propose the following first stage equation derived from our demand model:

$$\log(p_{jt}) = \text{PIRel. Altitude Change}_{jt} + \gamma S_{jt} + \alpha_{n(j)} + \alpha_t + X_{jt}\beta_1 + \tilde{u}_{jt} \quad (17)$$

where $\text{Rel. Altitude Change}_{jt}$ is the relative altitude change of the grid cell containing j from 2007 to t , $\alpha_{n(j)}$ are census tract $n(j)$ fixed effects, α_t are year and calendar month fixed effects, and X_{jt} are appraisal controls including age, type, number of bedrooms, and number of bathrooms. We assume that $\tilde{\xi}_{jt}$ is distributed joint normally with log prices, with constant variance σ and marginal expectation $\mathbb{E}(\tilde{\xi}_{jt} | \log(e_{jt})) = CF(\log(e_{jt}); \phi)$ for some parameter ϕ . Then we can re-write our redevelopment condition in (10) by adding and subtracting the control function and adding the controls from the first stage:

$$\begin{aligned} d_{jt} &= 1\left(\frac{1}{\sigma^*} \tilde{V}_{jt}^S \geq 0\right) \\ \frac{1}{\sigma^*} \tilde{V}_{jt}^S &= \frac{\eta}{\sigma^*} \log(p_{jt}) - \frac{\gamma(\eta+1)}{\sigma^*} S_{jt} + \frac{1}{\sigma^*} CF(\log(e_{jt}); \phi) + \alpha_{n(j)} + \alpha_t + X_{jt}\beta_2 + \frac{\tilde{\xi}_{jt}^* - \mu^*}{\sigma^*} \end{aligned} \quad (18)$$

where $\tilde{\xi}_{jt}^* = \tilde{\xi}_{jt}^S - \mathbb{E}(\tilde{\xi}_{jt}^S | \log(e_{jt}))$ is normally distributed with mean μ^* and standard deviation σ^* . Thus this is estimated via Probit, including the control function as a regressor.⁴¹ Because of the assumption of joint normality, the control function is a linear function of the first stage residuals, $CF(\log(e_{jt}); \phi) = \widehat{\phi \log(e)}_{jt}$, and we test robustness to mis-specification by showing robustness to higher order polynomial approximations of this function.

The immediate threat to the identification assumption that uneven grid sinking only affects prices through demand is that grid-level sinking itself induces changes in the costs that builders face when developing a plot. However, structured interviews with civil engineers working for construction firms in Mexico City suggest that correlation of construction costs with realized sinking on either the plot or neighborhood conditions is unlikely; construction

⁴¹We prove that the new error term $\frac{\tilde{\xi}_{jt}^* - \mu^*}{\sigma^*}$ is mean independent of prices in Appendix G.5.

code regulations require that engineers implement soil mechanics tests of the soil conditions of the plot they will build on, but these tests are not designed to predict future subsidence.⁴² To control for soil conditions and other local characteristics, we include census tract and seismic zone by year fixed effects, which absorb average static plot characteristics such as the type of soil and drainage, as well as changing construction code requirements which vary by seismic zone. In Section 5.3.2 we provide empirical evidence that trends in uneven sinking are uncorrelated with other supply trends.

Table 10 reports the results of estimating (18). Confidence intervals are estimated via clustered bootstrap to account for the fact that the control function is estimated from the first stage. Column (1) reports the first stage results from regressing log prices on uneven grid cell sinking and controls. Uneven sinking lowers prices conditional on tract fixed effects and unit-level controls, and with an F-statistic of 10.6 the first stage is sufficiently powered.

Column (2) reports the results of estimating the linear probability model via IV for reference, giving an estimate of 0.40 for the supply elasticity. Probit estimation including the residuals from the first stage as a control function in Column (3) also suggest that redevelopment responds positively to prices and realized sinking as the model predicts. While the magnitude of the coefficients is not interpretable due to the unidentified scale parameter, Equation (10) implies that we can estimate the elasticity as $\eta = \hat{\varepsilon}/(1 - \hat{\varepsilon})$, where $\hat{\varepsilon} = \beta^p/\beta_S \times \gamma$,⁴³ which implies a supply elasticity of 0.28. This estimate is robust to including a more flexible polynomial approximation for the control function in Column (5), which gives an almost identical estimate of the supply elasticity. Comparing these results to the estimates that exclude the control function in Column (6), we see that this function is crucial for addressing bias that drives the estimate of the elasticity towards zero. Our

⁴²The purpose of soil mechanics tests is to ensure that the structure itself does not induce sinking, and thus these report static characteristics according to the geology of the plot. Interviews with civil engineers operating in Mexico City suggest that these tests provide limited information about how much sinking has occurred beyond the static risk implied by the geology, and do not make predictions about how much future sinking will occur unrelated to the structure's impact.

⁴³Confidence intervals are calculated over estimates of ε^S in each bootstrap sample, and in each sample γ_b is drawn from a normal distribution centered around the point estimate with standard deviation equal to the standard error of this estimate.

estimate of a supply elasticity of 0.28 is in line with recent papers that measure within-city housing supply elasticities. Our estimate is near the lower range of the neighborhood-level elasticities estimated by [Baum-Snow and Han \(2024\)](#) for the United States, and corresponds to the maximum of the re-development elasticities estimated by [Rollet \(2025\)](#) for New York City.

5.3 Validation and robustness

5.3.1 Estimates of the cost of subsidence

Our estimates of the costs of subsidence are robust to using subsets of our fixed effects and linear trends. Table [A7](#) in the Appendix reports estimates of the effect of subsidence on appraisal values for different relaxations of these controls, and we estimate similar magnitude effects in all cases. Results are also robust to modeling potential measurement error in subsidence; Figure [B7](#) plots the distribution of p-values from a Monte Carlo simulation that models noise in the calculation of the subsidence rate distributed normal with mean zero and standard deviation of 10 millimeters, a conservative estimate of the measurement error for SAR Interferometry in other settings ([Liu et al., 2020](#); [Bawden et al., 2023](#)), showing that accounting for this uncertainty does not change results.

We next conduct a placebo test by testing for whether the subsidence of a plot's neighboring pixels affects prices. This serves as a test for whether the increased probability that my neighbors are re-developed introduces a confounder, as sinking neighborhoods could experience gentrification induced by new builds. In order to address the fact that we cannot observe the ages of neighboring properties, we run an analogous specification to [\(16\)](#) but in differences, as we can observe the change in sinking for neighbors. Table [A8](#) in the Appendix shows that sinking on neighboring plots is not correlated with housing values, giving confidence that we are measuring the impact of damage to the home itself, not other trends in the neighborhood.

Subsidence and seismic risk are very correlated in the cross section. If housing market

trends related to seismic concerns are evolving in way that is correlated with shocks to subsidence, then our estimates may pick up these trends. To test for this, we estimate Equation (16) excluding years after 2017, as the major earthquake that hit Mexico City in 2017 may have impacted the evolution of the housing market in ways that are correlated with sinking. Table A9 in the Appendix reports results, which if anything are stronger when limiting to the pre-2017 period, reflecting that our estimates pick up changes in sinking, not broad trends associated with the Eastern part of the city.

Our main pre-trends test looked for evidence that future sinking was correlated with rents, but we can also use our price data directly to test if changes in home prices predict changes in sinking. Figure B8 compares the relationship between price changes between appraisals and sinking between the appraisals (blue), and price changes and future sinking (pink). While sinking and price changes over the same period are negatively correlated, there is no significant relationship between lagged price changes and sinking between the next set of appraisals. Comparing coefficients on a regression of these, lagged prices are an insignificant predictor of sinking, and the point estimate on lagged prices is 66% that of the point estimate on contemporaneous sinking.⁴⁴

We verify that results are not driven by mechanical appraiser valuation of subsidence by dropping localities where the median difference between appraised and transaction values in the R04 data is greater than 1%. Table A10 reports results, which are quantitatively and qualitatively very similar to our main estimates.

The significance of our results is robust alternative ways of estimating standard errors. Table A11 reports the results from our different specifications using a 2-kilometer radius for calculating Conley standard errors. Estimates are generally more precise when using Conley standard errors, as differencing within property reduces the strong spatial correlation in outcomes.

⁴⁴Note that if home buyers use past sinking as a signal of future sinking even conditional on the home's location, then this test would not be model-consistent as forward-looking home buyers should incorporate their expectation of future sinking into prices today.

Finally, we test for whether changes in appraised values are driven by mortgage penalties on sinking homes. If banks charge higher interest rates on homes that are prone to sinking, then the changes in values we estimate may represent discounts that the market offers to offset these rates. Table A12 in the Appendix estimates the cross-sectional correlation of the sinking intensity of the census tract with the interest rate charged on mortgages on that tract using the R04 data, finding no evidence that banks assign differential interest rates to high sinking areas.

5.3.2 Supply estimation

We test for whether new developments in sinking areas are systematically different from developments in non-sinking areas. In particular, developers may adapt to sinking by building at lower heights or with different amenities, choices which could affect costs directly. Tables A13 and A14 in the Appendix show that we cannot reject that developments in sinking areas are built with similar heights and amenities as those in other areas; in terms of observables, developments seem to be similar regardless of past and future sinking.

Identification in our supply estimation requires that redevelopment trend similarly in areas with high versus low plot-level sinking and uneven versus uneven neighborhood sinking. We test for this by comparing trends in pixel-level development between high- and low-sinking intensity pixels. Intuitively, we compare trends between pixels that were never sinking quickly and pixels that started sinking quickly later in the panel. To do this, we classify a pixel as “high sinking” using a cut-off based on the distribution of sinking rates in 2020 (median, Q75), and classify a pixel as “treated” starting in the first year that the sinking rate in that pixel is at least the cut-off rate. Figure B9 shows the results of the Sun and Abraham (2021) estimates, which exclude always fast-sinking pixels. Not-yet-sinking pixels were trending similarly to never-sinking pixels before sinking accelerated. In fact, it is only after pixels start showing higher rates of sinking that high-sinking pixels show increased probability of development compared to never-sinking pixels.

6 The costs of subsidence and policy implications

We estimate the costs of subsidence by calculating the difference in welfare between the observed equilibrium and a counterfactual equilibrium in which all future sinking is set to zero ($\mathbb{E}_t(s_{j\tau}) = 0 \forall j, \tau > t$). We also conduct two alternative policy experiments to study the benefits of disclosure laws that reveal the true expected value of future subsidence to property managers. The first is the gains from implementing disclosure laws without addressing subsidence, which we model as a counterfactual in which sinking is unchanged but $\theta = 1$. Second, we estimate how costly subsidence would be in an environment of rational expectations by comparing a counterfactual equilibrium with $\theta = 1$ but sinking is as in baseline to one in which $\theta = 1$ and future sinking is zero.⁴⁵

6.1 The costs of subsidence

Figure 9 depicts the change in welfare between the counterfactuals we consider, expressed in billions of 2018 USD. The leftmost red bar depicts the welfare benefits from setting all expected future sinking to zero relative to the observed equilibrium, which gives an estimate of the total costs of subsidence. Sinking is very costly, leading to \$33 billion USD in economic loss, which annualized represents about 1% of Mexico City’s GDP. Almost all of these costs are borne by property managers, who lose out on lower-than-expected rents; these losses represent the “bad investment” losses that home owners make by over-paying for sinking homes that degrade faster than they expected. Subsidence also costs the developer, but only slightly: Expected future sinking depresses the value of the housing stock and therefore their profits, but this has a muted impact when information frictions preclude capitalization of these gains. Renters enjoy small gains as well, as the higher housing stock in the city lowers rents.

Next we consider a counterfactual in which sinking continues but there are no information

⁴⁵ Appendix Table A15 summarizes the parameters needed to calculate welfare and how each is estimated or calibrated, and details on how we find counterfactual equilibria are available in Appendix G.6.

frictions ($\theta = 1$). This creates a gain of \$18.2 billion USD, which represents 55% of the gains from completely eliminating subsidence. With no information frictions, property managers gain as they go from making negative profits to zero profits. Housing developers lose out in the no information frictions counterfactual relative to baseline, reflecting the downward adjustment in the inefficiently high housing stock that they benefited from under information frictions. Renters dislike the higher rents they pay when housing supply falls.

Finally, we can compare the total costs of subsidence (red bar) to what the costs of subsidence would be in a counterfactual with no information frictions, which is represented by the yellow rightmost bar. We see in this comparison that property managers are indifferent to the change in subsidence, as they make zero profit in both scenarios. The developer gains from the mitigation of subsidence, as they benefit from the increased value of the housing they build. With $\eta < 1$, this direct effect is augmented by the overall higher housing stock supplied in the no-sinking equilibrium.

It is also of note that policies that mitigate subsidence and policies that mitigate information frictions create very different set of winners and losers over space. We show in Figures B10 and B11 in the Appendix that mitigating subsidence leads to housing value gains for incumbent property managers in sinking areas and increases in density, whereas mitigating information frictions alone leads to price depreciation in sinking areas.

These estimates provide a measure of the total cost of subsidence at current levels; in order to price groundwater pumping as the externality-generating action, we must convert this to dollars per unit of water pumped. We do this using calibrated hydro-physical relationships between aquifer storage and subsidence in the Mexico City Valley; Appendix H provides details. Taking our total cost estimate together with the elevation-to-pumped volume conversion implies that subsidence costs the city \$0.89 per cubic meter pumped. Comparing this tax to the water tariffs Mexico City residents pay in Table 11, which are heavily subsidized for most residents, this amounts to an 52-293% increase over the average

marginal rate paid by residents, and would add 32-299% to the average total bill.⁴⁶ Such increases are likely politically infeasible, and we study other cost-effective policy options in the next section.

6.2 Cost-benefit of other recharge policies

If significantly increasing water tariffs is not possible, are there other cost-effective options for abating subsidence? We explore the potential cost-effectiveness of three policies that have been implemented at some point in Mexico City that would permit offsetting groundwater pumping: investment in wastewater recycling plants, building wastewater injection sites to artificially recharge the aquifer, and repairing leaks in the water delivery infrastructure that cause over 35% of urban water supply to be lost in transport ([SACMEX, 2012](#)).⁴⁷ These analyses should be taken as suggestive; while policy interest and previous investments in each of these options over the last 30 years in Mexico City provide some idea of potential costs ([SACMEX, 2012](#)), current and accurate cost data for these types of investments would improve these estimates. Detailed documentation of the assumptions made and cost sources for each of these are available in Appendix H.1.

Table 12 reports the results of these analyses. While wastewater recycling has the potential to offset the largest volume of water, the cost of building and operating these facilities means they are the least cost-effective option, and this is driven primarily by our estimate of how expensive it is to treat grey water. Wastewater injection, on the other hand, saves the least amount of water, but its benefits dramatically outweigh the costs. For these calculations, we assume that wells evenly affect subsidence across the city, but if wells are built near areas that are subsiding quickly then the imperfect connectivity of the aquifer

⁴⁶We assume that 60% of the water bill is taxed, the average share of water in Mexico City that comes from groundwater extraction.

⁴⁷We assume that all leaks are repaired on surface water sources *before* entering the basin, so that all water diverted from leaks would not have otherwise contributed to aquifer recharge. This is an important assumption, as [CONAGUA \(2024\)](#) estimate that most groundwater recharge on the Mexico Valley aquifer comes from water infrastructure leaks, so the groundwater impacts of repairing leaks within the city are unclear.

means that this would have a larger local impact on subsidence, potentially increasing the gains even further. Finally, leaks repair comes in as the cheapest (and least capital intensive) option, and benefits outweigh costs by 49%.

7 Conclusion

In summary, we conduct a comprehensive valuation of the costs of subsidence in Mexico City, finding that subsidence induces over 34 billion USD in costs in Mexico City. These losses are driven by accelerated depreciation of sinking homes, which experience loss of useful life and increased structural risk and cracks. Neighborhood impacts from uneven sinking over space also play an important role in lowering home values, as neighborhoods see significantly more flooding in response to uneven subsidence relative to surrounding areas. Despite these costs and how high-profile subsidence is in the city, we show that new homes do not fully capitalize the future costs of subsidence, and that these frictions amplify the total costs of this groundwater externality.

Importantly, our estimates exclude city-wide costs that are shared among residents. For example, while our estimates capture private housing market losses from increased probability of flooding, they do not capture expenditures incurred by the city government to repair water main breaks or sinkholes or replace macro-infrastructure as the main sewer line servicing the Mexico City that had to be replaced when subsidence altered the slope beyond repair ([SACMEX, 2012](#)). While these costs should be included for a full cost analysis, our estimates likely capture the largest part of the costs of subsidence, as our estimates are orders of magnitude larger than the costs of the entire budget of the water utility (\$528 million USD in 2024), the cost of the Cutzamala surface water system (\$33 million USD in 2021), or the cost of the recent drainage system replacement (\$65 million USD).

Our framework provides a general way of thinking about re-development in places that experience evolving environmental hazards such as climate impacts, erosion, or sea level

rise. Our model highlights the different economic role that *realizations* of environmental hazards play in driving re-development, as compared to expected *future* hazards that must be capitalized correctly into home values in order for the aggregate amount of housing in harm's way to be efficient. We find that information frictions that affect the capitalization of future environmental hazards, which have been found to be widespread in different contexts, can exacerbate the costs of these types of externalities by over-supplying housing in risky areas.

References

- Bagheri-Gavkosh, M., Hosseini, S.M., Ataei-Ashtiani, B., Sohani, Y., Ebrahimian, H., Morovat, F., Ashrafi, S., 2021. Land subsidence: A global challenge. *Science of The Total Environment* 778. doi:[10.1016/j.scitotenv.2021.146193](https://doi.org/10.1016/j.scitotenv.2021.146193).
- Bakkensen, L.A., Barrage, L., 2022. Going Underwater? Flood Risk Belief Heterogeneity and Coastal Home Price Dynamics. *The Review of Financial Studies* 35, 3666–3709. doi:<https://doi.org/10.1093/rfs/hhab122>.
- Bakkensen, L.A., Ding, X., Ma, L., 2019. Flood Risk and Salience: New Evidence from the Sunshine State. *Southern Economic Journal* 85, 1132–1158. doi:<https://doi.org/10.1002/soej.12327>.
- Balboni, C., 2025. In Harm's Way? Infrastructure Investments and the Persistence of Coastal Cities. *American Economic Review* 115. doi:[0.1257/aer.20191943](https://doi.org/10.1257/aer.20191943).
- Baum-Snow, N., Han, L., 2024. The Microgeography of Housing Supply. *Journal of Political Economy* 132. doi:<https://doi.org/10.1086/728110>.
- Bawden, G., Snead, M., Stork, S., Galloway, D., 2023. Measuring Human-Induced Land Subsidence from Space. Technical Report. USGS. URL: <https://pubs.usgs.gov/fs/fs06903/pdf/fs06903.pdf>.
- Bayer, P., Ferreira, F., McMillan, R., 2007. A Unified Framework for Measuring Preferences for Schools and Neighborhoods. *Journal of Political Economy* 115, 588–638. doi:[10.1086/522381](https://doi.org/10.1086/522381).
- Benetton, M., Emiliozzi, S., Guglielminetti, E., Loberto, M., Mistretta, A., 2023. Does climate change adaptation matter? Evidence from the City on the Water. mimeo URL: https://papers.ssrn.com/sol3/papers.cfm?abstract_id=4313434.
- Bishop, K.C., Murphy, A.D., 2019. Valuing Time-Varying Attributes Using the Hedonic Model: When Is a Dynamic Approach Necessary? *The Review of Economics and Statistics* 101, 134–145. doi:[10.1162/rest_a_00722](https://doi.org/10.1162/rest_a_00722).
- Blundell, R., Matzkin, R., 2014. Control functions in non-separable simultaneous equations models. *Quantitative Economics* 5, 271–295. doi:<http://dx.doi.org/10.3982/QE281>.
- Borchers, J., Carpenter, M., 2014. Land Subsidence from Groundwater Use in California. Technical Report. California Water Foundation. URL: https://cawaterlibrary.net/wp-content/uploads/2017/04/1397858208-SUBSIDENCEFULLREPORT_FINAL.pdf.
- Cabral-Cano, E., Dixon, T.H., Miralles-Wilhelm, F., Díaz-Molina, O., Sánchez-Zamora, O., Carande, R.E., 2008. Space geodetic imaging of rapid ground subsidence in Mexico City. *GSA Bulletin* 120, 1556–1566. doi:[10.1130/B26001.1](https://doi.org/10.1130/B26001.1).
- Carleton, T., Crews, L., Nath, I., 2024. Is the world running out of fresh water? *AEA Papers and Proceedings* 114, 31–35. URL: https://www.levicrews.com/files/p-wateruse_pp-paper.pdf, doi:[10.1257/pandp.20241008](https://doi.org/10.1257/pandp.20241008).

- Chaussard, E., Havazli, E., Fattahi, H., Cabral-Cano, E., Solano-Rojas, D., 2021. Over a Century of Sinking in Mexico City: No Hope for Significant Elevation and Storage Capacity Recovery. *Journal of Geophysical Research: Solid Earth* 126. doi:[10.1029/2020JB020648](https://doi.org/10.1029/2020JB020648).
- Cigna, F., Tapete, D., 2021. Present-day land subsidence rates, surface faulting hazard and risk in Mexico City with 2014–2020 Sentinel-1 IW InSAR. *Remote Sensing of Environment* 253, 112161. doi:[10.1016/j.rse.2020.112161](https://doi.org/10.1016/j.rse.2020.112161).
- CONAGUA, 2009. Situación del Subsector de Agua Potable, Alcantarillado y Saneamiento. Technical Report. CONAGUA. URL: <http://www.conagua.gob.mx/CONAGUA07/Publicaciones/Publicaciones/LibroAnexosYTablas-Situaci%C3%B3nSAPAS.pdf>.
- CONAGUA, 2024. Actualización de la Disponibilidad Media Anual de Agua en el Acuífero Zona Metropolitana de la Ciudad de México. Technical Report. Subdirección General Técnica, Gerencia de Aguas Subterráneas, CONAGUA. Ciudad de México. URL: https://sigagis.conagua.gob.mx/gas1/Edos_Acuiferos_18/cmdx/DR_0901.pdf.
- DellaVigna, S., 2018. Structural Behavioral Economics. *Handbook of Behavioral Economics: Applications and Foundations* 1 1, 613–723.
- Desmet, K., Kopp, R.E., Kulp, S.A., Nagy, D.K., Oppenheimer, M., Rossi-Hansberg, E., Strauss, B.H., 2021. Evaluating the Economic Cost of Coastal Flooding. *American Economic Journal: Macroeconomics* 13, 444–486. doi:[10.1257/mac.20180366](https://doi.org/10.1257/mac.20180366).
- Dickstein, M., Morales, E., 2018. What do exporters know? *The Quarterly Journal of Economics* 133, 1753–1801.
- Dranove, D., Jin, G.Z., 2010. Quality disclosure and certification: Theory and practice. *Journal of Economic Literature* 48, 935–63. URL: <https://www.aeaweb.org/articles?id=10.1257/jel.48.4.935>, doi:[10.1257/jel.48.4.935](https://doi.org/10.1257/jel.48.4.935).
- Falk, A., Becker, A., Dohmen, T., Huffman, D., Sunde, U., 2016. The Preference Survey Module: A Validated Instrument for Measuring Risk, Time, and Social Preferences. IZA Discussion Paper No. 9674 URL: <https://ssrn.com/abstract=2725035>.
- Fattahi, H., Simons, M., Agram, P., 2017. Insar Time-Series Estimation of the Ionospheric Phase Delay: An Extension of the Split Range-Spectrum Technique. *IEEE Transactions on Geoscience and Remote Sensing* 55, 5984–5996. doi:[10.1109/TGRS.2017.2718566](https://doi.org/10.1109/TGRS.2017.2718566).
- Fernández-Torres, E., Cabral-Cano, E., Solano-Rojas, D., Havazli, E., Salazar-Tlaczani, L., 2020. Land subsidence risk maps and InSAR based angular distortion structural vulnerability assessment: an example in Mexico City. *Proceedings of the International Association of Hydrological Sciences* 382, 583–587. doi:[10.5194/piahs-382-583-2020](https://doi.org/10.5194/piahs-382-583-2020).
- Fernández-Torres, E., Cabral-Cano, E., Salazar-Tlaczani, L.e.a., 2025. Economic risk of differential subsidence in Mexico City (2014–2022). *Nat Hazards* 121, 2507–2534. doi:<https://doi.org/10.1007/s11069-024-06891-9>.

- Fowler, L.C., 1981. Economic Consequences of Land Surface Subsidence. *Journal of the Irrigation and Drainage Division* 107, 151–159. doi:[10.1061/JRCEA4.0001344](https://doi.org/10.1061/JRCEA4.0001344).
- Frondel, M., Gerster, A., Vance, C., 2020. The power of mandatory quality disclosure: Evidence from the german housing market. *Journal of the Association of Environmental and Resource Economists* 7, 181–208. doi:[10.1086/705786](https://doi.org/10.1086/705786).
- Gallagher, J., 2014. Learning about an Infrequent Event: Evidence from Flood Insurance Take-Up in the United States. *American Economic Journal: Applied Economics* 6, 206–233. doi:[10.1257/app.6.3.206](https://doi.org/10.1257/app.6.3.206).
- Gambolati, G., Teatini, P., 2021. Land Subsidence and its Mitigation. *The Groundwater Project*.
- Gechter, M., Tsivanidis, N., 2025. Spatial spillovers from High-Rise Developments: Evidence from Mumbai Mills. mimeo .
- Gibson, M., Mullins, J.T., 2020. Climate Risk and Beliefs in New York Floodplains. *Journal of the Association of Environmental and Resource Economists* 7, 1069–1111. doi:[10.1086/710240](https://doi.org/10.1086/710240).
- Gobierno de la Ciudad de México, 2020. Agua para todos: Programa integral para mejorar la distribución y abastecimiento de agua potable. Technical Report. Informe de Gobierno. URL: [#rehabilitaci%C3%B3n-de-pozos](https://informadegobierno.cdmx.gob.mx/acciones/agua-para-todos-programa-integral-para-mejorar-la-distribucion-y-abastecimiento-de-agua-%C3%B3n-de-pozos).
- Gobierno del Distrito Federal, 2007. Programa de Manejo Sustentable del Agua para la Ciudad de México. Technical Report. SEGUIAGUA. URL: http://centro.paot.org.mx/documentos/paot/CD/ProgAgua_CDMX.pdf.
- Gonzalez-Navarro, M., Quintana-Domeque, C., 2016. Paving Streets for the Poor: Experimental Analysis of Infrastructure Effects. *The Review of Economics and Statistics* 98, 254–267. doi:[10.1162/REST_a_00553](https://doi.org/10.1162/REST_a_00553).
- Gourevitch, J.D., Kousky, C., Liao, Y.P., Nolte, C., Pollack, A.B., Porter, J.R., Weill, J.A., 2023. Unpriced climate risk and the potential consequences of overvaluation in US housing markets. *Nature Climate Change* 13, 250–257. doi:[10.1038/s41558-023-01594-8](https://doi.org/10.1038/s41558-023-01594-8).
- Hino, M., Burke, M., 2021. The effect of information about climate risk on property values. *Proceedings of the National Academy of Sciences* 118. doi:[10.1073/pnas.2003374118](https://doi.org/10.1073/pnas.2003374118).
- Hsiang, S., Kopp, R., Jina, A., Rising, J., Delgado, M., Mohan, S., Rasmussen, D.J., Muir-Wood, R., Wilson, P., Oppenheimer, M., Larsen, K., Houser, T., 2017. Estimating economic damage from climate change in the United States. *Science* 356, 1362–1369. doi:[10.1126/science.aal4369](https://doi.org/10.1126/science.aal4369).
- Hsiao, A., 2023. Sea Level Rise and Urban Adaptation in Jakarta. mimeo URL: https://allanhhsiao.com/files/Hsiao_jakarta.pdf.

Hu, B., Zhou, J., Xu, S., Chen, Z., Wang, J., Wang, D., Wang, L., Guo, J., Meng, W., 2013. Assessment of hazards and economic losses induced by land subsidence in Tianjin Binhai new area from 2011 to 2020 based on scenario analysis. *Natural Hazards* 66, 873–886. doi:[10.1007/s11069-012-0530-9](https://doi.org/10.1007/s11069-012-0530-9).

Ingeniería, C., 2021. ¿Sabes cuál es el costo de tratar las aguas residuales de tu colonia o vivienda? URL: <https://blog.cbr-ingenieria.com.mx/conoces-cu%C3%A1l-es-el-costo-de-tratar-las-aguas-residuales-de-tu-colonia-o-vivienda-imaginaste-no-hacerlo>.

Laibson, D., 1997. Golden Eggs and Hyperbolic Discounting. *Quarterly Journal of Economics* 112, 443–477.

Liu, L., Yu, J., Chen, B., Wang, Y., 2020. Urban subsidence monitoring by sbas-insar technique with multi-platform sar images: a case study of beijing plain, china. *European Journal of Remote Sensing* 53, 141–153. doi:[10.1080/22797254.2020.1728582](https://doi.org/10.1080/22797254.2020.1728582).

Liu, Z., Liu, P.W., Massoud, E., Farr, T.G., Lundgren, P., Famiglietti, J.S., 2019. Monitoring Groundwater Change in California's Central Valley Using Sentinel-1 and GRACE Observations. *Geosciences* 9, 436. doi:[10.3390/geosciences9100436](https://doi.org/10.3390/geosciences9100436). number: 10 Publisher: Multidisciplinary Digital Publishing Institute.

Lixin, Y., Jie, W., Chuanqing, S., Guo, J.W., Yanxiang, J., Liu, B., 2010. Land Subsidence Disaster Survey and Its Economic Loss Assessment in Tianjin, China. *Natural Hazards Review* 11, 35–41. doi:[10.1061/\(ASCE\)1527-6988\(2010\)11:1\(35\)](https://doi.org/10.1061/(ASCE)1527-6988(2010)11:1(35)).

Mahya, M., Kok, S., Cado van der Lelij, A., 2021. Economic assessment of subsidence in Semarang and Demak, Indonesia. Technical Report. Wetlands International. URL: <https://www.wetlands.org/publications/a-roadmap-to-address-land-subsidence-for-central-java/>.

Nanda, A., Ross, S.L., 2012. The Impact of Property Condition Disclosure Laws on Housing Prices: Evidence from an Event Study Using Propensity Scores. *The Journal of Real Estate Finance and Economics* 45, 88–109. URL: <https://doi.org/10.1007/s11146-009-9206-y>, doi:[10.1007/s11146-009-9206-y](https://doi.org/10.1007/s11146-009-9206-y).

Nicholls, R.J., Lincke, D., Hinkel, J., Brown, S., Vafeidis, A.T., Meyssignac, B., Hanson, S.E., Merkens, J.L., Fang, J., 2021. A global analysis of subsidence, relative sea-level change and coastal flood exposure. *Nature Climate Change* 11, 338–342. doi:[10.1038/s41558-021-00993-z](https://doi.org/10.1038/s41558-021-00993-z).

Novelo-Casanova, D., Suárez, G., Cabral-Cano, E., Fernández-Torres, E., Fuentes-Mariles, O., Havazli, E., Jaimes, M.A., López-Espinoza, E., Martin-Del Pozzo, A.L., Morales-Barrera, W., Morales-Rodríguez, H., Nieto-Torres, A., Rodríguez-Elizarrarás, S., Solano-Rojas, D., Velasco-Herrera, V., 2022. The Risk Atlas of Mexico City, Mexico: a tool for decision-making and disaster prevention. *Natural Hazards* 111, 411–437. doi:[10.1007/s11069-021-05059-z](https://doi.org/10.1007/s11069-021-05059-z).

- Ortega, F., Penaranda, F., Taspinar, S., 2025. When the Water Recedes and Home Prices Don't: Flood Risk Learning and Neighborhood Spillovers. mimeo .
- Ortega, F., Taspinar, S., 2018. Rising sea levels and sinking property values: Hurricane Sandy and New York's housing market. *Journal of Urban Economics* 106, 81–100. doi:<https://doi.org/10.1016/j.jue.2018.06.005>.
- Ospital, A., 2024. Urban Policy and Spatial Exposure to Environmental Risk. mimeo .
- Ostriker, A., Russo, A., 2023. The Effects of Floodplain Regulation on Housing Markets. mimeo URL: https://ostriker.github.io/papers/Ostriker-Russo_floodplain-regulations.pdf.
- Parsons, T., Wu, P.C., Wei, M.M., D'Hondt, S., 2023. The Weight of New York City: Possible Contributions to Subsidence From Anthropogenic Sources. *Earth's Future* 11. doi:<https://doi.org/10.1029/2022EF003465>.
- Peter, H., Jäggi, A., Fernández-Sánchez, J., Escobar, D., 2017. Sentinel-1A - First precise orbit determination results. *Advances in Space Research* 60. doi:[10.1016/j.asr.2017.05.034](https://doi.org/10.1016/j.asr.2017.05.034).
- Petkov, I., Ortega, F., 2025. Learning from experience: Flooding and insurance take-up in the flood zone and its periphery. *Journal of Risk and Insurance* 92, 212–356. doi:<https://doi.org/10.1111/jori.70002>.
- Petrin, A., Train, K., 2010. A Control Function Approach to Endogeneity in Consumer Choice Models. *Journal of Marketing Research* 47, 3–13. URL: <http://www.jstor.org/stable/20618950>.
- Press, A., 2022. Indonesia's capital is rapidly sinking into the sea. NPR URL: <https://www.npr.org/2022/01/26/1075720551/jakarta-indonesia-sinking-into-java-sea-new-capital>.
- Rodella, A.S., Zaveri, E., Bertone, F. (Eds.), 2023. The Hidden Wealth of Nations: The Economics of Groundwater in Times of Climate Change. World Bank. URL: <http://hdl.handle.net/10986/39917>. license: CC BY 3.0 IGO.
- Rodríguez Zamora, C., 2010. Estimation of a semi-parametric hazard model for Mexico's new housing market. *Bank for International Settlements Proceedings of the Fifth IFC Conference*, 587–599. URL: <https://www.bis.org/ifc/ifcb34ap.pdf>.
- Rollet, V., 2025. Can We Rebuild a City? The Dynamics of Urban Redevelopment. Unpublished .
- Rosen, S., 1974. Hedonic Prices and Implicit Markets: Product Differentiation in Pure Competition. *Journal of Political Economy* 82, 34–55. URL: <http://www.jstor.org/stable/1830899>. publisher: University of Chicago Press.

SACMEX, 2012. El Gran Reto del Agua en la Ciudad de México: Pasado, presente y prospectivas de solución para una de las ciudades más complejas del mundo. Mexico City.

Secretaría de Gestión Integral de Riesgos y Protección Civil, 2018. Causas y Consecuencias de la subsidencia en los cuadrantes Dos (Zona Poniente), Tres y Cuatro de la Zona Cero de la Ciudad de México, Anexo A. Technical Report. Secretaría de Gestión Integral de Riesgos y Protección Civil. Ciudad de México. URL: <https://www.atlas.cdmx.gob.mx/datospdf.html>.

Sinha, K., 2022. Fracking Disclosure, Collateral Value, and the Mortgage Market. *The Accounting Review* 97, 427–454. URL: <https://doi.org/10.2308/TAR-2020-0119>, doi:[10.2308/TAR-2020-0119](https://doi.org/10.2308/TAR-2020-0119).

Solano-Rojas, D., Cabral-Cano, E., Hernandez-Espriu, A., Wdowinski, S., 2015. The relationship of InSAR-GPS land subsidence and the groundwater level decrease in wells of the Mexico City Metropolitan Area. *Boletín de la Sociedad Geológica Mexicana* 67, 273–283. doi:[10.18268/bsgm2015v67n2a10](https://doi.org/10.18268/bsgm2015v67n2a10).

Sun, L., Abraham, S., 2021. Estimating dynamic treatment effects in event studies with heterogeneous treatment effects. *Journal of Econometrics* 225, 175–199. doi:[10.1016/j.jeconom.2020.09.006](https://doi.org/10.1016/j.jeconom.2020.09.006).

Wagner, K.R.H., 2022. Adaptation and Adverse Selection in Markets for Natural Disaster Insurance. *American Economic Journal: Economic Policy* 14, 380–421. doi:[10.1257/pol.20200378](https://doi.org/10.1257/pol.20200378).

Werner, A.D., Zhang, Q., Xue, L., Smerdon, B.D., Li, X., Zhu, X., Yu, L., Li, L., 2013. An Initial Inventory and Indexation of Groundwater Mega-Depletion Cases. *Water Resources Management* 27, 507–533. doi:[10.1007/s11269-012-0199-6](https://doi.org/10.1007/s11269-012-0199-6).

Willemse, W., Kok, S., Kuik, O., 2020. The effect of land subsidence on real estate values. *International Association of Hydrological Sciences* 382, 703–707. doi:<https://doi.org/10.5194/piahs-382-703-2020>.

Wu, Y.Y., Madson, A., 2024. Error Sources of Interferometric Synthetic Aperture Radar Satellites. *Remote sensing* 16. doi:<https://doi.org/10.3390/rs16020354>.

Yoo, J., Perrings, C., 2017. An externality of groundwater depletion: land subsidence and residential property prices in Phoenix, Arizona. *Journal of Environmental Economics and Policy* 6, 121–133. doi:[10.1080/21606544.2016.1226198](https://doi.org/10.1080/21606544.2016.1226198).

Yu, C., Li, Z., Penna, N., 2018a. Interferometric synthetic aperture radar atmospheric correction using a GPS-based iterative tropospheric decomposition model. *Remote Sensing of Environment* 204, 109–121.

Yu, C., Li, Z., Penna, N., Crippa, P., 2018b. Generic atmospheric correction model for Interferometric Synthetic Aperture Radar observations. *Journal of Geophysical Research: Solid Earth* 123, 9202–9222.

Yu, C., Penna, N., Li, Z., 2017. Generation of real-time mode high-resolution water vapor fields from GPS observations. *Journal of Geophysical Research: Atmospheres* 122, 2008–2025.

Yunjun, Z., Fattah, H., Amelung, F., 2019. Small baseline InSAR time series analysis: Unwrapping error correction and noise reduction. *Computers & Geosciences* 133.

A Tables

Table 1: Effect of future sinking on rents

<i>log Rent</i>	(1)	(2)	(3)	(4)
NPV future sinking (m)	-0.002 (0.008)	-0.011 (0.008)	-0.011 (0.008)	-0.013 (0.010)
N	702	702	702	702
Hedonic controls	X	X	X	X
Type x Borough FEs	X	X	X	X
Year FEs	X			
Year x Borough FEs		X	X	X
Locality FEs			X	X
N. bedrooms x age trends				X

* p < 0.1, ** p < 0.05, *** p < 0.01

Notes: The outcome in every column is the log rents. All regressions include controls for log household income, an indicator for having a solid roof, and property-level sinking from the time of construction to the year of observation. Standard errors clustered at the census tract.

Table 2: Impact of plot sinking on appraisal values

	AR(1)		Perfect foresight	
	3%	6%	3%	6%
Property-level sinking (m)	-0.06052*** (0.01968)	-0.06049*** (0.01968)	-0.06075*** (0.01992)	-0.06045*** (0.02001)
NPV future sinking	0.00009 (0.00095)	0.00061 (0.00386)	-0.00009 (0.00076)	0.00012 (0.00238)
Observations	129,424	129,424	129,424	129,424
θ	-0.002	-0.01	0.001	-0.002
SE	(0.016)	(0.064)	(0.012)	(0.039)
ATE: plot sinking	-0.92%	-0.92%	-0.92%	-0.92%
Mean sinking between observ. (m)	0.151	0.151	0.151	0.151
Property FEs	X	X	X	X
Age FEs	X	X	X	X
Zone x year FEs	X	X	X	X
Borough x age trends	X	X	X	X
N. bedrooms x age trends	X	X	X	X

* p < 0.1, ** p < 0.05, *** p < 0.01

Notes: The outcome in all regressions is the log appraised value of the home. All estimates include property, age, and seismic zone by year fixed effects, and include linear time trends by borough and the number of bedrooms. Estimation limited to properties with more than one appraisal. Standard errors clustered at the census tract. The Average Treatment Effect (ATE) is calculated by multiplying the reported coefficient by the average sinking between observations in meters.

Table 3: Price response to expected future sinking, new builds

	(1)	(2)	(3)	(4)
AR(1) expectations				
NPV future sinking	-0.006 (0.005)	-0.006 (0.005)	-0.004 (0.005)	-0.005 (0.004)
Observations	102,909	102,909	102,806	102,857
θ	0.100	0.100	0.066	0.083
Mean NPV future sinking	12.003	12.003	12.006	12.004
ATE: Future sinking	-7.43%	-6.92%	-4.59%	-5.89%
Grid cell FEs	X	X	X	X
Year FEs	X			
Year x Seismic Zone FEs		X	X	X
Hedonic controls			X	
Time trends by hedonic chars.				
Perfect foresight				
NPV future sinking	-0.008 (0.005)	-0.007 (0.005)	-0.004 (0.004)	-0.004 (0.004)
Observations	102,909	102,909	102,806	102,857
θ	0.133	0.117	0.067	0.067
Mean NPV future sinking	13.167	13.167	13.17	13.168
ATE: Future sinking	-10.28%	-9.07%	-5.38%	-5.09%
Grid cell FEs	X	X	X	X
Year FEs	X			
Year x Seismic Zone FEs		X	X	X
Hedonic controls			X	
Time trends by hedonic chars.				X

* p < 0.1, ** p < 0.05, *** p < 0.01

Notes: The outcome in all regressions is the log appraised value. Regressions limited to new builds. Standard errors clustered at the census tract. The Average Treatment Effect (ATE) is calculated by multiplying the reported coefficient by the average net present value of future sinking in meters assuming a 6% discount rate. “Ar(1) expectations” calculate the net present value as a function of the rate of sinking; “Perfect foresight” uses the observed sinking post sale through 2020, and then uses a fixed projected rate for subsequent years. Estimates of θ assume $\gamma = -0.060$.

Table 4: Survey evidence on sorting and attention to sinking

	Surprised by severity	Ex-post factors used	Ex-ante factors used
Sinking in last 5 years (m)	0.287* (0.145)	-0.020 (0.150)	-0.171* (0.101)
N	794	800	800
Mean Y (low sinking)	0.254	0.493	0.451
Strata FEs	X	X	X
Borough FEs	X	X	X
Education FEs	X	X	X
Respondent age FEs	X	X	X
Respondent gender FEs	X	X	X

* p <0.1, ** p <0.05, *** p <0.01

Notes: Outcomes in order of appearance are an indicator for using any ex-post factors (seeing effects in the home or neighborhoods) to infer future probability of having issues due to sinking, an indicator for using any ex-ante factors (asking an expert, asking around, the news, the risk zone, examining construction quality), and an indicator for reporting having considered sinking when they moved in. “Sinking in last 5 years” is the total property-level sinking over the last 5 years in meters. All specifications include survey strata, borough, respondent age, respondent gender, and respondent educational attainment fixed effects. All regressions weighted by sampling weights. Standard errors clustered at the census tract.

Table 5: Survey evidence: Sinking and structural issues

		Does your home have any issues with...?				
		Useful life remaining	Structural issues	Levelling issues	Cracks: Hallways	Cracks: Walls
		(1)	(2)	(3)	(4)	(5)
Sinking (m)		-4.408*** (1.643)	0.100*** (0.036)	0.053* (0.030)	0.033 (0.031)	0.078** (0.037)
Data source	Repeat appraisals		Survey	Survey	Survey	Survey
Observations	129,475		800	800	800	800
Mean Y	63.310		0.59	0.26	0.20	0.28

Notes: Standard errors clustered at the census tract. Column (1) regresses the appraised years of life remaining on total sinking on the property, controlling for property, age, and zone by year of appraisal fixed effects and time trends by borough, number of bedrooms, and type. These estimates exclude properties with only one appraisal. In Columns (2) through (5), all outcomes are indicators for reporting the stated issue in their home and the regressor is the total sinking on the property in meters from the year of construction (or 2007, whichever is later) to 2025. Columns (2) through (5) include survey strata, borough, respondent age, respondent gender, and respondent educational attainment fixed effects and are weighted by sampling weights.

Table 6: Survey evidence: Sinking and maintenance expenditure

	Any spending	log Spending (MXN)	log Years until next big investment	Any spending on non-sinking related issues
Total sinking on home (m)	0.002 (0.044)	0.443** (0.175)	-0.188** (0.089)	-0.004 (0.034)
N	625	359	616	623
Mean Y (low sinking)	0.578	9,152.879	6.707	0.301

* p <0.1, ** p <0.05, *** p <0.01

Notes: Standard errors clustered at the census tract. Outcomes in order of appearance are: An indicator for any spending on maintenance; log total spending on maintenance over the last 6 months; the log of respondent's estimated time in years to the next large investment in the home; and an indicator for the household mentioning any non-sinking category of response: electric work, remodeling, painting interiors or exteriors, additions, water-proofing, or replacing windows. "Total sinking on home" is the total subsidence on the property in meters from the year of construction (or 2007, whichever is later) to date. All specifications include survey strata, borough, respondent age, respondent gender, and respondent educational attainment fixed effects. All regressions weighted by sampling weights.

Table 7: Neighborhood sinking impacts home values and damages public infrastructure

	log appraised value		Reports issues with flooding		Reports issues with fissures	
	(1)	(2)	(3)	(4)	(5)	(6)
Property-level sinking (m)	-0.046** (0.020)	-0.055*** (0.020)	-0.026 (0.121)	-0.015 (0.116)	-0.005 (0.170)	-0.158 (0.132)
Abs. relative altitude change (m)	-0.161*** (0.059)		0.630*** (0.194)		-0.309 (0.513)	
SD of sinking within 500m (m)		-0.119** (0.048)		1.296 (2.995)		0.578** (2.265)
Data source	Repeat transactions		Survey		Survey	
Observations	129,427	16,438	800	800	800	800
Mean Y	0.112	0.112	0.620	0.620	0.621	0.621
Mean Sinking measure	0.151	0.151	0.263	0.263	0.263	0.263
Mean Unevenness measure	0.063	0.006	0.028	0.005	0.028	0.005

* p < 0.1, ** p < 0.05, *** p < 0.01

Notes: Standard errors clustered at the census tract. Columns (1) and (2) regress the log appraised value on sinking on the property and the cumulative change in relative altitude (Column (1)) and the standard deviation of sinking within the 500m grid cell (Column (2)). Both columns include property, age, and zone by year of appraisal fixed effects and time trends by borough, number of bedrooms, and type, and exclude properties with only one appraisal. Columns (3) through (6) regress an indicator for the household reporting that their neighborhood has issues with the infrastructure problem in the header on total sinking on the property since it was built and the cumulative relative altitude change since 2007 in Columns (3) and (5), and the average standard deviation of sinking from 2007-2020 in Columns (4) and (6). Columns (3) through (6) include strata, borough, education, respondent age, and gender fixed effects, and regressions are weighted by sample weights.

Table 8: Impact of sinking on the probability of re-development

	(1)	(2)	(3)
Sinking on the property (m)	0.0267*** (0.0040)	0.0053* (0.0030)	0.0052* (0.0029)
Relative altitude (m)	-0.0240* (0.0133)	-0.0181 (0.0124)	-0.0182 (0.0124)
log Price			-0.0005 (0.0017)
N	309,596	308,132	307,859
Mean Y	0.0091	0.0089	0.0089
Adj. R2	0.069	0.079	0.079
Census tract FEs	X	X	X
Borough x year FEs	X	X	X
Hedonic controls		X	X

* p < 0.1, ** p < 0.05, *** p < 0.01

Notes: The outcome in all regressions is an indicator for the appraisal being associated with a new development within 5 years of the appraisal. Specifications with hedonic controls include fixed effects for the type (apartment, single family, etc.) and amenity classification (economical to luxury), square footage, number of bedrooms, number of bathrooms, number of parking spaces, age, plot size, built area, and number of floors. Standard errors clustered at the census tract.

Table 9: Impact of sinking on the probability of new development

	Pr. development on the Pixel		
	(1)	(2)	(3)
Pixel-level sinking (m)	0.00049*** (0.00016)	0.00067* (0.00036)	0.00041*** (0.00015)
Observations	1,500,497	1,500,497	1,500,497
Mean Y	0.005	0.005	0.005
Mean sinking (m)	0.34	0.34	0.34
Pixel FEs	X	X	X
Year FEs	X		
Zone x Year FEs		X	
Borough x year FEs			X

* p < 0.1, ** p < 0.05, *** p < 0.01

Notes: The outcome in all regressions is an indicator for construction beginning on a new development in the pixel-year. All specification include pixel fixed effects; (1) includes year fixed effects, (2) includes year by seismic zone fixed effects, and (3) includes borough by year fixed effects. Standard errors clustered at the census tract.

Table 10: Supply elasticity estimates

	First stage (1)	IV (2)	Probit (3)	Probit, AME (4)	Probit, Flexible CF (5)	Probit, no CF (6)
Relative altitude change (m)	-0.006 [-0.009, -0.002]					
log Price		0.403 [-0.074, 1.398]	5.935 [0.101, 24.653]	0.273 [0.002, 1.106]	5.952 [0.217, 24.719]	0.010 [-0.148, 0.215]
Property-level sinking (m)	-0.121 [-0.164, -0.084]	0.091 [0.026, 0.255]	1.654 [0.705, 4.867]	0.076 [0.031, 0.228]	1.660 [0.720, 4.887]	0.895 [0.347, 1.805]
u			-5.927 [-24.660, 0.016]	-0.272 [-1.107, 0.000]	-6.068 [-24.949, -0.304]	
u^2					-0.237 [-0.818, 0.122]	
u^3					0.295 [-0.046, 0.608]	
Share redeveloped	0.027	0.027	0.027	0.027	0.027	0.027
Observations	101,888	101,888	101,888	101,888	101,888	101,888
Tract FEs	X	X	X	X	X	X
Year FEs	X	X	X	X	X	X
Calendar month FEs	X	X	X	X	X	X
Type FEs	X	X	X	X	X	X
Amenity FEs	X	X	X	X	X	X
Bed, bath, age controls	X	X	X	X	X	X
F stat (KPR)	10.563					
Estimated elasticity		0.403 [-0.074, 1.398]	0.281 [0.005, 0.873]	0.273 [0.002, 1.106]	0.281 [0.014, 0.873]	0.001 [-0.017, 0.019]
95% CI						

Notes: The outcome in Column (1) is the log transaction price; the outcome in Columns (2)-(6) is an indicator for the plot being redeveloped. Brackets under each estimate report the 95% confidence interval. Standard errors clustered at the census tract in the first stage and linear probability model; confidence intervals calculated from bootstrapped sampling of census tracts in Columns (3)-(6), with 1,000 bootstrap samples drawn of 235 census tracts sampled in each. All estimates control for age, age^2 , the number of bedrooms, the number of bathrooms, and fixed effects for the census tract, year, month of transaction, type (apartment, single family, etc.), and amenity classification (economy, semi-luxury, or luxury). Average marginal effects calculated over the sample with each observation assigned the relevant estimated fixed effects.

Table 11: Pigouvian tax on groundwater pumping and water consumption, rates

	Very low income	Low income	Middle income	Unsubsidized
Share of HHs	0.243	0.42	0.113	0.225
Avg. consumption (m ³)	23.35	29.427	27.294	35.098
Avg. marginal rate	\$0.303	\$0.574	\$1.167	\$1.691
Average bi-monthly bill	\$4.175	\$13.154	\$22.106	\$59.34
Tax as % of marginal rate	292.81%	154.44%	75.98%	52.44%
Tax as % of bill	297.56%	119.03%	65.69%	31.47%

Notes: Rates from the 2024 schedule. Average consumption estimated from city block averages reported in 2019. All monetary values converted to 2018 USD using a 19 MXN/USD exchange rate, and deflating 2024 prices to 2018. “Marginal rates” refer to the marginal price of water at average city block consumption per household.

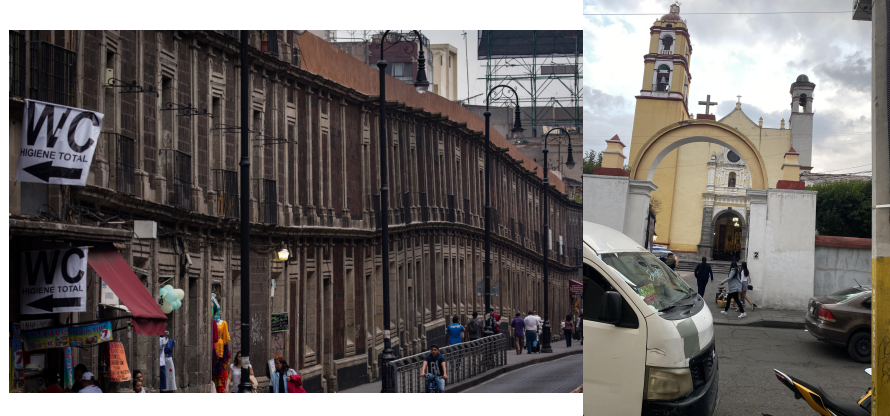
Table 12: Cost-benefit analysis

	Wastewater recycling	Wastewater injection	Repairing leaks
Total water saved (hm ³ /year)	1261.44	22.08	25.55
NPV of benefits, annualized	\$263.5	\$4.89	\$22.65
NPV of costs, annualized	\$3039.84	\$0.28	\$15.2
Benefit-cost ratio	0.09	17.27	1.49

Notes: Monetary values expressed in millions of 2018 USD. 6% discounting rate used.

B Figures

Figure 1: Structures affected by subsidence in Mexico City



(a) Building distorted by uneven sinking in one side in Texcoco, downtown Mexico City

(b) Church sinking to



(c) Building whose foundation is exposed on one side as pavement sinks unevenly around it, downtown Mexico City



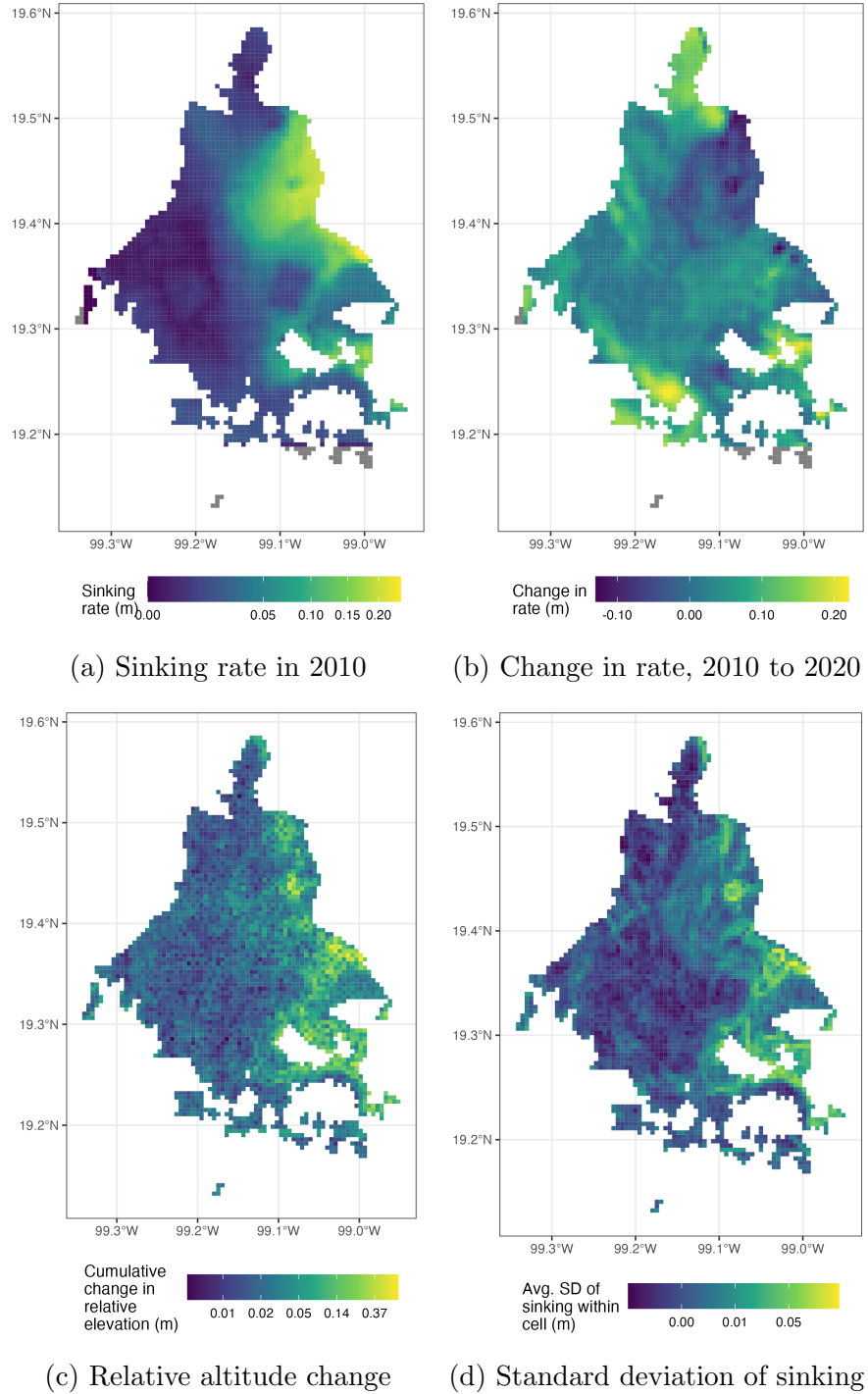
(d) Sinkhole, Coyoacán



(e) Wall tilting into sidewalk, Venustiano Carranza

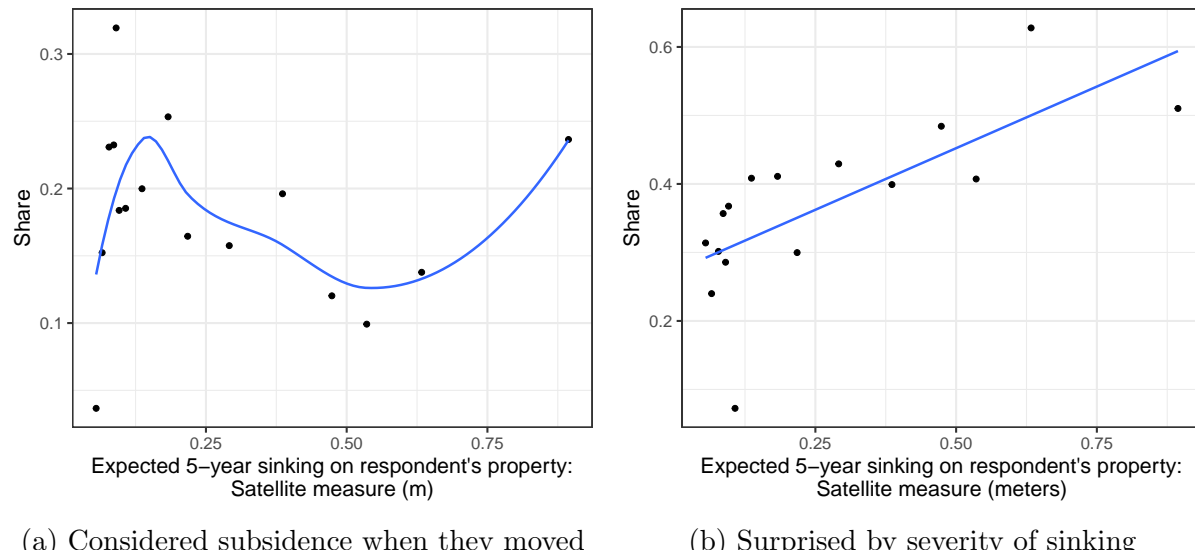
Notes: Subfigure (a) is from the New York Times, article “Mexico City, Parched and Sinking, Faces a Water Crisis”. Sub figure (b) is author’s photograph from Texcoco, a city in the greater Mexico City metropolitan area located on the former lake bed. Subfigure (c) is author’s photograph from the historic center of Mexico City. Subfigures (d) and (e) are from the Mexico City government’s Subsidence Atlas ([Secretaría de Gestión Integral de Riesgos y Protección Civil, 2018](#)).

Figure 2: Subsidence rates in Mexico City



Notes: Map extent limited to grid cells with positive population within the state of Mexico City. Cells in grey do not have data in 2010. Panel (a) plots the sinking rate at the pixel level in 2010. Panel (b) plots the change in the sinking rate from 2010 to 2020. Panel (c) plots the total cumulative relative elevation change from 2007 to 2020. Panel (d) plots the average standard deviation of sinking, which averages the cross sectional standard deviation across years.

Figure 3: Sinking against attention and surprise

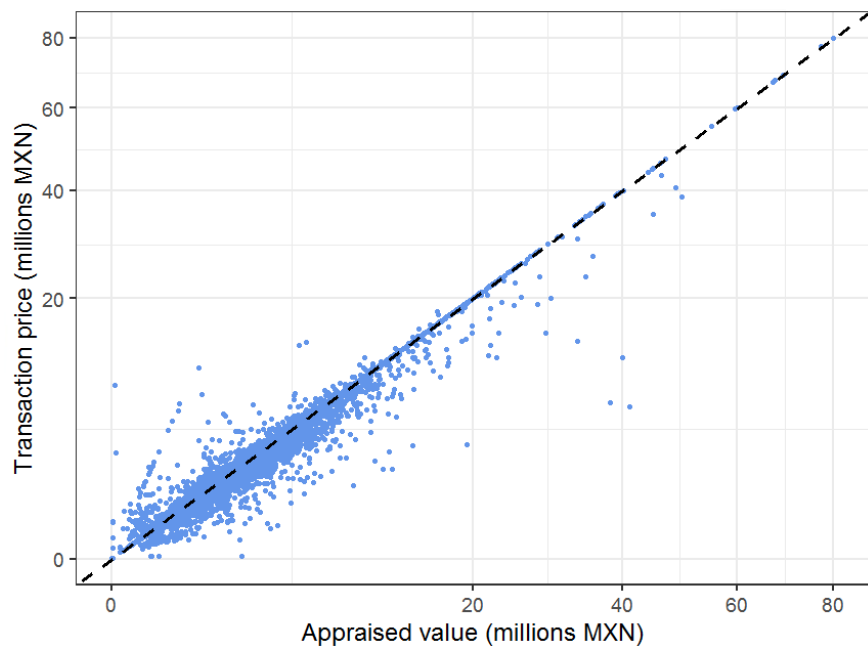


Notes: Each plot calculates the average outcome within 16 quantile bins of expected 5-year plot-level sinking, estimated as $5\bar{s}_j$ where \bar{s}_j is the average sinking rate on the plot. Panel (a) plots the average of an indicator for the respondent reporting they considered subsidence when deciding where to live. Panel (b) plots the average of an indicator for the respondent reporting that the issues related to subsidence have been more severe than they anticipated. Linear line of best fit plotted in Panel (a); non-linear relationship in (b) approximated with Loess regression.

Figure 4: Market clearing

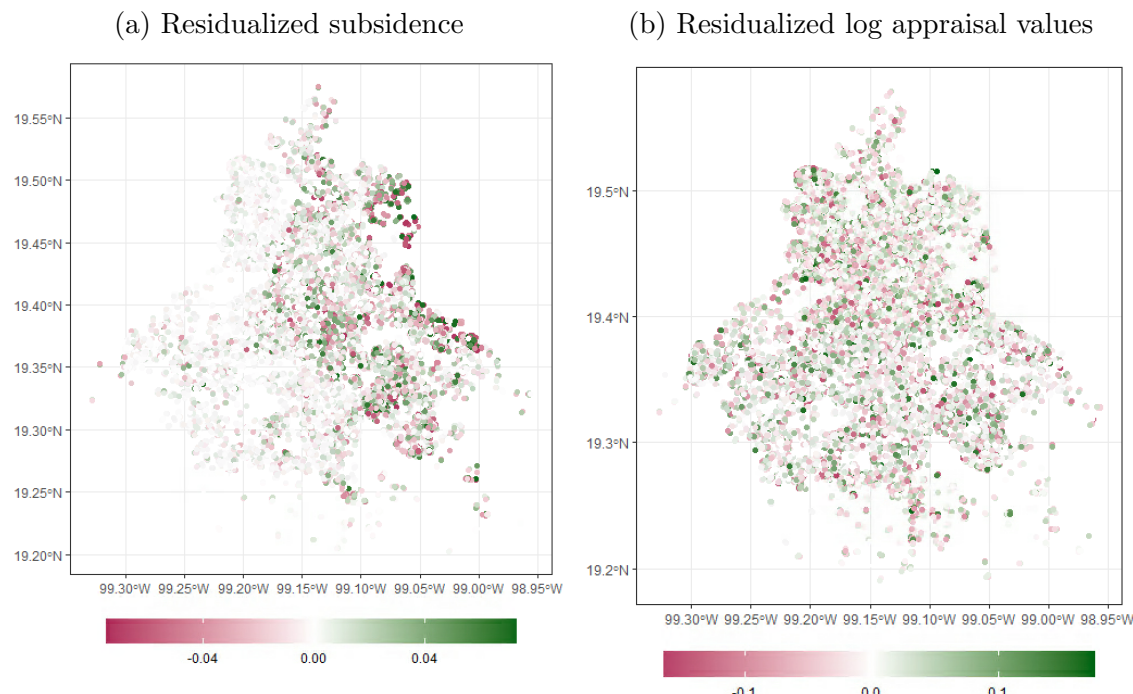


Figure 5: Appraisals and transaction prices



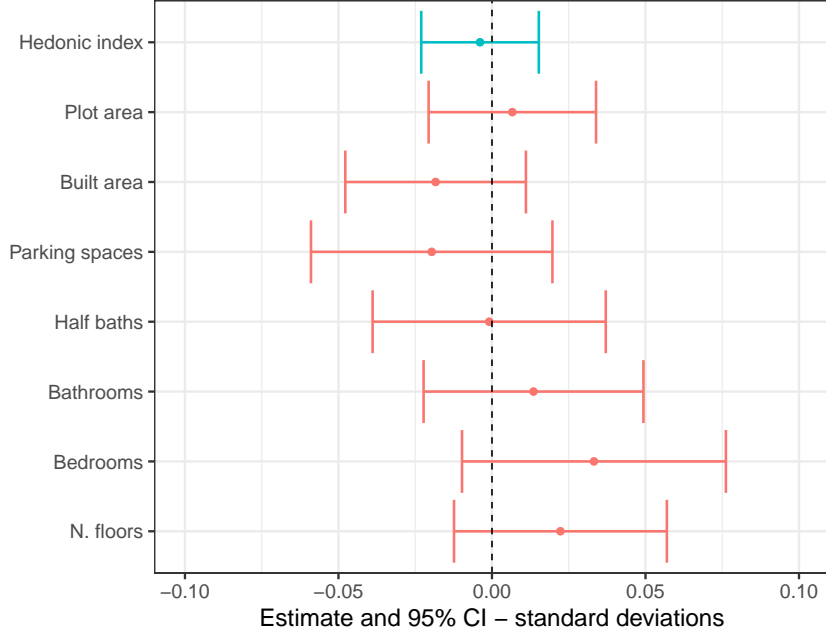
Notes: Each point represents an appraisal-transaction price pair from the mortgage data; a random sample of 50,000 pairs was drawn from the full sample of 5,645,851. The dashed line is the 45° line. The slope and adjusted R^2 reported are from a regression of the transaction price on the appraised value with no intercept.

Figure 6: Residualized prices and sinking



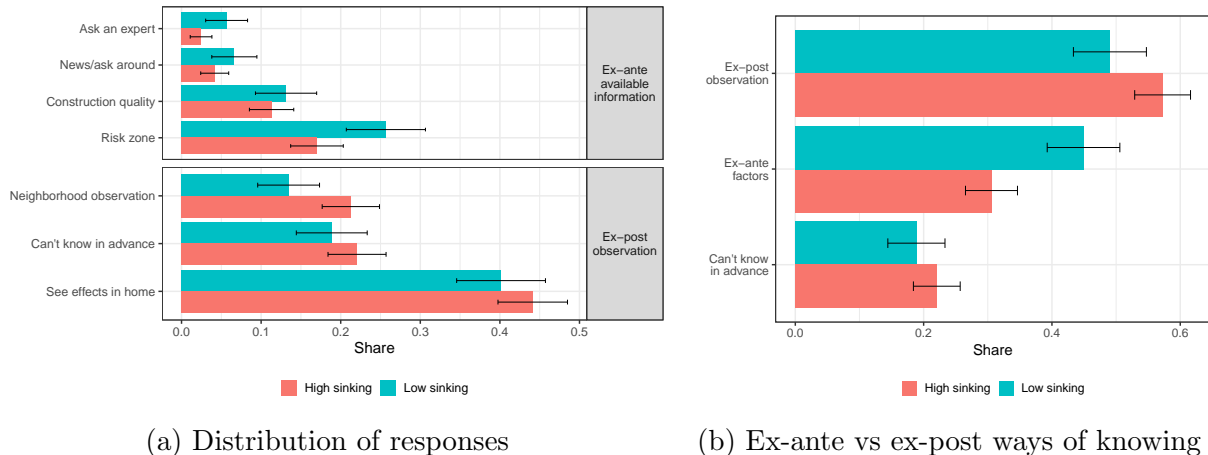
Notes: Each point plots the residual from a regression of the outcome on transaction, age, year of appraisal by zone fixed effects and linear trends by the number of bedrooms and borough. Residuals censored at the 1% and 99% percentiles and pseudo-log transformation applied to color scheme for visual clarity. Points jittered by a factor of 0.002 (maximum displacement of approximately 222 meters) to facilitate visualization of multiple points per property.

Figure 7: Pre-trends test: Subsidence and market composition



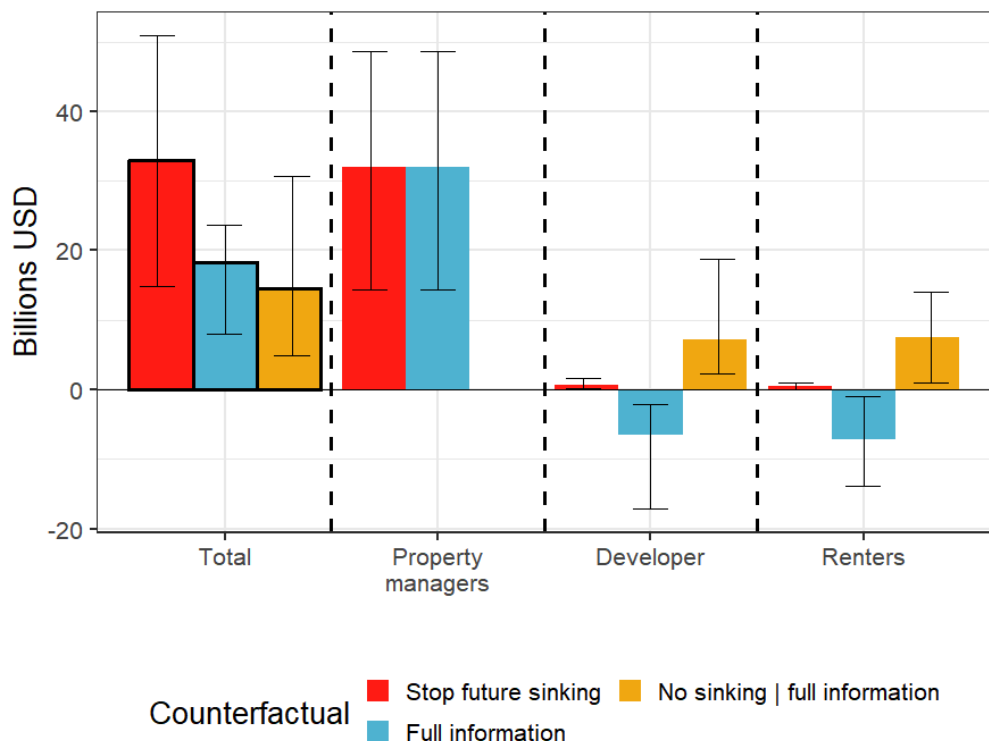
Notes: Plots coefficients and 95% confidence intervals for separate regressions of the outcome on sinking to date on the property in meters. The hedonic index is the simple average of the Z-score of plot area, built area, parking spaces, half baths, bathrooms and bedrooms. All outcomes are standardized by the mean and standard deviation of the variable. Each regression mimics the main specification as closely as possible, replacing the outcome with the attribute listed in the y axis on plot-level sinking, 500 meter grid fixed effects, vintage by year of sale fixed effects, and linear trends by borough and seismic zone. Standard errors clustered at the census tract.

Figure 8: How can you know if a home will have issues with subsidence in the future?



Notes: Each bar plots the average of an indicator for the respondent mentioning a way of knowing that a house will have future issues with sinking in that category, weighted by the population weights and separated by the high-sinking and low-sinking strata. Black bars represent the 95% confidence interval around the mean. The right figure groups ex-ante and ex-post mechanisms and reports the mean for each.

Figure 9: Welfare benefits of counterfactual policies



Notes: Each bar height represents the change in surplus by market participant for the counterfactual minus a baseline equilibrium, expressed in terms of billions of 2018 US dollars. “Stop future sinking” sets $\mathbb{E}(s_{j\tau}) = 0 \forall j, \tau > t$ and compares to the observed equilibrium. “Full information” sets $\theta = 1$ and keeps observed sinking, relative to the observed equilibrium. “No sinking | full information” shows the benefits of a counterfactual with $\theta = 1$ and $\mathbb{E}(s_{j\tau}) = 0 \forall j, \tau > t$ relative to a counterfactual with observed sinking but $\theta = 1$. Error bars mark the 5th to the 95th percentile range of estimates from 1,000 samples γ and η from normal distributions centered around their point estimates with standard deviation given by the standard error of the estimate.

C Table Appendix

Table A1: Appraised values and transaction prices

	Price	Price	% deviation	% deviation
Intercept		0.049*** (0.008)	0.041*** (0.005)	
Appraised value	0.967*** (0.004)	0.958*** (0.003)		
Sinking intensity (m)			0.006 (0.007)	0.007 (0.007)
Observations	5,645,851	5,645,851	5,645,851	5,645,851
Mean Y	2.048	2.048	0.044	0.044
Adj. R2	0.528	0.528	0	0.007
Loan controls				X

* p < 0.1, ** p < 0.05, *** p < 0.01

Notes: The outcome in Columns (1) and (2) is the transaction price in millions of pesos. The explanatory variable in (1) and (2) is the appraised value in millions of pesos. The outcome in Column (3) is the percent deviation in appraised values from transaction values, $|p_{transac} - p_{appraised}|/p_{transac}$. The explanatory variable in Column (3) is average total sinking in the locality from 2007 to 2020. Standard errors in all specifications are clustered at the locality.

Table A2: Repeat sales sample compared to the full appraisal sample

	(1)	(2)	(3)	Mean Y
Single-family home	-0.166*** (0.007)	-0.151*** (0.007)	-0.067*** (0.004)	0.196
Apartment	0.171*** (0.007)	0.155*** (0.007)	0.070*** (0.004)	0.794
Empty lot	-0.001 (0.000)	-0.000 (0.000)	0.001 (0.000)	0.004
Communal property	-0.002*** (0.001)	-0.003*** (0.001)	-0.002*** (0.000)	0.004
Medium class	-0.005 (0.013)	-0.014 (0.011)	-0.015** (0.007)	0.622
Plus class	-0.047*** (0.009)	-0.017*** (0.006)	-0.000 (0.003)	0.171
Luxury class	-0.020*** (0.002)	-0.013*** (0.002)	-0.002 (0.001)	0.035
Age	-5.518*** (0.283)	-5.196*** (0.264)	-2.191*** (0.164)	12.931
Plot size (sq. m)	122.636 (76.546)	150.028*** (47.630)	40.917 (32.436)	523.763
Construction size (sq. m)	-35.146*** (1.344)	-28.396*** (1.353)	-12.113*** (0.645)	97.059
N. floors	-0.237*** (0.033)	-0.199*** (0.034)	-0.205*** (0.043)	1.832
N. bedrooms	-0.241*** (0.012)	-0.212*** (0.011)	-0.096*** (0.008)	2.353
N. bathrooms	-0.309*** (0.019)	-0.219*** (0.015)	-0.077*** (0.008)	1.644
N. parking	-0.210*** (0.021)	-0.136*** (0.018)	-0.041*** (0.010)	1.129
Price (millions MXN)	-0.766*** (0.049)	-0.555*** (0.044)	-0.171*** (0.015)	2.224
Sinking to date (m)	-0.004 (0.011)	-0.038*** (0.009)	-0.014*** (0.004)	0.181
Rel. altitude (m)	0.193 (0.180)	0.130 (0.155)	-0.048 (0.071)	0.338
N. observations	322538	322538	322538	322538
Borough x Year FEs		X	X	
Census tract FEs			X	

* p < 0.1, ** p < 0.05, *** p < 0.01

Notes: Each row is the coefficient of a separate regression where the outcome is listed in the row label and the explanatory variable is an indicator for being included in the repeat sales sample. All regressions include an intercept and cluster standard errors at the census tract level. The last column reports the overall mean of the outcome in each row.

Table A3: Survey evidence for information frictions: Limiting to respondents who have moved in the last 10 years

	Surprised by severity	Ex-post factors used	Ex-ante factors used
Sinking in last 5 years (m)	0.213*** (0.000)	1.863*** (0.000)	-1.144*** (0.000)
N	61	61	61
Mean Y (low sinking)	0.262	0.45	0.368
Strata FEs	X	X	X
Borough FEs	X	X	X
Education FEs	X	X	X
Respondent age FEs	X	X	X
Respondent gender FEs	X	X	X

* p <0.1, ** p <0.05, *** p <0.01

Notes: Data limited to respondents who report moving to their current unit within the last 10 years. Outcomes in order of appearance are an indicator for using any ex-post factors (seeing effects in the home or neighborhoods) to infer future probability of having issues due to sinking, an indicator for using any ex-ante factors (asking an expert, asking around, the news, the risk zone, examining construction quality), and an indicator for reporting that sinking has been more severe than they anticipated. “Sinking in last 5 years (m)” is the total subsidence on the property over the last 5 years. All specifications include survey strata, borough, respondent age, respondent gender, and respondent educational attainment fixed effects. All regressions weighted by sampling weights. Standard errors clustered at the census tract.

Table A4: Subsidence and sorting on risk, discounting preferences

	Discounting		Risk aversion	
	(1)	(2)	(3)	(4)
Sinking in last 5 years (m)	-0.208 (0.450)		0.163 (0.309)	
Relative altitude change in last 5 years (m)		1.504 (0.944)		1.253* (0.682)
N	396	396	362	362
Mean Y (low sinking)	0.671	0.671	0.624	0.624
Strata FEs	X	X	X	X
Borough FEs	X	X	X	X
Education FEs	X	X	X	X
Respondent age FEs	X	X	X	X
Respondent gender FEs	X	X	X	X

* p <0.1, ** p <0.05, *** p <0.01

Notes: Outcomes in order of appearance are the implied discount rate and risk aversion coefficient measured by Falk instruments. Respondents had a random 50% change on being asked the discounting or risk aversion questions, with 400 being surveyed on each each. “Sinking in last 5 years (m)” is the total subsidence on the property over the last 5 years. All specifications include survey strata, borough, respondent age, respondent gender, and respondent educational attainment fixed effects. All regressions weighted by sampling weights. Standard errors clustered at the census tract.

Table A5: Impact of plot sinking on appraised useful life remaining

	(1)	(2)	(3)	(4)
Property-level sinking (m)	-3.23374*** (1.14822)	-4.83280*** (1.48152)	-4.10111** (1.66468)	-4.40771*** (1.64326)
Observations	129,475	129,475	129,475	129,475
ATE: plot sinking	-48.81%	-72.95%	-61.91%	-66.54%
Mean sinking between observ. (m)	0.151	0.151	0.151	0.151
Property FEs	X	X	X	X
Year FEs	X	X	X	X
Age FEs	X	X	X	X
Zone x year FEs		X	X	X
Borough x age trends			X	X
N. bedrooms x age trends				X

* p < 0.1, ** p < 0.05, *** p < 0.01

Notes: The outcome in all regressions is the appraised useful years of life remaining. All estimates include property, age, and year of appraisal fixed effects. Estimation limited to properties with more than one appraisal. Standard errors clustered at the census tract. The Average Treatment Effect (ATE) is calculated by multiplying the reported coefficient by the average sinking between observations in meters.

Table A6: Impact of plot sinking on maintenance expenditures

	(1)	(2)	(3)	(4)
Property-level sinking (m)	0.016 (0.012)	0.023** (0.010)	0.022** (0.010)	0.023** (0.010)
log HH income	0.062*** (0.012)	0.063*** (0.012)	0.063*** (0.012)	0.062*** (0.012)
N	5,607	5,607	5,607	5,607
Mean dept. variable	0.117	0.117	0.117	0.117
Age bin FEs	X	X	X	X
Type x Borough FEs	X	X	X	X
N. room FEs	X	X	X	X
N. bedroom FEs	X	X	X	X
Year FEs	X			
Year x Borough FEs		X	X	X
Locality FEs			X	X
N. bedroom x age trends				X

* p < 0.1, ** p < 0.05, *** p < 0.01

Notes: The outcome in all regressions is an indicator for incurring any maintenance spending. Standard errors clustered at the locality. All regressions include controls for log household income and an indicator for having a solid roof.

Table A7: Impact of sinking is stable across specifications

	(1)	(2)	(3)	(4)
Property-level sinking (m)	-0.099*** (0.014)	-0.095*** (0.015)	-0.061*** (0.020)	-0.060*** (0.020)
Observations	129,431	129,431	129,431	129,427
ATE: plot sinking	-1.49%	-1.44%	-0.92%	-0.92%
Mean sinking between observ. (m)	0.151	0.151	0.151	0.151
Property FEs	X	X	X	X
Year FEs	X	X	X	X
Age FEs	X	X	X	X
Zone x year FEs		X	X	X
Borough x age trends			X	X
N. bedrooms x age trends				X

* p < 0.1, ** p < 0.05, *** p < 0.01

Notes: Standard errors clustered at the census tract. The outcome in all columns is the log appraised value. All estimates include property, age, and year fixed effects. Estimation limited to properties with more than one appraisal. The Average Treatment Effect (ATE) is calculated by multiplying the reported coefficient by the average subsidence between observations in meters.

Table A8: Impact of sinking on neighboring pixels on appraisal values

	(1)	(2)	(3)	(4)
Property-level sinking (m)	-0.08965*** (0.01582)	-0.09683*** (0.01887)	-0.06815*** (0.01977)	-0.06175*** (0.02008)
Sinking on neighboring properties (m)	0.00541 (0.00364)	-0.00221 (0.00502)	0.00052 (0.00482)	0.00139 (0.00482)
Observations	16,438	16,438	16,437	16,437
Mean sinking between observ. (m)	0.034	0.034	0.034	0.034
Start year x end year FEs	X			
Zone x start year x end year FEs		X	X	X
Borough x age trends			X	X
N. bedrooms x age trends				X
Binned floor space x age trends				X

* p < 0.1, ** p < 0.05, *** p < 0.01

Notes: Standard errors clustered at the census tract. The outcome in every column is the change in log appraised value. All estimates difference between subsequent appraisals in the same property. “Start year x End year FEs” are fixed effects by year of appraisal by year of last appraisal, which control for the change in age between appraisals.

Table A9: Repeat appraisals results: Pre-2017 earthquake

	(1)	(2)	(3)	(4)
Property-level sinking (m)	-0.115*** (0.027)	-0.113*** (0.02847)	-0.084*** (0.032)	-0.083** (0.032)
Observations	78,453	78,453	78,453	78,453
ATE: plot sinking	-1.28%	-1.26%	-0.94%	-0.92%
Mean sinking between observ. (m)	0.112	0.112	0.112	0.112
Property FEs	X	X	X	X
Year FEs	X	X	X	X
Age FEs	X	X	X	X
Zone x year FEs		X	X	X
Borough x age trends			X	X
N. bedrooms x age trends				X

* p < 0.1, ** p < 0.05, *** p < 0.01

Notes: Standard errors clustered at the census tract. The outcome in every column is the log appraised value. All estimates include property, age, and year fixed effects. Estimation limited to properties with more than one appraisal. The Average Treatment Effect (ATE) is calculated by multiplying the reported coefficient by the average subsidence between observations in meters. Limited to appraisals for transactions before 2017.

Table A10: Repeat appraisals, Excluding localities with large differences between appraisals and transaction prices

	(1)	(2)	(3)	(4)
Property-level sinking (m)	-0.099*** (0.014)	-0.095*** (0.015)	-0.061*** (0.020)	-0.061*** (0.020)
Observations	129,228	129,228	129,228	129,224
ATE: plot sinking	-1.49%	-1.44%	-0.92%	-0.92%
Mean sinking between observ. (m)	0.151	0.151	0.151	0.151
Property FEs	X	X	X	X
Year FEs	X	X	X	X
Age FEs	X	X	X	X
Zone x year FEs		X	X	X
Borough x age trends			X	X
N. bedrooms x age trends				X

* p < 0.1, ** p < 0.05, *** p < 0.01

Notes: Estimation limited to localities where the median difference between appraisal values and transaction prices is greater than 1%. The outcome in every column is the log appraised value. All estimates include property, age, and year fixed effects. Estimation limited to properties with more than one appraisal. Standard errors clustered at the census tract. The Average Treatment Effect (ATE) is calculated by multiplying the reported coefficient by the average subsidence between observations in meters.

Table A11: Significance is robust to using Conley standard errors

	(1)	(2)	(3)	(4)
Property-level sinking (m)	-0.099*** (0.020)	-0.095*** (0.020)	-0.061*** (0.021)	-0.060*** (0.022)
Observations	129,431	129,431	129,431	129,427
ATE: plot sinking	-1.49%	-1.44%	-0.92%	-0.92%
Mean sinking between observ. (m)	0.151	0.151	0.151	0.151
Property FEs	X	X	X	X
Year FEs	X	X	X	X
Age FEs	X	X	X	X
Zone x year FEs		X	X	X
Borough x age trends			X	X
N. bedrooms x age trends				X

* p < 0.1, ** p < 0.05, *** p < 0.01

Notes: Standard errors calculated using 2-kilometer radius for pooled Conley standard error calculation. The outcome in all columns is the log appraised value. All estimates include property, age, and year fixed effects. Estimation limited to properties with more than one appraisal. The Average Treatment Effect (ATE) is calculated by multiplying the reported coefficient by the average subsidence between observations in meters.

Table A12: Interest rates for mortgages are uncorrelated with tract-level sinking

	(1)	(2)
Intercept	10.135*** (0.037)	
Sinking intensity (m)	0.080 (0.047)	0.005 (0.031)
Observations	5,645,851	5,645,851
Mean Y	10.171	10.171
Adj. R2	0.001	0.217
Loan controls		X

* p < 0.1, ** p < 0.05, *** p < 0.01

Notes: Regression of the interest rate (in percentage points) charged on a mortgage on the total sinking in meters on the census tract from 2007 to 2020. Column (2) includes controls for the appraised value of the home, the borrower's income and the down payment as a share of the value, as well as bank and month fixed effects. Standard errors clustered at the census tract.

Table A13: Effect of sinking on the height of new developments

	(1)	(2)	(3)	(4)
Panel A				
Sinking pre-construction (m)	0.128 (0.348)	0.443 (0.333)	0.121 (0.339)	0.115 (0.360)
Observations	13,628	13,628	13,608	13,608
ATE: plot sinking	2.72%	9.43%	2.58%	2.45%
Mean sinking (m)	0.213	0.213	0.213	0.213
500m grid FEs	X	X	X	X
Year started x Year finished FEs	X			
Year started x Zone x Year finished FEs		X	X	X
Hedonic controls			X	X
Linear trends by hedonic char.				X
Panel B				
Sinking pre-construction (m)	0.430 (0.380)	0.535 (0.373)	0.061 (0.365)	0.049 (0.380)
Relative elevation change (m)	-11.552* (6.159)	-4.479 (4.458)	1.357 (4.117)	1.254 (4.050)
NPV future sinking (m)	0.019 (0.042)	0.004 (0.040)	0.046 (0.034)	0.047 (0.034)
Observations	13,628	13,628	13,608	13,608
ATE: plot sinking	9.15%	11.38%	1.29%	1.05%
ATE: Relative altitude change	-14.74%	-5.71%	1.73%	1.6%
ATE: Future sinking	16.87%	3.27%	40.7%	41.82%
Mean sinking (m)	0.213	0.213	0.213	0.213
Mean relative altitude change (m)	0.013	0.013	0.013	0.013
Mean NPV future sinking (m)	8.943	8.943	8.942	8.942
500m grid FEs	X	X	X	X
Year started x Year finished FEs	X			
Year started x Zone x Year finished FEs		X	X	X
Hedonic controls			X	X
Linear trends by hedonic char.				X

* p < 0.1, ** p < 0.05, *** p < 0.01

Notes: The outcome in all specifications is the height (number of floors) of the development. Standard errors clustered at the census tract. The Average Treatment Effect (ATE) is calculated by multiplying the reported coefficient by the average subsidence between observations in meters.

Table A14: Effect of sinking on the amenities of new developments

<i>Amenity index</i>	(1)	(2)	(3)	(4)	(5)	(6)	(7)	(8)	(9)	(10)
Sinking pre-construction (m)	0.057 (0.108)	0.029 (0.110)	0.084 (0.109)	0.051 (0.111)	0.084 (0.110)	0.046 (0.112)				
Relative elevation change (m)		-0.979 (0.751)	-0.909 (0.739)	-0.972 (0.764)	-0.870 (0.759)	-0.621 (0.736)	-0.745 (0.738)	-0.608 (0.744)	-0.714 (0.755)	
NPV future sinking (m)				0.000 (0.009)	0.003 (0.009)			0.001 (0.009)	0.003 (0.009)	
Observations	13,610	13,610	13,610	13,610	13,610	13,610	13,616	13,616	13,616	13,616
ATE: plot sinking	1.22%	0.61%	1.8%	1.08%	1.79%	0.98%				
ATE: Relative altitude change			-1.25%	-1.16%	-1.24%	-1.11%	-0.79%	-0.95%	-0.78%	-0.91%
ATE: Future sinking					0.36%	2.29%				
Mean sinking (m)	0.213	0.213	0.213	0.213	0.213	0.213				
Mean relative altitude change (m)										
Mean NPV future sinking (m)										
500m grid FEs	X	X	X	X	X	X				
Year started x Year finished FEs	X	X	X	X	X	X				
Year started x Zone x Year finished FEs		X	X	X	X	X	X	X	X	X

* p < 0.1, ** p < 0.05, *** p < 0.01

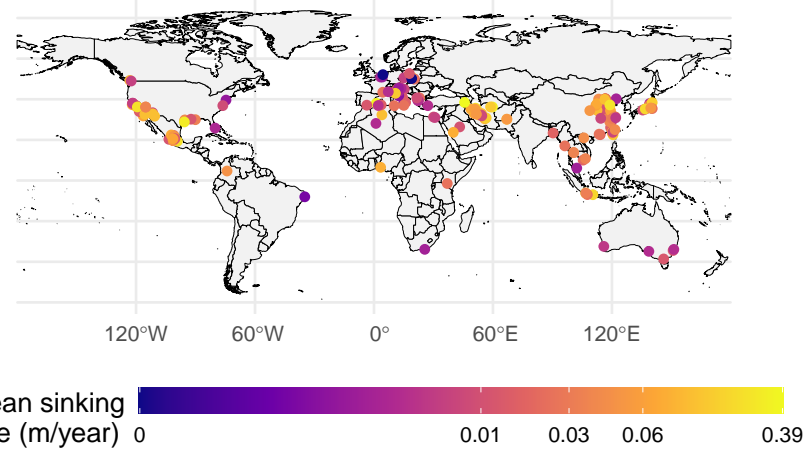
Notes: The outcome in all specifications is the amenity score of the development, which takes the simple average of standardized values for the floor space, construction space, number of bathrooms, number of bedrooms, number of parking spaces, and indicators for the presence of a gym, security desk, pool, and green space. Standard errors clustered at the census tract. The Average Treatment Effect (ATE) is calculated by multiplying the reported coefficient by the average subsidence between observations in meters.

Table A15: Parameters needed for welfare analysis

	Value	Interpretation	How estimated/calibrated
γ	0.06	Disutility from subsidence	Repeat transactions estimation
θ	0.08	Extent of information frictions	Value of future sinking in new home price
η	0.28	Supply elasticity	Redevelopment estimation
ρ	1/1.06	Discount factor	Chosen to reflect a 6% social discount rate
μ	1.111	Mean of log cost shocks	Calibrated from distribution of structural residual in data
σ	0.413	Standard deviation of log cost shocks	Calibrated from distribution of structural residual in data
$\tilde{\xi}_{jt}^S$	(vector)	log cost shocks	Exactly matched to data using equilibrium conditions
e_{jt}	(vector)	Unobserved demand shifters	Exactly matched to data using equilibrium conditions
D	2.2	Demolition cost	Calibrated to match mean redevelopment probability of 2.7%

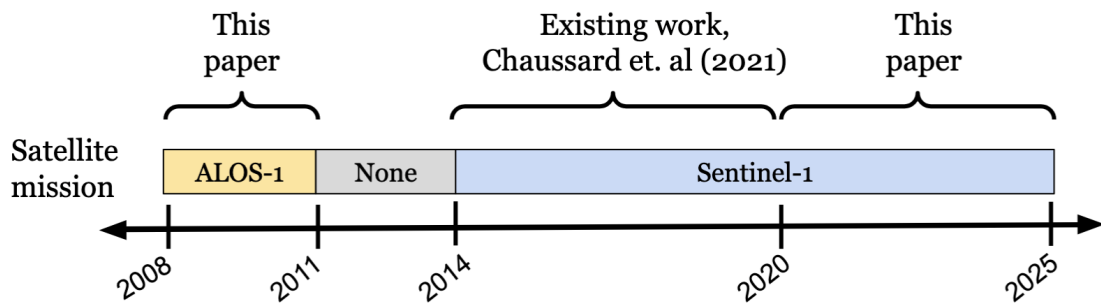
D Figure Appendix

Figure B1: Subsidence rates from the geophysics literature



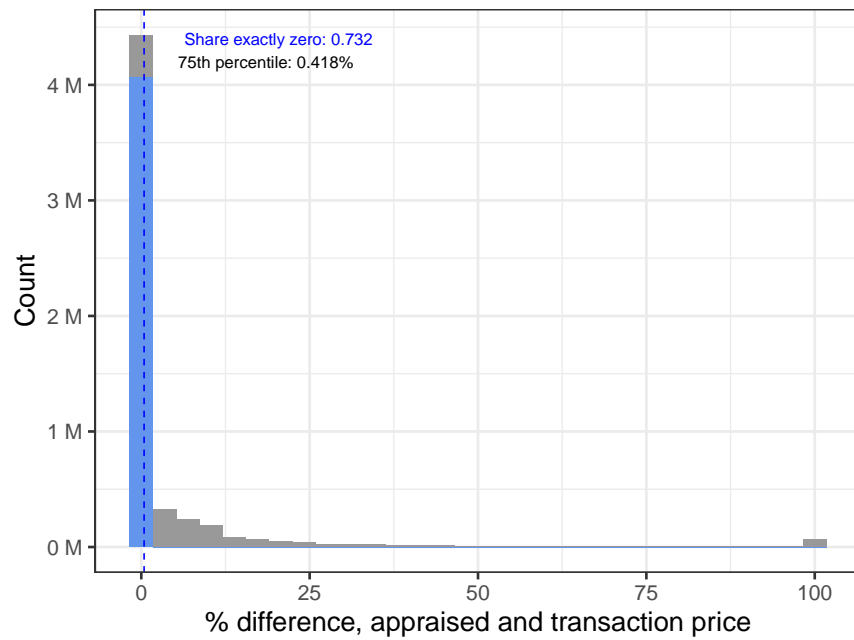
Notes: Figure adapted from data reported in [Bagheri-Gavkosh et al. \(2021\)](#), who survey geophysical studies of land subsidence published before 2021. The median study included in the survey calculated subsidence rates starting in 2001 and ending in 2010. Points are colored by the mean subsidence rate estimated in the study when available, and the maximum rate when that is the only measure reported.

Figure B2: Timeline of satellite data measures



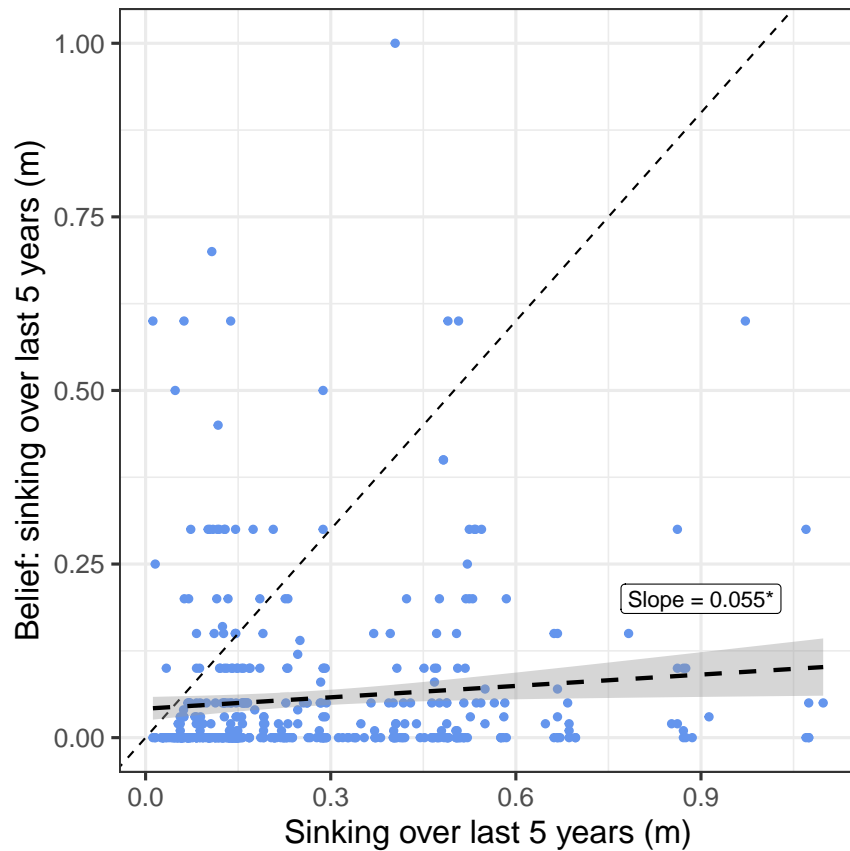
Notes: [Chaussard et al. \(2021\)](#) provided data from 2014-2020. Original interferometry performed from 2008-2011 using ALOS-1 data, and 2021-2025 using Sentinel-1 data.

Figure B3: Distribution of deviations of appraised and transaction values



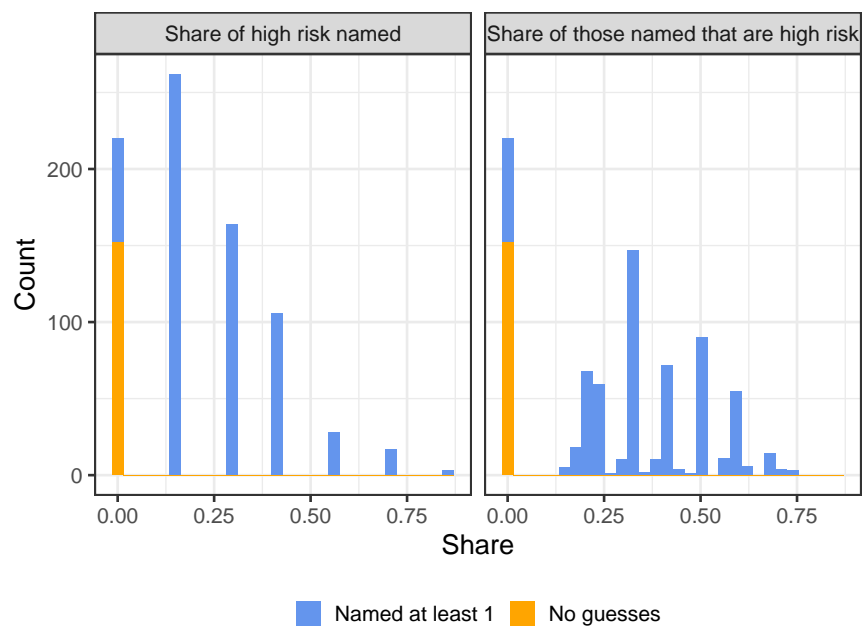
Notes: Height of the bars represents the number of appraisals with the given percentage difference between appraised and transaction values, measured as $100 \times (p^{appr} - p^{transac})/p^{transac}$. Values winzorized at the 99th percentile for visual clarity. Exact zero values colored in blue.

Figure B4: Beliefs about past sinking versus satellite measures



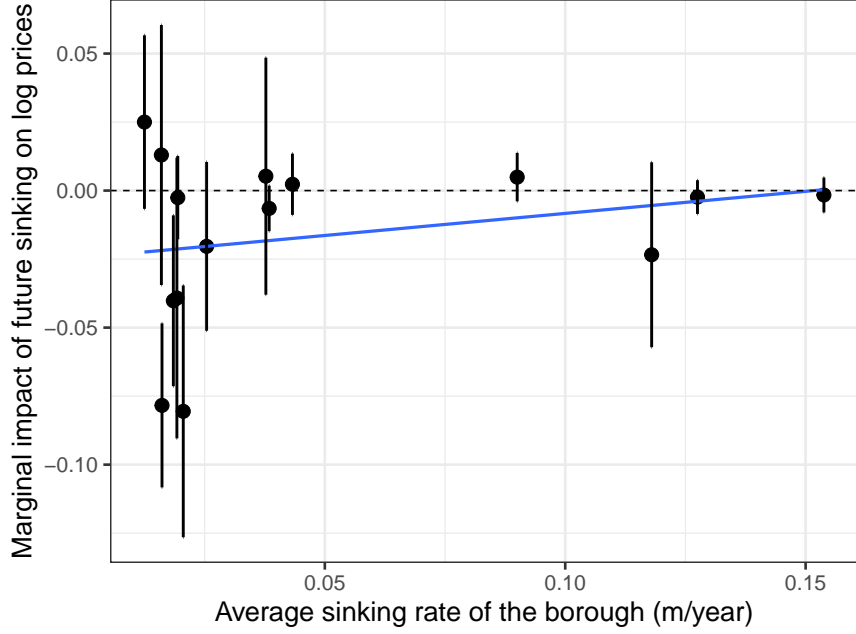
Notes: Each point plots the respondent's report of how much their plot has sunk in the last five years against the satellite measure of how much that plot has sunk. The dotted line plots the 45° line. The thick dashed line with prediction interval represents the line of best fit from a linear regression.

Figure B5: Evaluating respondent beliefs about the geography of sinking



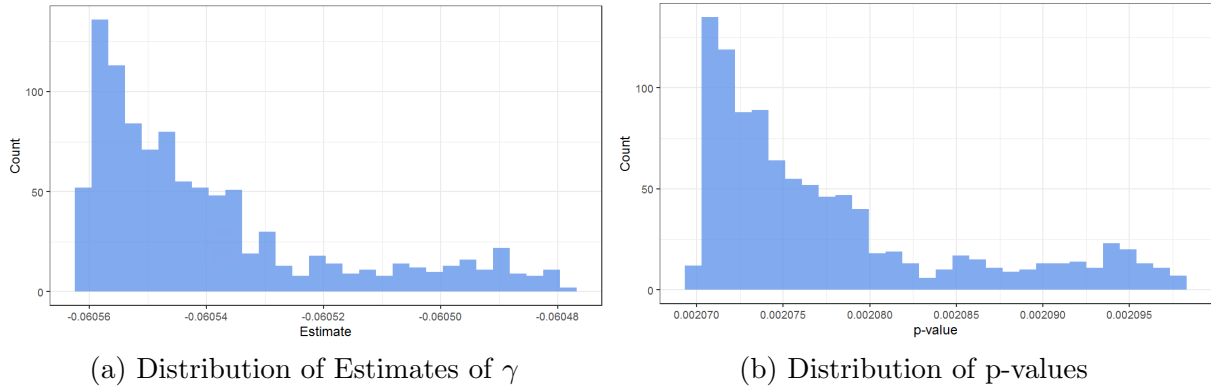
Notes: Each bar plots the number of responses that scored a given “grade” according to two metrics. The right panel scores the share of the seven boroughs considered high sinking risk that the respondent named in response to the question “Which boroughs in Mexico City have issues with subsidence?”. The left panel scores the share of named boroughs that are in the seven high risk boroughs. Respondents who could not name any boroughs in response to the question are marked in yellow and are assigned a score of zero.

Figure B6: Capitalization of future sinking by borough



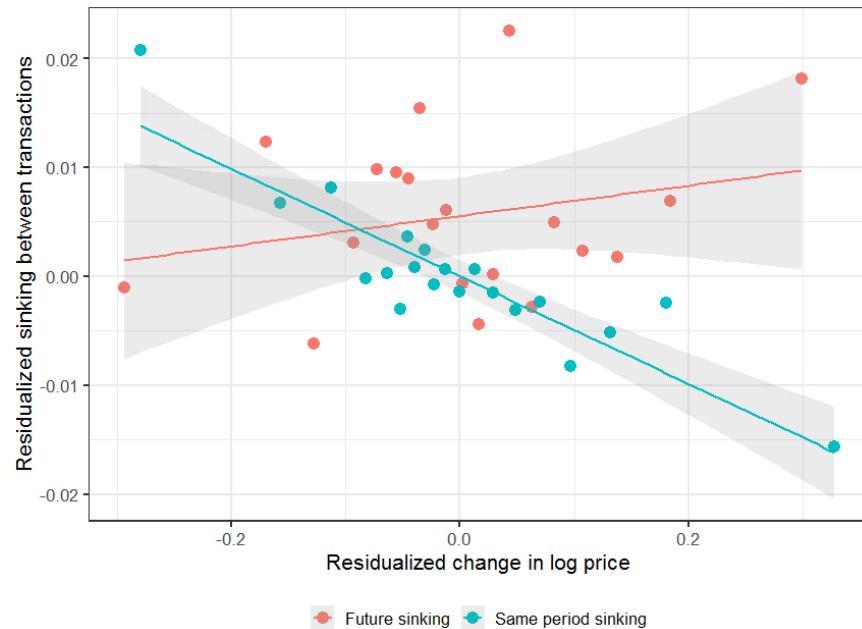
Notes: Each point with error bar represents the regression coefficient and 95% confidence interval of the interaction of a borough fixed effect with the net present value of future sinking specified using an AR(1) process and 6% discount rate. Estimation is limited to new builds. All estimates include fixed effects by 500m-grid cell, seismic zone by year, amenity class, number of bathrooms, number of floors, and number of parking spaces. Standard errors clustered at the grid cell. The blue line fits a linear regression through the point estimates.

Figure B7: Monte Carlo estimates simulating measurement error in subsidence



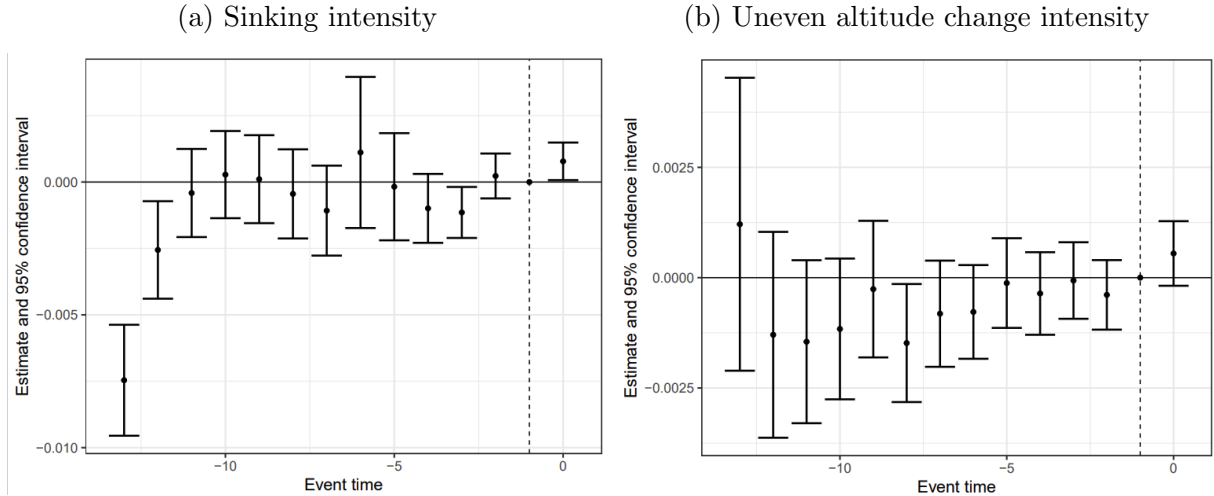
Notes: Each plot shows the frequency of estimates of γ (Figure (a)) and its associated p-value (Figure (b)) given 1,000 draws of data in which each models total subsidence as $\tilde{S}_{jt} = S_{jt} + \sum_{i=0}^{Age_{jt}} e_{ij}$, where e_{ij} is drawn from a normal distribution with mean zero and standard deviation of 0.01 meters, simulating a 10 millimeter per year white noise measurement error associated with the measured sinking rate. Each point estimate is from a regression of log prices on \tilde{S}_{jt} and property, age, and zone by year of appraisal fixed effects and time trends by borough, number of bedrooms, and type. Estimates exclude properties with only one appraisal. Standard errors clustered at the census tract.

Figure B8: Pre-trends test



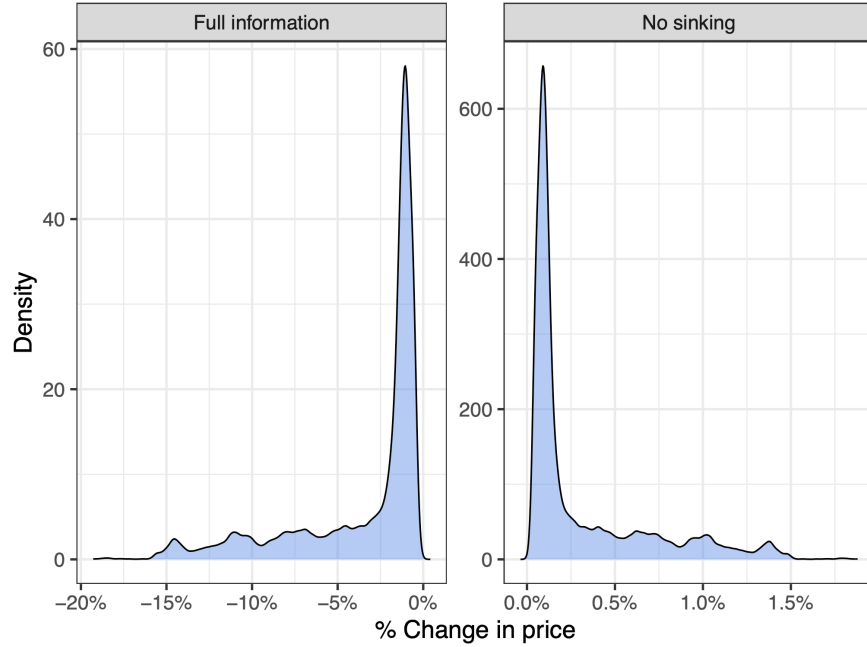
Notes: Points represent mean residualized sinking between transactions for 20 quantile bins of the residualized change in log price between appraisals. Residualization of both variables is done on property, age, and year of appraisal by seismic zone fixed effects. Lines represent the line of best fit through these binned values; grey areas represent 95% prediction intervals. The slopes reported are from a regression of the sinking between appraisals on the change in log price (lagged or contemporaneous), residualized as in the plot. P-values calculated using standard errors clustered at the census tract.

Figure B9: Pre-trends in pixel-level development



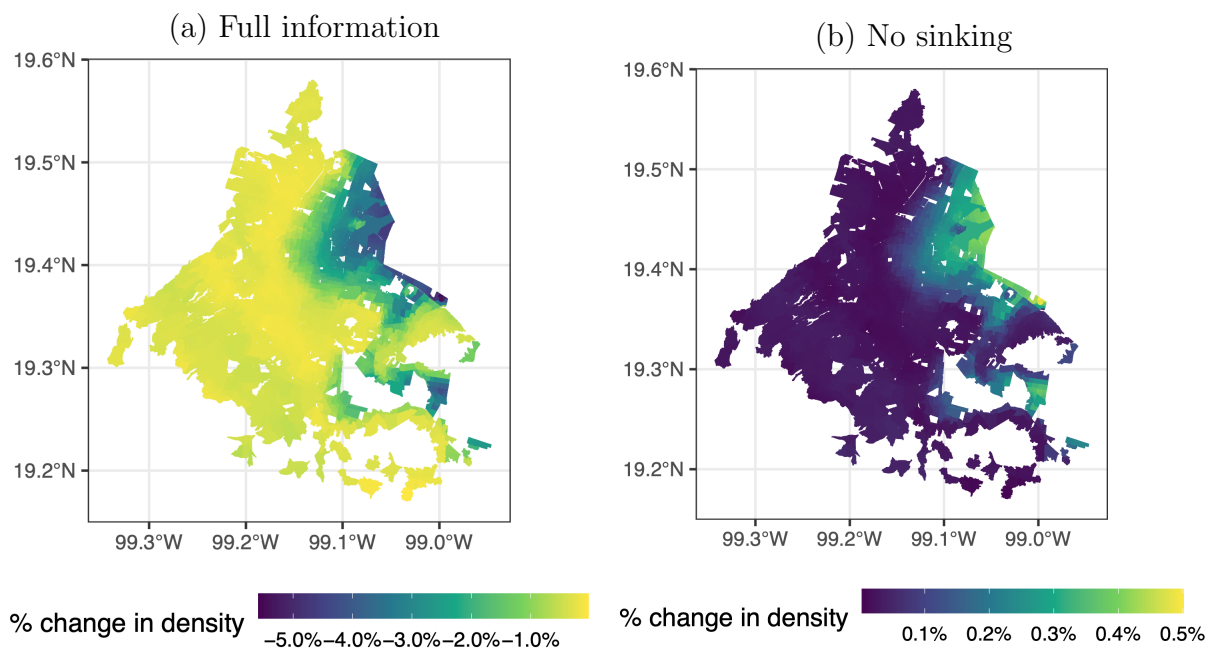
Notes: Depicts point estimates and 95% confidence intervals from a regression of an indicator for any development occurring on the pixel on an indicator for being a high-sinking pixel in 2020 (Panel (a)) or a highly-unevenly sinking pixel as measured by the cumulative relative altitude change (Panel (b)) in different periods. Periods denoted on the horizontal axis are the year relative to the first year that the pixel achieved a sinking intensity above the cut-off. Relative periods < 10 are grouped into the -10 period. All regressions include pixel and year fixed effects. Point estimates estimated using [Sun and Abraham \(2021\)](#) staggered event study estimator. Standard errors clustered at the pixel.

Figure B10: Price changes in counterfactuals relative to the observed equilibrium



Notes: Each plot shows the density of the percentage change in price in the counterfactual relative to observed prices. The left figure counterfactual is relative to an alternative where sinking remains unchanged but there are no information frictions ($\theta = 1$). The right figure counterfactual is relative to an alternative equilibrium where subsidence is zero.

Figure B11: Change in density under full information relative to the observed equilibrium



Notes: Fill colors per census tract represent the percentage change in the number of units per plot between (a) a counterfactual calculated with no information frictions and the observed housing density, and (b) a counterfactual calculated with no future sinking and the observed housing density.

E Data Appendix

E.1 Subsidence data

Subsidence calculated from Sentinel-1 measures (2014-2020) at the pixel level (90 by 90 meter resolution) using the C-band was directly provided by Chaussard et al. (2021). I create an annual pixel-level measure of sinking by mimicking their methodology for creating the average pixel-level analysis reported in their paper by estimating a linear regression of cumulative vertical deformation on time for each pixel, the slope of which is an estimate of the sinking in that period. This method is preferred to directly integrating sinking at each time step, which is sensitive to estimates contaminated by error or low coherence (Chaussard et al., 2021). In our setting the linear projection helps remove measurement error that may be related to construction itself, as a change in building height, if detected at all by the satellite, would be smoothed over by the other measurements.

We create annual, pixel-level measures of subsidence for 2007-2011 using ALOS-1 ascending track L-band SAR acquisitions for the Mexico Valley. We process the raw Level-1 data using the ISCE full stack processing framework (Interferometric synthetic aperture radar Scientific Computing Environment) and use MintPy algorithms to correct for tropospheric distortions and unwrapping errors and produce the final corrected time series values (Yunjun et al., 2019) and GACOS to do tropospheric corrections (Yu et al., 2018b,a, 2017). Given the high signal-to-noise ratio in sinking in central Mexico, I do not filter on coherence to maximize the coverage of the data.

Using the same process, we create annual, pixel-level measures of subsidence for 2021-2025 using Sentinel-1 ascending track C-band SAR acquisitions for the Mexico Valley. We process the raw Level-1 data using the ISCE full stack processing framework (Interferometric synthetic aperture radar Scientific Computing Environment) and use MintPy algorithms to correct for tropospheric distortions (using GACOS) and unwrapping errors. I do not filter on coherence.

In order to create a harmonized panel of pixels, I create a regular $100\text{m} \times 100\text{m}$ pixel overlay that spans the two spatial extents of the ALOS and Sentinel data and take an intersection-weighted average of the original pixel subsidence rates. From this grid I interpolate linearly from 2011-2013.

E.1.1 Measurement error

In the direct measures of subsidence produced by SAR interferometry, measurement error arises from four main sources: (i) errors in the characterization of the exact orbit location, which is required to properly compare multiple passes; (ii) errors arising from tropospheric or ionospheric conditions that affect measurement, in particular water vapor; (iii) unwrapping errors, which occur when “unwrapping” the phase length which is modular 2π , and (iv) temporal decorrelation, where measurements jump in the 2π range due to irregular backscatter. We discuss the role for these in our measurements and the magnitude of errors from these sources.

Orbital location errors Errors in characterizing the exact location of the satellite in space at each pass can result in long wavelength phase ramps which essentially represent a

level shift in subsidence that is common to every pixel. These are relatively straightforward to identify in interferograms, and the MintPy algorithm we use to generate the time series implements a linear “de-ramping” of the time series. That said, before de-ramping, the accuracy of orbit information depends on the satellite. The Sentinel-1 orbit information, used in our analysis from 2014-2025, is extremely accurate, and Sentinel’s orbit products have an accuracy typically below 5cm in 3D in terms of the exact location of the satellite ([Peter et al., 2017](#)). This results in negligible orbit errors in the resulting interferometry process. As an older satellite, the ALOS-1 satellite achieves an accuracy of around 40 centimeters in 3D in terms of the satellite’s location in space, so de-ramping is more important for this satellite product.

Tropospheric and ionospheric errors Changes in tropospheric and ionospheric conditions can distort interferograms, which manifests as a phase ramp similar to orbital location errors. We correct for differences in the troposphere by using GACOS hourly temperature, pressure, and water vapor measurements to adjust measurements using MintPy. The magnitude of ionospheric distortions is inversely proportional to the band frequency; in the case of the C-band, which is relatively high frequency, these errors are minimal, on the order of <5 millimeters. For the lower frequency L-band, the ionosphere plays a more important role, but its importance is highly dependent on context; ionospheric errors are at their worst during periods of high solar activity, during the day at equatorial and polar locations. The ALOS-1 satellite has a sun-synchronous orbit, so it’s ascending orbit passed over Mexico City around 10:30PM local time. The nighttime pass together with the fact that Mexico City is near mid-latitude ranges at 19° latitude means that ionospheric errors are somewhat mitigated, and our de-ramping also decreases ionospheric delay ([Chaussard et al., 2021](#)).

Unwrapping errors Unwrapping errors result from too large of a phase difference between passes, and rather than affecting measurements directly it affects the ability to produce a measurement at all in some places. Unwrapping errors can arise from several sources; those most relevant to our setting include (i) too fast of ground deformation; and (ii) steep slopes that mean that measurement is sensitive to the exact line-of-sight of the satellite. Our area of interest does not have particularly steep slopes, as urbanized Mexico City is located within a valley. How fast is “too-fast” of deformation depends on the band, as the phase is wrapped around half the radar’s wavelength. For the Sentinel-1 C-band, this means that if displacement exceeds 2.8 centimeters between passes, which occur every 6 days, then displacement would not be able to be estimated. Thus, subsidence would need to exceed a rate of 1.7 meters per year to be undetectable, a rate observed for dramatic events such sudden, discrete events such as volcanic eruptions or ice sheet collapses, but not observed in our sample. The L-band measures we use from the ALOS-1 satellite are able to detect up to 11.8 centimeters between passes, and our average pass frequency is 90 days, so sinking would have to exceed 47.9 centimeters per year to be undetectable, which is almost double the maximum rate observed in our data.

Temporal decorrelation The primary source of temporal decorrelation is changes in the ground surface that cause measurements to behave differently between passes, for example changes in vegetative density or snow cover. These sources of error are minimized in urban settings, where concrete provides a time-consistent radar signature. This is diagnosable using the average coherence in the signal between satellite passes, which when

limiting to Mexico City in our data is over 0.9 on a scale from 0 to 1 almost everywhere.

Summing up By focusing on an urban setting and using state-of-the-art tools for conducting interferometry with tropospheric corrections and linear de-ramping, we minimize the role for measurement error in our analysis. Other studies in urban areas use GPS stations that provide ground measures at discrete points, and find measurement errors on the order of less than millimeters per year (see: 1.5mm/year in Beijing ([Liu et al., 2020](#)); 9mm/year in the Antelope Valley, CA ([Bawden et al., 2023](#))). Assuming we achieve similar accuracy (1.5mm), our measurement error would be an order of magnitude of around 2.1% of the average sinking rate of 7 centimeters/year.

E.1.2 Does development cause subsidence?

While historic buildings in Mexico City such as the Palace of Fine Arts have been known to cause sinking because of their own weight, modern construction code requirements seek to prevent this through soil studies, including underground levels that offset the weight of the building, and using pylons that “anchor” the building into the ground instead of sitting on top of the soil.

We test whether development causes subsidence by estimating the following specification:

$$s_{pt+\tau} = \beta_1 (\text{Development}_{pt}) + \theta s_{pt-1} + \alpha_p + \alpha_{tg(p)} \quad (19)$$

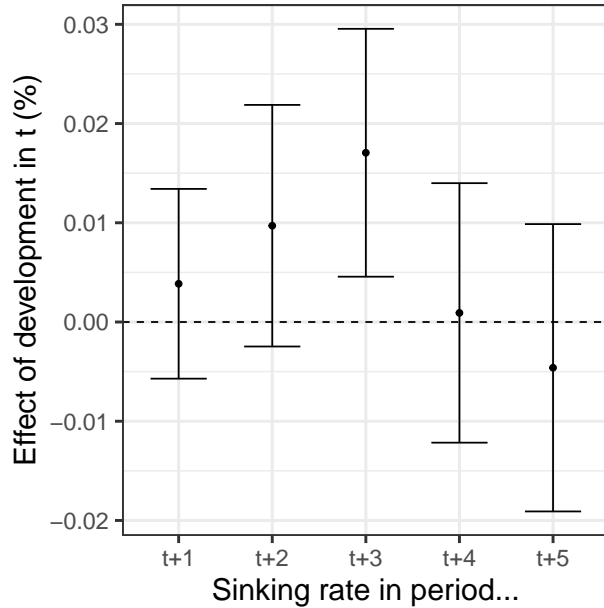
where $s_{pt+\tau}$ is the sinking rate on pixel p in period $t + \tau$ and $1(\text{Development}_{pt})$ is an indicator for a new development occurring in pt . s_{pt-1} is the lagged sinking rate, a necessary control given that sinking leads to more development. We also control for pixel fixed effects α_p and seismic zone by year fixed effects $\alpha_{g(p)t}$. To avoid confounding the effect of multiple developments, we limit estimation to the sample of pixels that had either one or no developments over the period. Standard errors are clustered at the pixel.

Figure B12 reports $\hat{\beta}$ for $\tau \in [1, 5]$, transformed to be reported as a percent of the average sinking rate. Most coefficients are statistically insignificant, except for sinking three years after construction ended. However, the value of the coefficient is economically minor; a development in t increases the rate of sinking in $t + 3$ by less than 2%. This is generally consistent with studies from Mexico City and elsewhere that find that the role of human development in causing land subsidence is minor ([Chaussard et al., 2021](#); [Parsons et al., 2023](#)). The fact that the coefficients are small and largely insignificant also assuages concerns that construction impedes measurement of subsidence by masking as positive elevation gain.

E.2 Survey design and implementation

The survey was designed to be representative of Mexico City housing units, with stratification on two broad zones of high and low sinking from 2007-2020 defined at the borough level. Within strata, census tracts were sampled with probabilities drawn from the number of housing units in that tract in the 2020 census; 80 tracts were randomly sampled, and 10 households were surveyed per tract. Seven boroughs were designated as high-risk with average total sinking above 0.36 meters from 2020-2024. IRB exemption was obtained through the UC Berkeley Office for the Protection of Human Subjects.

Figure B12: Impact of development on future sinking rates



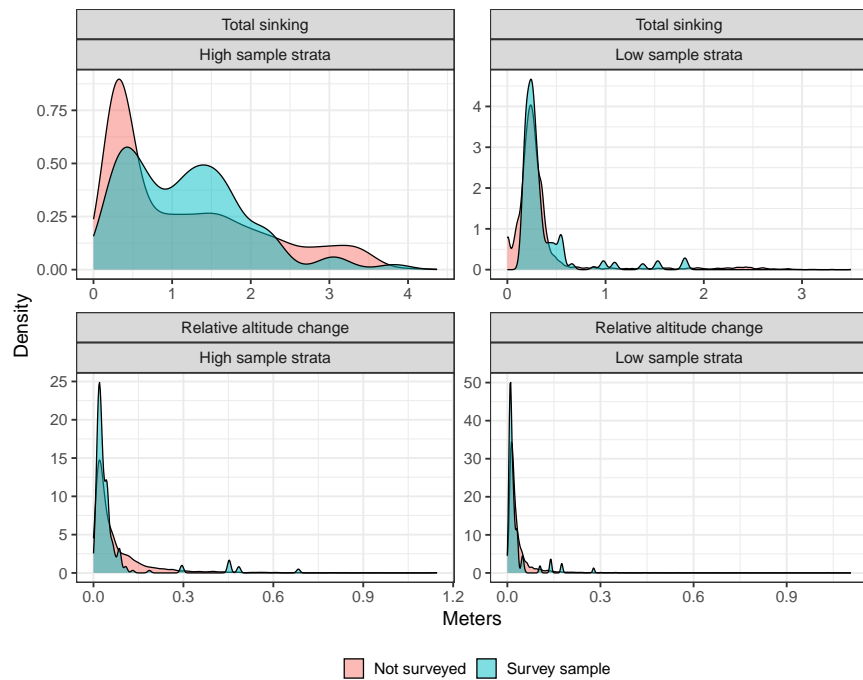
Notes: Plots $\hat{\beta}/\bar{s}$, where \bar{s} is the average sinking rate over the panel, and 95% confidence interval from estimating Equation (19) for $\tau \in [1, 5]$. Standard errors clustered at the pixel.

The surveyed homes provide good representation of sinking across the city; Figure B13 reports the distribution of average total sinking and total relative altitude loss from 2008–2020 for surveyed and non-surveyed tracts. The distributions are very similar, with some more mass in the surveyed tracts at mid-levels of sinking coming from the distribution of housing units over space within high-risk boroughs.

Table A16 reports comparisons of our resident and unit outcomes with the 2022 Income and Expenditure Survey (ENIGH). Despite the three-year difference and different sampling strategy (housing units versus residents), outcomes are broadly comparable though statistically differentiable between our survey and the ENIGH. Given the sample restriction on homeowners of any tenure and renters with at least 5 years in the unit, our sample is 73% homeowners (compare to 60% in the ENIGH). Looking within homeowners in Table A16, we see that survey respondents are more likely to inhabit single-family homes and live in self-built homes as compared to commercially built homes. Respondents are also significantly older on average. These differences likely highlight selection into being contactable by the survey firm. Reassuringly, our respondents are not meaningfully more educated on average; a 0.58 difference in educational attainment represents an approximate difference of 1.5 years of schooling.⁴⁸

⁴⁸Middle and high school education in Mexico each last 3 years, so the difference between “Middle school incomplete” and “Middle school complete” is approximately 1.5 years.

Figure B13: Distribution of subsidence in surveyed and non-surveyed census tracts



Notes: Each plot is the distribution of average total sinking from 2008-2020 at the census tract level and the total relative altitude change from 2008-2020 on surveyed and non-surveyed tracts, reported separately for the high-sinking strata ($N=500$) and the low-sinking strata ($N=300$).

Table A16: Balance of survey outcomes against the 2022 ENIGH

	Full sample		Owners only		Diff, full sample	Diff, owners sample
	ENIGH	Our survey	ENIGH	Our survey		
Unit characteristics						
Single-family home	Mean	0.66	0.78	0.70	0.79	0.12***
	SD	(0.437)	(0.412)	(0.409)	(0.401)	(0.019)
	N	2541	800	1595	581	3341
Apartment	Mean	0.31	0.22	0.27	0.21	-0.09***
	SD	(0.422)	(0.412)	(0.392)	(0.401)	(0.019)
	N	2541	800	1595	581	3341
Age of home	Mean	26.82	38.82	30.39	42.28	4.5***
	SD	(20.285)	(22.713)	(19.471)	(22.387)	(0.96)
	N	2092	800	1471	581	2892
Self-built	Mean	0.28	0.63	0.47	0.67	0.16***
	SD	(0.49)	(0.483)	(0.49)	(0.47)	(0.023)
	N	1597	800	1597	581	2397
Commercially built	Mean	0.26	0.22	0.44	0.23	-0.22***
	SD	(0.465)	(0.409)	(0.465)	(0.42)	(0.021)
	N	1597	800	1597	581	2397
Respondent characteristics						
Female	Mean	0.54	0.57	0.54	0.56	0.04***
	SD	(0.499)	(0.496)	(0.499)	(0.498)	(0.019)
	N	8421	800	5449	581	9221
Age (respondent)	Mean	38.45	52.94	41.63	53.73	14.55***
	SD	(21.547)	(16.762)	(22.135)	(17.086)	(0.671)
	N	8421	800	5449	581	9221
Education	Mean	4.23	6.12	4.44	6.24	0.71***
	SD	(3.541)	(3.081)	(3.563)	(3.118)	(0.123)
	N	6505	800	4221	581	7305
						4802

Notes: Means and standard deviations are weighed by sample weights to the population. Differences are conditional on strata fixed effects and use heteroskedasticity-robust standard errors. Stars represent p-values less than 0.10 (*), 0.05 (**), and less than 0.01 (***).

E.3 Appraisal data

E.3.1 Appraised useful life remaining

We investigate whether appraised values for the years of useful life remaining follow systematic rules that would preclude us from exploiting true variation in the home's physical state. If appraisers use fixed rules based on some property characteristic or age to assess the useful life left, then regressions that include property and year of appraisal by year of last appraisal fixed effects would control for all possible variation in this variable.

To investigate this, we define the implied duration of the property's useful life by adding the age at time of appraisal to the appraised years of useful life remaining. Then, we investigate the extent to which the modal value of these implied useful lifespans by the property's borough, type (basic, medium, luxury amenities), vintage, and year of appraisal explains the appraised useful lifespan. We find that there are systematic patterns in the modal appraised useful life, with different boroughs and vintages receiving common appraised useful lifespans of 65, 70, 75, or 80 years. However, there are also substantial deviations from these rules of thumb.

Figure B14 plots the difference between the appraised useful lifespan and the rule of thumb value implied by the property's location, type, vintage, and year of appraisal. While differences are centered around zero, there are appraised useful lifespans that differ substantially from the rule of thumb value. If we define the rule of thumb excluding vintage, we find that newer homes appear to be built with longer useful lives, a finding consistent with technological improvements over time that increase the durability of homes.

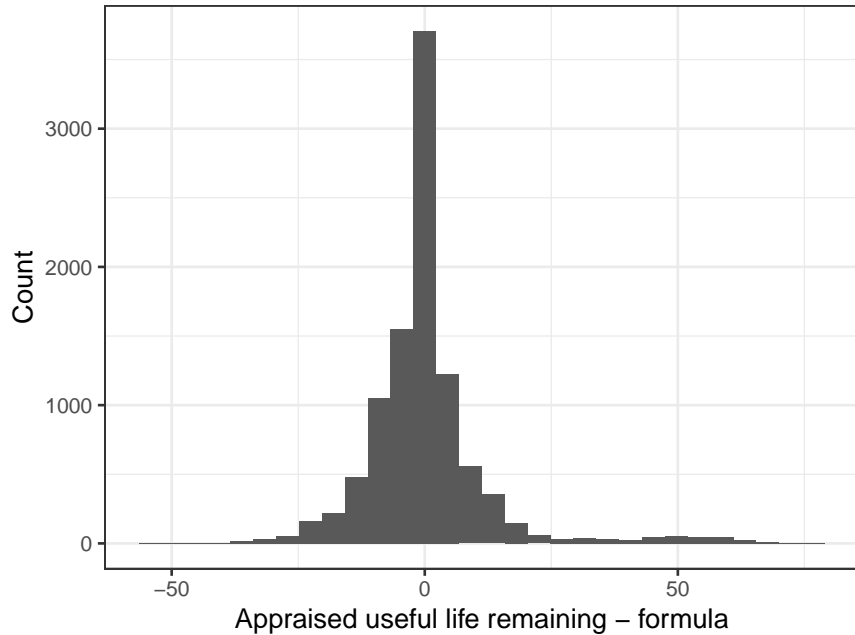
E.4 Housing developer data

We aggregate the quarterly development panel into a dataset of developments by calculating averages of characteristics of the modal unit and its asking price that are weighted by the number of units reported sold in that period. To create a dataset of new units developed, we expand the data by the number of units sold, assigning to each the modal price and characteristics reported in that quarter.

E.4.1 Coverage of the new housing market

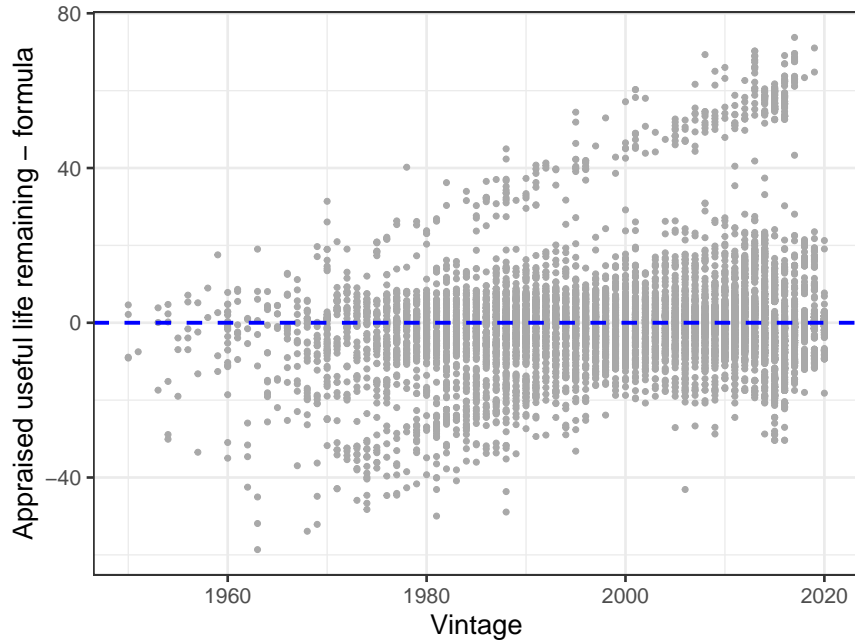
Across Mexico, the Central Bank reports that the DIME covers about 60% of new homes, given that developers account for 60% of new unit construction. We compare the units reported built in the DIME to the number of appraisals per year to get a better idea of the DIME coverage in Figure B16. Units reported sold by the DIME surpass even the total number of appraisals in some years, and is consistently around double the number of appraisals for new builds (blue line). This is likely because the appraisal data is missing transactions that did not involve a mortgage, a significant share (around 70%). While conclusions about coverage should be tempered by this fact, we see this as suggestive that the DIME covers a significant share of new development in Mexico City.

Figure B14: Deviations of appraised useful lifespan from rule of thumb values



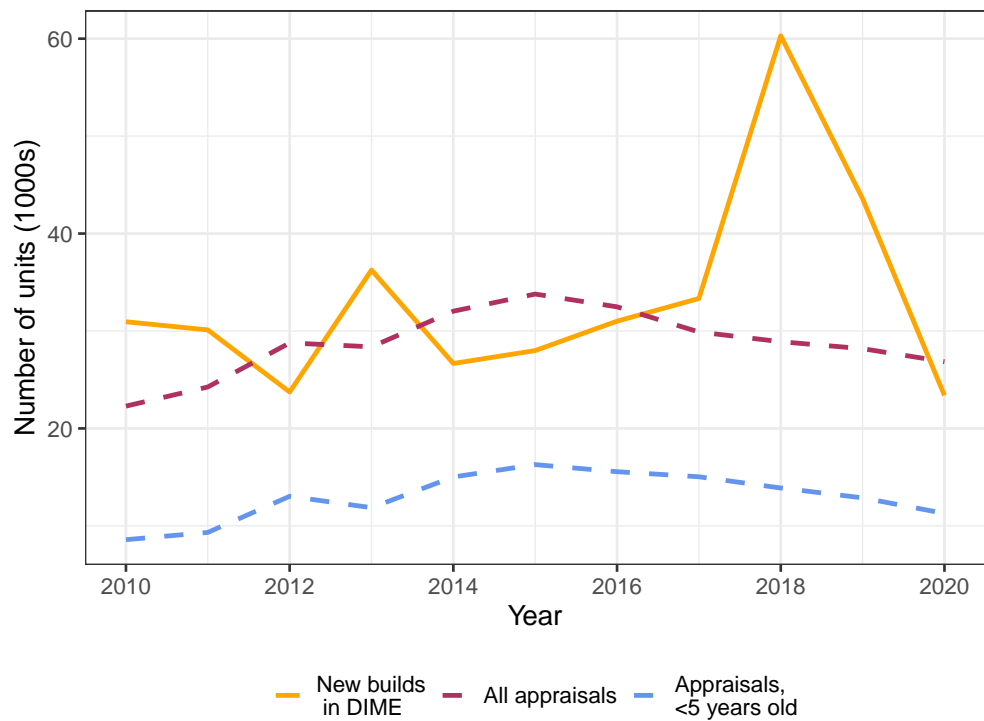
Notes: Histogram of the appraised useful lifespan minus the implied rule of thumb using a 10,000-observation random sample from the data. The rule of thumb is defined as the modal appraised useful lifespan for properties that are located in the same borough, built in the same year, appraised in the same year, and are of the same type.

Figure B15: Deviations of appraised useful lifespan from rule of thumb values



Notes: The rule of thumb is defined as the modal appraised useful lifespan for properties that are located in the same borough, appraised in the same year, and are of the same type, but does not control for vintage.

Figure B16: Total number of newly developed units and appraisals



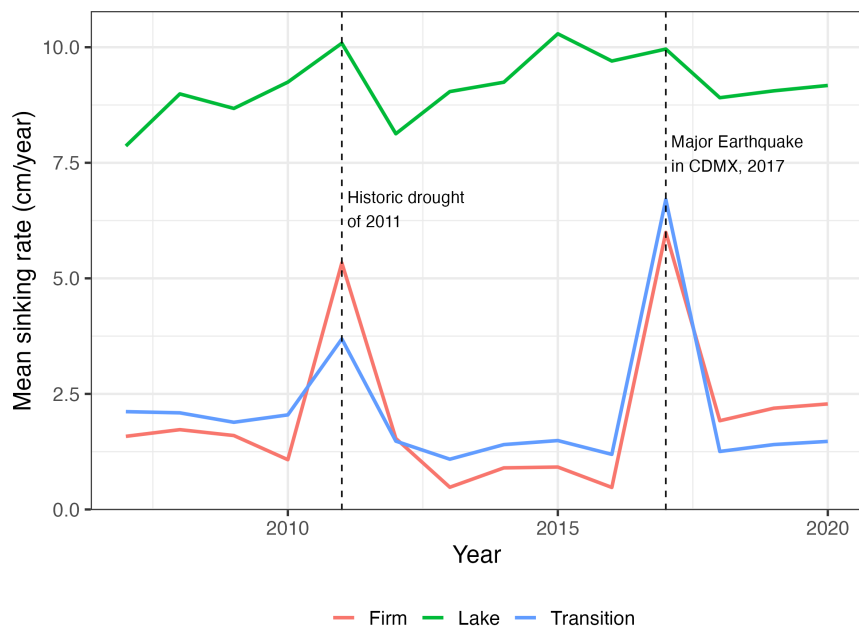
Plots the total number of units per year. The solid orange line plots the total number of units reported sold by the DIME. The dashed lines represent the total number of appraisals (maroon) and the total number of appraisals that are reported less than 5 years since construction (blue).

F Predictability of subsidence over time and space

As seen in Figure 2, subsidence intensity is very serially correlated over space, with the fastest rates of sinking concentrated over the historic lake and the surrounding “transition” zone defined in the construction code. Subsidence is also highly serially correlated; at the pixel level, the lagged subsidence rate has a correlation of 0.85 with the contemporaneous subsidence rate.

However, how sinking has evolved over time varies substantially in Mexico City. First, how sinking rates respond to shocks that affect groundwater levels or geophysical stability depends on zone. Figure B17 plots subsidence rates over time by broad categories of the geophysical environment defined in the construction code. While subsidence rates are consistently high in the lake zone, the more resistant Firm and Transition zones are more responsive to shocks; each experiences a spike in subsidence rates during the drought of 2011 and the large earthquake of 2017. In particular after the earthquake, rates in the Firm zone experienced a level shift up in the sinking rate.

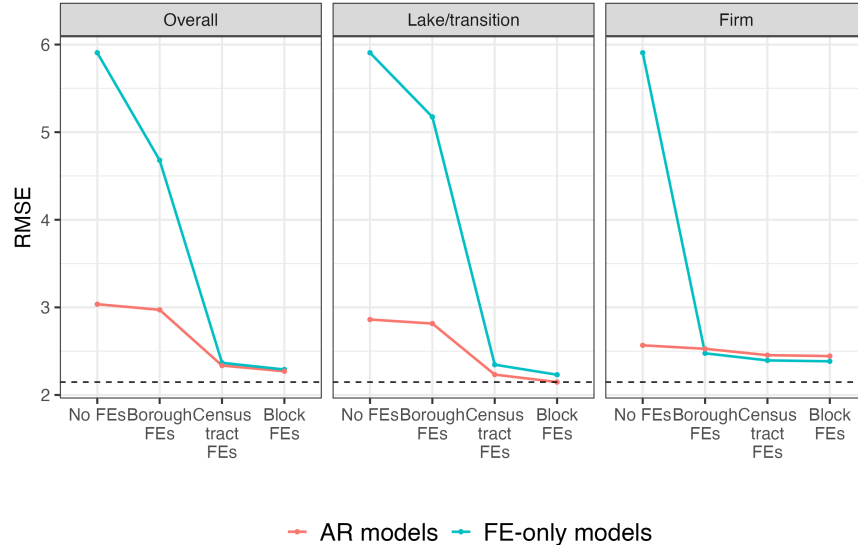
Figure B17: Subsidence rates over time



Notes: Lines represent simple averages of subsidence rates by year and seismic zone as defined by the construction code.

While past sinking is strongly correlated with current sinking (Table A17), it does not provide much additional predictive power conditional on fine enough geographic information. Figure B18 compares the RMSE for models with different levels of granularity of spatial fixed effects that either include or exclude the lagged subsidence rate as a predictor of the contemporaneous rate. This highlights that starting around the census tract level, lagged subsidence contains little additional information above this geographic average.

Figure B18: Predictive models of subsidence rates



Notes: Points plot the RMSE of regressions that include different levels of fixed effects and autoregressive terms. Points and lines in blue include only the fixed effects indicated on the horizontal axis, which range from no fixed effects (simple intercept model) to city block-level fixed effects. Pink points and lines include these same fixed effects, and additionally the lagged sinking rate.

Table A17: AR(1) predictive models of the subsidence rate

	Overall				Lake/transition				Firm			
	(1)	(2)	(3)	(4)	(5)	(6)	(7)	(8)	(9)	(10)	(11)	(12)
Intercept	0.698*** (0.004)				0.621*** (0.006)				1.801*** (0.006)			
Lagged sinking rate	0.877*** (0.001)	0.797*** (0.056)	0.151*** (0.012)	0.095*** (0.002)	0.922*** (0.001)	0.863*** (0.031)	0.232*** (0.014)	0.152*** (0.003)	0.117*** (0.002)	0.083 (0.085)	0.023* (0.014)	0.015*** (0.003)
Observations	821.716	821.716	821.716	821.716	507.539	507.539	507.539	507.539	314.177	314.177	314.177	314.177
RMSE	3.04	2.97	2.34	2.27	2.86	2.82	2.23	2.15	2.57	2.53	2.45	2.44
R squared	0.74	0.75	0.85	0.86	0.81	0.82	0.89	0.89	0.01	0.04	0.10	0.11
Borough FEs	X				X				X			
Census tract FEs		X				X				X		
Block FEs			X				X			X		

* p < 0.1, ** p < 0.05, *** p < 0.01

Notes: The unit of observation is a city block-year. Standard errors in parentheses assume iid errors.

G Theory Appendix

G.1 Linearization of expectation terms

First, consider a first-order approximation of $g(S_{i\tau}^{t+1}) = \exp(\gamma S_{i\tau}^{t+1})$ around $S_{i\tau}^{t+1} = \mathbb{E}(S_{i\tau}^{t+1})$:

$$\begin{aligned} g(S_{i\tau}^{t+1}) &= \exp(\gamma \mathbb{E}(S_{i\tau}^{t+1})) + \gamma \exp(\gamma \mathbb{E}(S_{i\tau}^{t+1})) \times (S_{i\tau}^{t+1} - \mathbb{E}(S_{i\tau}^{t+1})) + R(S_{i\tau}^{t+1}) \\ \Rightarrow \mathbb{E}(g(S_{i\tau}^{t+1})) &= \exp(\gamma \mathbb{E}(S_{i\tau}^{t+1})) + \mathbb{E}(R(S_{i\tau}^{t+1})) \end{aligned}$$

The remainder term $R(S_{i\tau}^{t+1})$ will be a function of higher-order moments of size:

$$\frac{\gamma^n}{n!} (S_{i\tau}^{t+1} - \mathbb{E}_t(S_{i\tau}^{t+1}))^n$$

which will be small if the moments of the distribution of sinking grow at a slower rate than $\frac{\gamma^n}{n!}$. For instance, note that the second-order approximation would also include the variance:

$$\begin{aligned} g(S_{i\tau}^{t+1}) &\approx \exp(\gamma \mathbb{E}(S_{i\tau}^{t+1})) + \gamma \exp(\gamma \mathbb{E}(S_{i\tau}^{t+1})) (S_{i\tau}^{t+1} - \mathbb{E}(S_{i\tau}^{t+1})) \\ &\quad + \frac{\gamma^2}{2} \exp(\gamma \mathbb{E}(S_{i\tau}^{t+1})) (S_{i\tau}^{t+1} - \mathbb{E}(S_{i\tau}^{t+1}))^2 \\ \Rightarrow \mathbb{E}(g(S_{i\tau}^{t+1})) &\approx \exp(\gamma \mathbb{E}(S_{i\tau}^{t+1})) + \frac{\gamma^2}{2} \exp(\gamma \mathbb{E}_t(S_{j\tau}^{t+1})) \text{Var}(S_{i\tau}^{t+1}) \end{aligned}$$

which is small in the time series of plot-level sinking.

Now we linearize the log terms. Consider a first-order Taylor series approximation of:

$$\begin{aligned} f(\mathbb{E}_t(\{\tilde{\lambda}_{ju}\}), \mathbb{E}_t(\{e_{ju}\}), \mathbb{E}_t(\{s_{iu}\}_u)) &= \\ \log \left(\exp(-\tilde{\lambda}_{jt} + e_{jt}) + \sum_{\tau=t+1}^{\infty} \rho^{\tau-t} \exp(\gamma \mathbb{E}_t\{S_{i\tau}^{t+1}\} - \mathbb{E}_t(\tilde{\lambda}_{j\tau}) + \mathbb{E}_t(e_{j\tau})) \right) \\ &= \log \left(\exp(-\tilde{\lambda}_{jt} + e_{jt}) + \sum_{\tau=t+1}^{\infty} \rho^{\tau-t} \exp(-\mathbb{E}_t(\tilde{\lambda}_{j\tau}) + \mathbb{E}_t(e_{j\tau}) + \sum_{u=t+1}^{\tau} \gamma \mathbb{E}_t(s_{iu})) \right) \end{aligned}$$

around $\tilde{\mathbb{E}}_t(s_{iu}) = 0$, $\mathbb{E}_t(e_{ju}) = e_{jt}$, and $\mathbb{E}_t(\tilde{\lambda}_{ju}) = \lambda_{jt} \forall u > t$:

$$\begin{aligned} f(\{\mathbb{E}_t(\tilde{\lambda}_{ju})\}, \{\mathbb{E}_t(e_{ju})\}, \{\mathbb{E}_t(s_{iu})\}) &\approx f(\tilde{\lambda}_{jt}, e_{jt}, \vec{0}) \\ &\quad + \sum_{u=t+1}^{\infty} \frac{\partial f}{\partial \tilde{\lambda}_{ju}} \Big|_{\tilde{\lambda}_{jt}, e_{jt}, \vec{0}} \times (\mathbb{E}_t(\tilde{\lambda}_{ju}) - \lambda_{jt}) \\ &\quad + \sum_{u=t+1}^{\infty} \frac{\partial f}{\partial e_{ju}} \Big|_{\tilde{\lambda}_{jt}, e_{jt}, \vec{0}} \times (\mathbb{E}_t(e_{ju}) - e_{jt}) \\ &\quad + \sum_{u=t+1}^{\infty} \frac{\partial f}{\partial \mathbb{E}_t(s_{iu})} \Big|_{\tilde{\lambda}_{jt}, e_{jt}, \vec{0}} \times (\mathbb{E}_t(s_{iu}) - 0) \end{aligned}$$

Note that:

$$\begin{aligned}
f(\tilde{\lambda}_{jt}, e_{jt}, \vec{0}) &= \log \left(\frac{\exp(e_{jt} - \tilde{\lambda}_{jt})}{1 - \rho} \right) \\
\frac{\partial f}{\partial \tilde{\lambda}_{ju}} \Big|_{\tilde{\lambda}_{jt}, e_{jt}, \vec{0}} &= - \left(\frac{1 - \rho}{\exp(e_{jt} - \tilde{\lambda}_{jt})} \right) \rho^{u-t} \exp(e_{jt} - \tilde{\lambda}_{jt}) = -(1 - \rho) \rho^{u-t} \\
\frac{\partial f}{\partial e_{ju}} \Big|_{\tilde{\lambda}_{jt}, e_{jt}, \vec{0}} &= \left(\frac{1 - \rho}{\exp(e_{jt} - \tilde{\lambda}_{jt})} \right) \exp(e_{jt} - \tilde{\lambda}_{jt}) \rho^{u-t} = (1 - \rho) \rho^{u-t} \\
\frac{\partial f}{\partial \tilde{\mathbb{E}}_t(s_{ju})} \Big|_{\tilde{\lambda}_{jt}, e_{jt}, \vec{0}} &= \left(\frac{1 - \rho}{\exp(e_{jt} - \tilde{\lambda}_{jt})} \right) \times \exp(e_{jt} - \tilde{\lambda}_{jt}) \frac{\gamma \rho^{u-t}}{1 - \rho} = \gamma \rho^{u-t}
\end{aligned}$$

Thus:

$$\begin{aligned}
f(\{\mathbb{E}_t(\tilde{\lambda}_{ju})\}, \{\mathbb{E}_t(e_{ju})\}, \{\tilde{\mathbb{E}}_t(s_{iu})\}) &\approx e_{jt} - \tilde{\lambda}_{jt} - \log(1 - \rho) \\
&\quad + (1 - \rho) \sum_{\tau=t+1}^{\infty} \rho^{\tau-t} (\mathbb{E}_t(e_{j\tau}) - e_{jt} - (\mathbb{E}_t(\tilde{\lambda}_{j\tau}) - \tilde{\lambda}_{jt})) \\
&\quad + \gamma \sum_{\tau=t+1}^{\infty} \rho^{\tau-t} \tilde{\mathbb{E}}_t(s_{j\tau})
\end{aligned}$$

G.2 Calculating expectations of future sinking

We create two measures of expectations of future sinking. The first assumes that sinking rates follow an AR(1) process at the plot level, such that:

$$s_{it+1} = \mu_i + \phi s_{it} + e_{it+1} \tag{20}$$

We estimate the parameters of this function, namely, $\{\mu_i\}_i$ and ϕ , and define the expected value of the sinking rate in each period as:

$$\mathbb{E}_t(s_{it+\tau}) = \mu_i (1 - \phi^{\tau-t}) + \phi^{\tau-t} s_{it} \tag{21}$$

with the expected value of total sinking in τ being the sum of the expectations of sinking rates from $t+1$ to τ . Solving for the net present value of these terms from $t+1$ to infinity gives:

$$\sum_{\tau=t+1}^{\infty} \rho^{\tau-t} \mathbb{E}_t(S_{i\tau}^t) = \frac{\rho}{1 - \rho} \mu_i + \frac{\rho \phi}{1 - \rho \phi} (s_{it} - \mu_i) \tag{22}$$

For expectations that follow perfect foresight, we use the realized sinking on the plot from $t+1$ to 2025, and use a plot-specific estimate of the rate from 2025-on for sinking after

that date. The expectation term under perfect foresight is:

$$\sum_{\tau=t+1}^{\infty} \rho^{\tau-t} \mathbb{E}_t(S_{i\tau}^t) = \sum_{\tau=t+1}^{2024} \rho^{\tau-t} S_{i\tau}^t + \frac{\rho^{2025-t}}{1-\rho} \hat{s}_i \quad (23)$$

G.3 Welfare calculations

G.3.1 Renters

Per-period surplus per renter in the housing unit market is:

$$CS_j^i = R_j(0) \log \left(\sum_j \exp\{-\log(R_j(0)) + Z_j \delta + e_j\} \right) + C$$

We measure the welfare loss to consumers Δ^D as the equivalence variation required to compensate home buyers for the impacts of subsidence relative to the benchmark. Because of the size of the system, it is too computationally intensive to calculate an equivalent variation for each consumer, so we find the average equivalent variation as:

$$\begin{aligned} & \Delta_t^D \text{ such that:} \\ & \frac{1}{J} \sum_j CS_{jt}^i = \frac{1}{J} \sum_j R_j(0) \log \left(\sum_j \exp\{-\log(R_j(0) + \Delta_t^D) + Z_j \delta + e_{jt}\} \right) \end{aligned} \quad (24)$$

While a building is not redeveloped, rents must adjust so that equilibrium demand on the plot is equal to the (fixed) supply of housing on the plot, so we can express mean utility in each period as a function of utility in the period when the building is new ($S_{jt} = 0$) with rental price $R_j^*(0)$.

G.3.2 Property managers

Expected manager surplus is their profits under rational expectations:

$$\Pi_t = \sum_j H_{jt} \left(\mathbb{E} \left(\sum_{\tau=t}^{\infty} \rho^{\tau-t} R_{j\tau} \right) - p_{jt} \right) \quad (25)$$

G.3.3 Producer surplus

Per-period producer surplus in the housing unit market is:

$$\begin{aligned} PS_t(\{S\}_j; \theta) &= \mathbb{E}(\pi_{jt}^*) \\ &= Pr(\exp(\tilde{\xi}_{jt}^S) \tilde{\eta} p_{jt}(0)^{\eta+1} - p_{jt} H_{jt-1} D > 0) \times \\ &\quad \mathbb{E}(\exp(\tilde{\xi}_{jt}^S) \tilde{\eta} p_{jt}(0)^{\eta+1} - p_{jt} H_{jt-1} D | \exp(\tilde{\xi}_{jt}^S) \tilde{\eta} p_{jt}(0)^{\eta+1} - p_{jt} H_{jt-1} D > 0) \end{aligned}$$

with expectations defined over cost shocks. The firm earns positive profits for:

$$\begin{aligned}\tilde{\xi}_{jt}^S &> -(\log(\tilde{\eta}) + (\eta + 1) \log(p_{jt}(0)) - \log(p_{jt}) - \log(H_{jt-1}) - \log(D)) \iff \\ \tilde{\xi}_{jt}^S &> -(\log(\tilde{\eta}) + \eta \log(p_{jt}) - \gamma(1 + \eta)S_{jt} - \log(H_{jt-1}) - \log(D)) := -\tilde{\pi}_{jt} \\ \iff \xi_{jt}^* &> \exp(-\tilde{\pi}_{jt}), \quad \xi_{jt}^* = \exp(\tilde{\xi}_{jt}^S)\end{aligned}$$

So the expected value is:

$$\begin{aligned}\mathbb{E}(\pi_{jt}^*) &= Pr(\xi_{jt}^* > \exp(-\tilde{\pi}_{jt})) \frac{\tilde{\eta} p_{jt}(0)^{\eta+1} \int_{\exp(-\tilde{\pi}_{jt})}^{\infty} \xi_{jt}^* f(\xi_{jt}^*) d\xi_{jt}^* - p_{jt} H_{jt-1} D}{Pr(\xi_{jt}^* > \exp(-\tilde{\pi}_{jt}))} \\ &= \tilde{\eta} p_{jt}(0)^{\eta+1} \int_{\exp(-\tilde{\pi}_{jt})}^{\infty} \xi_{jt}^* f(\xi_{jt}^*) d\xi_{jt}^* - p_{jt} H_{jt-1} D Pr(\xi_{jt}^* > \exp(-\tilde{\pi}))\end{aligned}$$

If $\tilde{\xi}_{jt}^S \sim N(\mu, \sigma^2)$, then ξ_{jt}^* has a log-normal distribution and the incomplete integral from above (removing indices for clarity) is:

$$\begin{aligned}\int_{\exp(-\tilde{\pi})}^{\infty} \xi^* f(\xi^*) d\xi^* &= \int_{\exp(-\tilde{\pi})}^{\infty} \exp(\tilde{\xi}) f(\xi^*) d\xi^* \\ &= \int_{\exp(-\tilde{\pi})}^{\infty} \frac{\exp(\tilde{\xi})}{\xi^* \sigma \sqrt{2\pi}} \exp\left(-\frac{(\log(\xi^*) - \mu)^2}{2\sigma^2}\right) d\xi^*\end{aligned}$$

Let $\tilde{\xi} = \log(\xi^*) \Rightarrow d\tilde{\xi} = 1/\xi^* d\xi^*$ and $\xi^* = \exp(\tilde{\pi}) \Rightarrow \tilde{\xi} = \tilde{\pi}$. Then:

$$\begin{aligned}\int_{\exp(-\tilde{\pi})}^{\infty} \xi^* f(\xi^*) d\xi^* &= \int_{-\tilde{\pi}}^{\infty} \frac{1}{\sigma \sqrt{2\pi}} \exp(\tilde{\xi}) \exp\left(-\frac{(\tilde{\xi} - \mu)^2}{2\sigma^2}\right) d\tilde{\xi} \\ &= \int_{-\tilde{\pi}}^{\infty} \frac{1}{\sigma \sqrt{2\pi}} \exp\left(-\frac{1}{2\sigma}(\tilde{\xi}^2 - 2\tilde{\xi}\mu + \mu^2 - 2\sigma^2\tilde{\xi})\right) d\tilde{\xi} \\ &= \int_{-\tilde{\pi}}^{\infty} \frac{1}{\sigma \sqrt{2\pi}} \exp\left(-\frac{1}{2\sigma^2}(\tilde{\xi}^2 - 2\tilde{\xi}(\mu + \sigma^2) + \mu^2 + 2\mu\sigma^2 + \sigma^4 - 2\mu\sigma^2 - \sigma^4)\right) d\tilde{\xi} \\ &= \int_{-\tilde{\pi}}^{\infty} \frac{1}{\sigma \sqrt{2\pi}} \exp\left(-\frac{(\tilde{\xi} - (\mu + \sigma^2))^2}{2\sigma^2} + \mu + \sigma^2/2\right) d\tilde{\xi} \\ &= \exp(\mu + \sigma^2/2) \int_{-\tilde{\pi}}^{\infty} \frac{1}{\sigma \sqrt{2\pi}} \exp\left(-\frac{(\tilde{\xi} - (\mu + \sigma^2))^2}{2\sigma^2}\right) d\tilde{\xi} \\ &= \exp(\mu + \sigma^2/2) \left(1 - \Phi\left(\frac{-\tilde{\pi} - (\mu + \sigma^2)}{\sigma}\right)\right) \\ &= \exp(\mu + \sigma^2/2) \Phi\left(\frac{\mu + \sigma^2 + \tilde{\pi}}{\sigma}\right)\end{aligned}$$

Giving:

$$\mathbb{E}(\pi_{jt}^*) = \tilde{\eta} p_{jt}(0)^{1+\eta} \exp(\mu + \sigma^2/2) \Phi\left(\frac{\mu + \sigma^2 + \tilde{\pi}_{jt}}{\sigma}\right) - p_{jt} H_{jt-1} D \Phi\left(\frac{\mu + \tilde{\pi}_{jt}}{\sigma}\right) \quad (26)$$

G.4 Propositions about changes in consumer, producer surplus

Consider the counterfactuals defined as follows:

C1 All future expected sinking is zero: $NPVS_{jt} := \sum_{\tau=t+1}^{\infty} \rho^{\tau-t} \mathbb{E}_t(s_{j\tau}) = 0 \forall j, t.$

C1 Mexico City experiences no sinking ever. That is, $NPVS_{jt} = S_{jt} = 0 \forall j, t.$

C3 Information frictions are resolved: $\theta \rightarrow 1.$

We evaluate each derivative “in the long run”, where the long-run is long enough that housing on a plot has a chance to be redeveloped and update to a new equilibrium. In the long-run, given a demand shock (as all of our counterfactuals represent), the new equilibrium represents a movement along the supply curve, and we know the elasticity of this supply curve is η :

$$\frac{\partial \log(H_{jt})}{\partial \log(p_{jt}(0))} = \eta \Rightarrow \frac{\partial \log(H_{jt})}{\partial X_{jt}} = \eta \frac{\partial \log(p_{jt}(0))}{\partial X_{jt}}$$

for some demand shifter X_{jt} .

G.4.1 Change in the probability of redevelopment

The probability that a plot is developed is:

$$Pr(\text{Redev}_{jt}) = \Phi\left(\frac{\mu + \tilde{\pi}_{jt}}{\sigma}\right), \quad \tilde{\pi}_{jt} = \log(\tilde{\eta}) + \eta \log(p_{jt}(0)) - \gamma S_{jt} - \log(H_{jt}) - \log(D)$$

In counterfactual **C1**:

$$\begin{aligned} \frac{\partial Pr(\text{Redev}_{jt})}{\partial NPVS_{jt}} &\propto \eta \frac{\partial \log(p_{jt}(0))}{\partial NPVS_{jt}} - \frac{\partial \log(H_{jt})}{\partial NPVS_{jt}} \\ &= \eta \frac{\partial \log(p_{jt}(0))}{\partial NPVS_{jt}} - \eta \frac{\partial \log(p_{jt}(0))}{\partial NPVS_{jt}} = 0 \end{aligned}$$

In counterfactual **C2**:

$$\frac{\partial Pr(\text{Redev}_{jt})}{\partial S_{jt}} \propto \frac{\partial Pr(\text{Redev}_{jt})}{\partial NPVS_{jt}} \frac{\partial NPVS_{jt}}{\partial S_{jt}} - \gamma = -\gamma > 0$$

In counterfactual **C3**:

$$\frac{\partial Pr(\text{Redev}_{jt})}{\partial \theta} \propto \eta \frac{\partial \log(p_{jt}(0))}{\partial \theta} - \frac{\partial \log(H_{jt})}{\partial \theta} = 0$$

G.4.2 Change in producer surplus

Expected profits are:

$$PS_{jt} = \tilde{\eta} p_{jt}(0)^{\eta+1} \exp(\mu + \sigma^2/2) \Phi\left(\frac{\mu + \sigma^2 + \tilde{\pi}_{jt}}{\sigma}\right) - \exp(\gamma S_{jt}) p_{jt}(0) H_{jt} D \Phi\left(\frac{\mu + \tilde{\pi}_{jt}}{\sigma}\right)$$

Let $\Xi(\tilde{\pi}_{jt}) = \exp(\mu + \sigma^2/2) \Phi\left(\frac{\mu + \sigma^2 + \tilde{\pi}_{jt}}{\sigma}\right)$ in the following, and recall that:

$$\frac{\partial \Xi(\tilde{\pi}_{jt})}{\partial NPVS_{jt}} = \frac{\partial \Xi(\tilde{\pi}_{jt})}{\partial \theta} = 0$$

In counterfactual **C1**:

$$\begin{aligned} \frac{\partial PS_{jt}}{\partial NPVS_{jt}} &= \Xi(\tilde{\pi}_{jt}) \tilde{\eta} (\eta + 1) p_{jt}(0)^\eta \frac{\partial p_{jt}(0)}{\partial NPVS_{jt}} \\ &\quad - \exp(\gamma S_{jt}) D \Phi\left(\frac{\mu + \tilde{\pi}_{jt}}{\sigma}\right) \left(\frac{\partial p_{jt}(0)}{\partial NPVS_{jt}} H_{jt} + \frac{\partial H_{jt}}{\partial NPVS_{jt}} p_{jt}(0) \right) \\ &= \Xi(\tilde{\pi}_{jt}) \tilde{\eta} (\eta + 1) p_{jt}(0)^\eta \frac{\partial p_{jt}(0)}{\partial NPVS_{jt}} \\ &\quad - \exp(\gamma S_{jt}) D \Phi\left(\frac{\mu + \tilde{\pi}_{jt}}{\sigma}\right) \left(\frac{\partial p_{jt}(0)}{\partial NPVS_{jt}} H_{jt} + \eta \frac{\partial p_{jt}(0)}{\partial NPVS_{jt}} H_{jt} \right) \\ &= \frac{\eta + 1}{p_{jt}(0)} \frac{\partial p_{jt}(0)}{\partial NPVS_{jt}} H_{jt} \left(\Xi(\tilde{\pi}_{jt}) \tilde{\eta} p_{jt}(0)^{\eta+1} - p_{jt} H_{jt} D \Phi\left(\frac{\mu + \tilde{\pi}_{jt}}{\sigma}\right) \right) \\ &= (\eta + 1) \frac{\partial \log(p_{jt}(0))}{\partial NPVS_{jt}} PS_{jt} = (\eta + 1) \gamma \theta PS_{jt} \leq 0 \end{aligned}$$

In counterfactual **C2**:

The change in producer surplus is equal to that of **C1**, plus the change due to the change in S_{jt} :

$$\begin{aligned} \frac{\partial PS_{jt}}{\partial S_{jt}} &= \underbrace{\frac{\partial PS_{jt}}{\partial NPVS_{jt}} \frac{\partial NPVS_{jt}}{\partial S_{jt}}}_{\leq 0} \underbrace{- \gamma p_{jt} H_{jt} D \Phi\left(\frac{\mu + \tilde{\pi}_{jt}}{\sigma}\right)}_{> 0} \\ &\quad - \underbrace{\frac{\gamma}{\sigma} \left(\tilde{\eta} p_{jt}(0)^{\eta+1} \exp(\mu + \sigma^2/2) \phi\left(\frac{\mu + \sigma^2 + \tilde{\pi}}{\sigma}\right) - p_{jt} H_{jt} D \phi\left(\frac{\mu + \tilde{\pi}}{\sigma}\right) \right)}_{\leq 0} \end{aligned}$$

The sign of this derivative is unknown. However, some patterns emerge:

- As very high or low $\tilde{\pi}_{jt}$, the last term goes to zero, and there is little impact through the changed probability of re-development.
- For values of $\tilde{\pi}_{jt}$ near the middle of the distribution, where cost shocks are more marginal to the decision to develop, things are more complicated for this term.

- Sending this term to zero, we see that benefits are not clear to producers. Subsidence benefits them by lowering the cost of development (term 2), but it also lowers revenues (term 3). As $\theta \rightarrow 0$, the costs channel wins.

In C3:

$$\begin{aligned}\frac{\partial PS_{jt}}{\partial \theta} &= \frac{\partial \tilde{\pi}_{jt}}{\partial \theta} \left(\tilde{\eta} p_{jt}(0)^{\eta+1} \exp(\mu + \sigma^2/2) \phi \left(\frac{\mu + \sigma^2 + \tilde{\pi}}{\sigma} \right) - p_{jt} H_{jt} D \phi \left(\frac{\mu + \tilde{\pi}}{\sigma} \right) \right) \\ &\quad + \frac{\partial \log(p_{jt}(0))}{\partial \theta} (\eta + 1) PS_{jt} \\ &= \frac{\partial \log(p_{jt}(0))}{\partial \theta} (\eta + 1) PS_{jt} \leq 0\end{aligned}$$

Information frictions unambiguously increase producer surplus by decreasing revenue.

G.5 Proof of validity of control function

The full structural supply model is:

$$\begin{aligned}d_{jt} &= 1 \left(\tilde{V}_{jt}^S \geq 0 \right) \\ \tilde{V}_{jt}^S &= \log(\tilde{\eta}) + \eta \log(p_{jt}) - \gamma(1 + \eta) S_{jt} - \log(H_{jt-1}) - \log(D) + \log(\xi_{jt}^S) \\ \log(p_{jt}) &= \gamma S_{jt} + \text{PIRel. altitude change}_{jt} + u_{jt}\end{aligned}$$

The proof follows [Blundell and Matzkin \(2014\)](#), in showing that the residual $\log(u_{jt})$ satisfies control function separability, which follows naturally from the linearity of the first stage:

$$r^2(\tilde{V}_{jt}^S, \log(p_{jt}), Z_{jt}) = u_{jt} = \underbrace{\log(p_{jt}) - \gamma S_{jt} - \text{PIRel. altitude change}_{jt}}_{q(\log(p_{jt}), Z_{jt})}$$

Note that $v(q(\log(p_{jt}), \text{Rel. altitude change}_{jt}), r^1(\log(p_{jt}))) = q(\log(p_{jt}), \text{Rel. altitude change}_{jt})$, so q is strictly increasing in \bar{p}_{jt} and $v()$ is strictly increasing in $q()$. Thus, the structural inverse of the system satisfied control function separability, and a control function can be derived from the first stage to estimate the second stage.

G.6 Computing counterfactuals

Given our sparse data on prices, we seek to estimate counterfactual prices and housing densities using a dataset of plots as a single cross-section. To do this, we consider a steady state in which the joint distribution of the underlying random variables that generate the equilibrium, $(\xi_{jt}^S, \varepsilon_{jt}^i, e_{jt}, s_{jt})$ is time-invarying and approximately non-stochastic given the large number of plots we consider (985,862). The intuition of this steady state is that while the draws of cost and preference shocks are stochastic, given enough plots the distribution of $(p_{jt}(0), H_{jt})$ is constant in each period and can be treated as fixed. In the steady state, we drop the t subscript to emphasize the independence of time.

The equilibrium is most easily expressed in terms of log prices and log relative housing relative to the outside option. Let $\tilde{\lambda}_j = \log(\lambda_j) - \log(\lambda_0)$; in equilibrium, $\tilde{\lambda}_j = \log(H_j) - \log(H_0)$. The equilibrium is characterized by:

$$\tilde{\lambda}_j^D = -\log(R_j(0)) + Z_j \delta + e_j \quad (27)$$

$$\tilde{\lambda}_j^S = \eta \log\left(\frac{\eta}{1+\eta}\right) + \eta \log(p_j(0)) + \tilde{\xi}_j^S - \log(H_{0t}^S) \quad (28)$$

$$\tilde{\lambda}_j^D \approx -\log(p_{jt}(0)) + Z_j \delta + e_j + \gamma \theta \sum_{\tau=t}^{\infty} \rho^{\tau-t} \mathbb{E}_t(s_{j\tau}) \quad (29)$$

The last equation is derived directly from Equation (15) evaluated at $S_{jt} = 0$.

Given data on the plot level on $(\tilde{\lambda}_j, \log(p_j(0)), Z_j, \sum_{\tau=t}^{\infty} \rho^{\tau-t} \mathbb{E}_t(s_{j\tau}))$ and estimates or calibrated values of the parameters $(\gamma, \theta, \delta, \eta, \rho)$, we first solve the previous equations exactly to back out $(e_j, \tilde{\xi}_j)$. From the inferred values of $\tilde{\xi}_j$, we calibrate μ and σ as the mean and standard deviation of these shocks.

In order to calculate welfare under different counterfactuals, for example setting $\mathbb{E}_t(s_{j\tau}) = 0$ or $\theta = 1$, we alter these parameters and, holding $(Z_j, e_j, \tilde{\xi}_j^S)$ fixed, solve the system for alternative vectors of prices and relative housing supply that clear the housing market on each plot.

G.7 Proof that the new error function is independent of prices

In order for the control function approach to provide unbiased estimation of the coefficient on prices, prices and the (modified) error term must be independent. We prove that here:

$$\begin{aligned} \mathbb{E}(\tilde{\xi}_{jt}^* | \log(p_{jt})) &= \mathbb{E}\left(\mathbb{E}\left(\tilde{\xi}_{jt}^* | \log(p_{jt}), Z_{jt}\right) | \log(p_{jt})\right) \\ &= \mathbb{E}\left(\mathbb{E}\left(\tilde{\xi}_{jt}^S - \mathbb{E}(\tilde{\xi}_{jt} | \log(e_{jt})) | \log(p_{jt}), Z_{jt}\right) | \log(p_{jt})\right) \\ &= \mathbb{E}\left(\mathbb{E}\left(\tilde{\xi}_{jt}^S | \log(p_{jt}), Z_{jt}\right) - \mathbb{E}\left(\mathbb{E}(\tilde{\xi}_{jt}^S | \log(e_{jt})) | \log(p_{jt}), Z_{jt}\right) | \log(p_{jt})\right) \\ &= \mathbb{E}\left(\mathbb{E}\left(\tilde{\xi}_{jt}^S | \log(p_{jt}), Z_{jt}\right) - \mathbb{E}\left(\mathbb{E}(\tilde{\xi}_{jt} | \log(e_{jt})) | \log(e_{jt}), Z_{jt}\right) | \log(p_{jt})\right) \\ &= \mathbb{E}\left(\mathbb{E}\left(\tilde{\xi}_{jt}^S | \log(e_{jt}), Z_{jt}\right) - \mathbb{E}\left(\tilde{\xi}_{jt} | \log(e_{jt})\right) | \log(p_{jt})\right) \\ &= \mathbb{E}\left(\mathbb{E}\left(\tilde{\xi}_{jt}^S | \log(e_{jt})\right) - \mathbb{E}\left(\tilde{\xi}_{jt} | \log(e_{jt})\right) | \log(p_{jt})\right) = \mathbb{E}(0 | \log(p_{jt})) = 0 \end{aligned}$$

H Cost-benefit Appendix

Our empirical estimates provide a measure of the total cost of subsidence, which expressed in terms of dollars per meter of average elevation loss is:

$$\frac{\text{Total cost}}{\text{meter of elevation loss}} = \frac{\text{Total cost}}{NPVS} = \frac{1}{0.931} \text{Total cost} \quad (30)$$

In order to price the externality-generating action, groundwater pumping, we must convert this to dollars per unit of water pumped.

Subsidence is caused by low groundwater tables. We estimate the response of subsidence rates to changes in aquifer storage by taking the average change in subsidence rates over the 13-year period in our panel, and estimating the dosage-response of subsidence rates to changes in aquifer storage:

$$\Delta s = \frac{\Delta s}{\Delta V} \times \Delta V \quad (31)$$

$$\Delta s = \frac{0.0361}{\underbrace{-111 \times 13}_{\substack{\text{Annual loss} \times T = \\ \text{Total loss} \\ \text{over 13 years}}}} \Delta V$$

Here Δs is the change in the annual subsidence rate (change in m /year), and ΔV is the net loss in aquifer storage (millions of cubic meters, or hectometers hm^3). We take the annual net loss in aquifer storage from [CONAGUA \(2024\)](#); details from this report on aquifer demand over this period are described in Table A18.⁴⁹

Table A18: Aquifer demand

	Annual volume (hm^3)
Natural recharge	151.4
Recharge from drinking water leaks	361.4
Total recharge	512.8
Pumping for drinking water	448.5
Other pumping	175.3
Total extraction	623.8
Net volume change per year	-111

Notes: Source: [CONAGUA \(2024\)](#).

Solving this formula for ΔV and assuming no change in recharge implies that aquifer storage would need to increase by a total of 2,495 hm^3 in order to fully abate average

⁴⁹This expression extracts away from dynamics; how long it would take for a higher water table to translate to slower sinking rates is difficult to answer but crucial question for policy. While it may take decades for higher aquifer levels to translate to fully abated sinking, interventions that locally rise water tables such as wastewater injection sites have seen rapid abatement of subsidence.

subsidence rates of 6 cm/year, the equivalent of reducing total pumping by a third for the next 26 years, according to:

$$\Delta V = (\text{Recharge} - (1 - r)\text{Pumping}) \times Y$$

$$2495 = (512.8 - (1 - r)623.8) \times Y$$

where r is the percentage reduction in pumping, and Y is the number of years this reduction is sustained for. Note that in terms of pumping, a permanent change in the pumping rate is required to induce a net loss in storage.

H.1 Cost-benefit of other recharge policies

Here we discuss the costs and benefits of these policies, a challenging task given the lack of detailed information on the cost structure of some of these interventions. We discuss how we construct the costs and benefits of each of the explored policies, with emphasis on the limitations of these estimates.

- *Wastewater recycling:* Our primary source for information the costs and benefits of investing in wastewater recycling plants comes from the 2007-2012 Plan for Sustainable Water Management in Mexico City ([Gobierno del Distrito Federal, 2007](#)). This document describes an investment in building 6 macro-sites for secondary wastewater treatment. We assume a useful life of 50 years once built following engineering guidance. In the absence of information on operating costs, which can be substantial for wastewater treatment, we use a value of \$2.9 MXN per liter treated which is taken from an engineering blog from Mexico ([Ingeniería, 2021](#)).⁵⁰ Note that construction costs may have evolved substantially between 2007 and now, and better estimates of operating costs are necessary for comprehensive analysis.
- *Injection of treated wastewater:* We take information on the costs and productivity of absorption wells from [SACMEX \(2012\)](#), which detail investments in 2012 made in developing new wells. We set annual operating costs to \$1.25 million MXN by assigning half the annual budget assigned to absorption wells and new deep wells in [Gobierno de la Ciudad de México \(2020\)](#). We assume a 5-year construction period.
- *Repairing water main leaks:* We take reports of the costs and efficiency of efforts to repair leaks in the system from [Gobierno de la Ciudad de México \(2020\)](#). Repairing leaks may have contradictory impacts on the aquifer; [CONAGUA \(2024\)](#) estimate that most recharge on the aquifer comes from lost water in the Mexico City system, and considering that some of that water is imported from outside the watershed would imply that some of this recharge is additional to what is pumped. We take an optimistic scenario and assume that all leaks that are addressed are done on parts of the system *prior* to entering the city, which would make all water saved additional. However, given that our cost estimates are calculated using efforts conducted *within* the city,

⁵⁰We chose the midpoint of the range they specify since these are secondary treatment sites.

it is unclear whether we over- or under-estimate these relative to the true costs of repairing leaks outside the city. While infrastructure outside the city is exposed and therefore less costly to work on than buried lines, these lines are also larger and more economically costly to shut down.